Aryl and Alkyl Migration Strategies for the Functionalization and Application of 1,2-Azaborines:

Author: Jonathan E. Deegan

Boston College

Graduate School of the Morrissey College of Arts and Sciences

Department of Chemistry

ARYL AND ALKYL MIGRATION STRATEGIES FOR THE FUNCTIONALIZATION AND APPLICATION OF 1,2-AZABORINES

A thesis

by

JONATHAN EDWARD DEEGAN

submitted in partial fulfillment of the requirements

for the degree of

Master of Science

August 2019

Aryl and Alkyl Migration Strategies for the Functionalization and Application of 1,2-Azaborines

by

JONATHAN EDWARD DEEGAN

Thesis Advisor:

Professor Shih-Yuan Liu, Ph.D.

ABSTRACT: As *BN*-*CC* isosterism becomes an increasingly valuable strategy to expand chemical space and increase molecular diversity, methods for functionalizing and utilizing *BN*-heteroarenes remain limited in comparison to those for all-carbon arenes. Described herein are initial studies aimed at developing methods for the late-stage functionalization of substituted 1,2-azaborines through controlled aryl and alkyl migrations. Furthermore, investigations into the application of *B*-aryl and *B*-alkyl 1,2-azaborines as transmetalation reagents in Suzuki-Miyaura cross-coupling reactions are presented.

For Anna

Acknowledgements

Though cliché, no expression describes my educational experience as accurately as the adage "it takes a village to raise a child." The following work would not have been possible without the kindness, support, and mentorship of countless individuals from whom I have had the distinct privilege to learn.

I must first express a tremendous amount of gratitude to my academic and scientific advisor, Prof. Shih-Yuan Liu, not only for granting me the opportunity to join his research group, but more so for his patience and guidance throughout my time at BC. Prof. Liu's artistry and devotion to his craft are unparalleled, and I will undoubtedly carry the lessons I've learned under his tutelage with me as I move forward in my career. I would also like to offer special thanks to Prof. Marc Snapper and Prof. X. Peter Zhang for serving on my thesis committee.

Many thanks are due to every member of the BC community that, knowingly or unknowingly, has helped me find direction throughout my graduate studies. In particular, I would like to sincerely thank Prof. Holly Deak for encouraging me to pursue my passion for STEM education, and for serving as an exemplary role model both in and out of the classroom.

Additionally, I would like to thank my mentors at Loyola University MD, the Christmann Group at the Freie Universität Berlin, my BC classmates, and my colleagues in the Liu group for constantly serving as sources of strength, wisdom, and inspiration.

Lastly, and most importantly, I must thank my mother, my father, and all of my family and friends, whose love, support, and tolerance of my absence were pivotal to the completion of this work.

Table of Contents

List of Figures

List of Schemes

List of Tables

List of Abbreviations

Ac	acetyl
Ad	adamantyl
Ar	arene
BDE	bond dissociation energy
BIPHEP	2,2'-bis(diphenylphosphino)biphenyl
Bn	benzyl
br	broad
Bu	butyl
cod	1,5-cyclooctadiene
CPME	cyclopentyl methyl ether
Cy	cyclohexane
d	doublet
dba	dibenzylideneacetone
dd	doublet of doublets
DDQ	2,3-dichloro-5,6-dicyano-1,4-benzoquinone
ddt	doublet of doublet of triplets
dq	doublet of quartets
dppb	1,4-bis(diphenylphosphino)butane
dppp	1,4-bis(diphenylphosphino)propane
dppf	1,1'-bis(diphenylphosphino)ferrocene
dtbpy	4,4′-di-*tert*-butyl-2,2′-dipyridyl
E	electrophile
Et	ethyl
equiv	equivalents
G2	second-generation palladacycle precatalyst
GC-MS	gas chromatography-mass spectrometry
h	hour(s)
(Het)	hetero
i	iso
IPr	1,3-bis-(2,6-diisopropylphenyl)imidazolinium chloride
JohnPhos	2-(biphenyl)di-*tert*-butylphosphine
KHMDS	potassium bis(trimethylsilyl)amide
L	ligand
m	multiplet
Me	methyl
Mes	mesityl (i.e. 1,3,5-trimethylbenzene)
Ms	mesyl (i.e. methanesulfonyl)
MTBE	methyl *tert*-butyl ether
neo	neopentyl
NMR	nuclear magnetic resonance spectroscopy
Nu	nucleophile
OTf	triflate (i.e. trifluoromethanesulfonate)

o-Tol	*ortho*-tolyl
PG	protecting group
Ph	phenyl
pin	pinacolato
Pr	propyl
q	quartet
QPhos	1,2,3,4,5-pentaphenyl-1'-(di-*tert*-butylphosphino)ferrocene
RCM	ring-closing metathesis
RT	room temperature
RuPhos	2-dicyclohexylphosphino-2′,6′-diisopropoxybiphenyl
s	singlet
SPhos	2-dicyclohexylphosphino-2′,6′-dimethoxybiphenyl
t	*tert*
t	triplet
td	triplet of doublets
TBS	*tert*-butyldimethylsilyl
THF	tetrahydrofuran
XPhos	2-dicyclohexylphosphino-2′,4′,6′-triisopropylbiphenyl

CHAPTER 1
Aryl and Alkyl Migration Strategies for the Functionalization and Application of 1,2-Azaborines

1.1 Introduction to *BN-CC* Isosterism

Though the definition varies between disciplines, the term "isosterism" was first introduced by Irving Langmuir in one of his seminal works, "Isomorphism, Isosterism, and Covalence." In his writing, Langmuir used isosterism to describe atoms, compounds, or groups of atoms that possess the same number and arrangement of electrons, but differ in the charges on their atomic nuclei.[1] By analyzing and comparing the physical properties of various molecules, Langmuir characterized twenty-one groups of isosteres. This served as the first occurrence of isosterism's use as a tool to compare the observable characteristics of different chemical species (**Table 1.1**).

Table 1.1 Groups of Isosteres Characterized by Langmuir[1]

Group	Isosteres
1	H^-, He, Li^+
2	O^{2-}, F^-, Ne, Na^+, Mg^{2+}, Al^{3+}
3	S^{2-}, Cl^-, Ar, K^+, Ca^{2+}
4	Cu^+, Zn^{2+}
5	Br^-, Kr, Rb^+, Sr^{2+}
6	Ag^+, Cd^{2+}
7	I^-, Xe, Cs^+, Ba^{2+}
8	N_2, CO, CN^-
9	CH_4, NH_4^+
10	CO_2, N_2O, N_3^-, CNO^-
11	NO_3^-, CO_3^{2-}
12	NO_2^-, O_3
13	HF, OH^-
14	ClO_4^-, SO_4^{2-}, PO_4^{3-}
15	ClO_3^-, SO_3^{2-}, PO_3^{3-}
16	SO_3, PO_3^-
17	$S_2O_6^{2-}$, $P_2O_6^{4-}$
18	$S_2O_7^{2-}$, $P_2O_7^{4-}$
19	SiH_4, PH_4^+
20	MnO^{4-}, CrO_4^{2-}
21	SeO_4^{2-}, AsO_4^{3-}

[1] Langmuir, I. *J. Am. Chem. Soc.* **1919**, *41*, 1543–1559.

To some extent, Langmuir's "Isomorphism, Isosterism, and Covalence" elaborated upon an article he had published a few months prior—"The Arrangement of Electrons in Atoms and Molecules."[2] While the idea of isosterism was complementary to his theories on bonding and atomic structure, this concept largely became entwined with the atomic theory of the time, and was not viewed as a separate concept for nearly another decade.[3]

Since Langmuir's coining of the term in 1919, isosterism has been shown to be a valuable chemical strategy, largely owing to the work of Grimm[4] and Erlenmeyer.[5] For many organic chemists, the modern interpretation of isosterism is broad, and simply describes molecules or groups which have the same number of atoms (isostructural) and the same total number of electrons arranged in a similar manner (isoelectronic). Another interpretation of Langmuir's theory—bioisosterism—has emerged as a fundamental strategy in medicinal chemistry,[6] and specifically defines the phenomenon of isoelectronic atoms and molecules displaying comparable biological activities.[7]

One of the simplest bioisosteric relationships can be found between the hydroxyl and thiol functional groups. The comparable electronic structure of these moieties allows them to be interchanged without significantly altering the physical properties of their respective molecules. Despite this isosteric relationship, however, the relative differences

---

[2] Langmuir, I. *J. Am. Chem. Soc.* **1919**, *41*, 868–934.
[3] (a) Bradlow, H. L.; Vanderwerf, C. A.; Kleinberg, J. *J. Chem. Educ.* **1947**, *24*, 433–435; (b) Wermuth, C. G. in *The Practice of Medicinal Chemistry*, 2nd ed.; Academic Press: San Diego, 1996, p 203–237.
[4] (a) Grimm, H. G.; Gunther, M.; Tittus, H. *Z. physik. Chem.* **1931**, *14*, 169; (b) Grimm, H. G. *Z. Elektrochem.* **1925**, *31*, 474–480; (c) Grimm, H. G. *Naturwissenschaften* **1929**, *17*, 557–564.
[5] (a) Erlenmeyer, H.; Leo, M. *Helv. Chim. Acta* **1933**, *16*, 897–904; (b) Erlenmeyer, H.; Leo, M. *Helv. Chim. Acta* **1932**, *15*, 1180; (c) Erlenmeyer, H.; Berger, E.; Leo, M. *Helv. Chim. Acta* **1933**, *16*, 733–738.
[6] Lima, L. M.; Barreiro, E. J. *Curr. Med. Chem.* **2005**, *12*, 23–49.
[7] (a) Gaikwad, P. L.; Gandhi, P. S.; Jagdale, D. M.; Kadam, V. J. *Am. J. PharmTech Res.* **2012**, *2*, 1; (b) Ali, G.; Subhan, F.; Islam, N. U.; Khan, I.; Rauf, K.; Samiullah; Abbas, M.; Rauf, A. *J. Chem. Soc. Pak.* **2014**, *36*, 150–169.

in sulfur's fundamental properties compared to oxygen's—such as lower electronegativity, an increased van der Waals radius, and reduced hydrogen bonding ability—result in thiol-containing molecules displaying significantly different biological activities than their hydroxy-containing analogues.[8] A demonstrative example can be observed through the comparison of the anti-inflammatory activities of different benzylidene derivatives in rat leukemia cells (**Table 1.2**).[9] When thiazole scaffold **1.1** is substituted with a free hydroxyl moiety, the molecule exhibits anti-inflammatory activity by inhibiting two enzymes, 5-lipoxygenase (LO) and cyclooxygenase (CO),[10] which are responsible for the production of proinflammatory prostaglandins.[11]

Table 1.2 An Example of Pharmacodynamic Modulation between –OH and –SH Moieties[9]

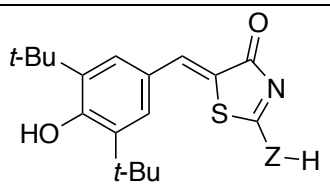

1.1

Z	Electronegativity	van der Waals Radius (Å)	H-Bond Strength (kcal/mol)	5-LO IC_{50} (μM)	CO IC_{50} (μM)
O	3.51	1.58	23	1.4	0.35
S	2.32	1.81	1.1	0.38	0.012

Upon replacement of the hydroxyl functional group with an isosteric thiol moiety, the IC_{50} was significantly reduced for both 5-lipoxygenase and cyclooxygenase, indicating enhanced potency toward both enzymes. Although the specific factor that causes this

[8] (a) Biswal, H. S.; Shirhatti, P. R.; Wategaonkar, S. *J. Phys. Chem. A* **2010**, *114*, 6944–6955; (b) Batsanov, S. S. *Inorganic Materials* **2001**, *37*, 871–885; (c) Steiner, T. *Angew. Chem. Int. Ed.* **2002**, *41*, 48–76.
[9] Patani, G. A.; LaVoie, E. J. *Chem. Rev.* **1996**, *9*, 3147–3176.
[10] Unangst, P. C.; Connor, D. T.; Cetenko, W. A.; Sorenson, R. J.; Kostlan, C. R.; Sircar, J. C.; Wright, C. D.; Schrier, D. J.; Dyer, R. D. *J. Med. Chem.* **1994**, *37*, 322–328.
[11] Vane, J. R. *Nature* **1971**, *231*, 232–235.

modulation of inhibition remains unclear, the use of this substitution strategy in the design of novel anti-inflammatory drugs supports sulfur as a valid bioisostere of oxygen, and altogether demonstrates the potential for isosterism to have practical applications across a variety of research areas.

In particular, isosterism has proven invaluable as a tool to highlight previously unrecognized relationships among compounds and identify new areas of research.[12] One example can be found in *BN-CC* isosterism—one variant of which is the substitution of a *C=C* unit with an isostructural and isoelectronic *B–N* unit. In recent years, *BN-CC* isosterism has gained increased attention as a useful strategy to generate diversity among synthetic targets and reagents, primarily by allowing for the modification of a compound's electronic properties without significantly altering the molecule's steric profile.[13]

Figure 1.1 Isosteric Relationship and Differences in Molecular Properties between Ethene and Aminoborane[14]

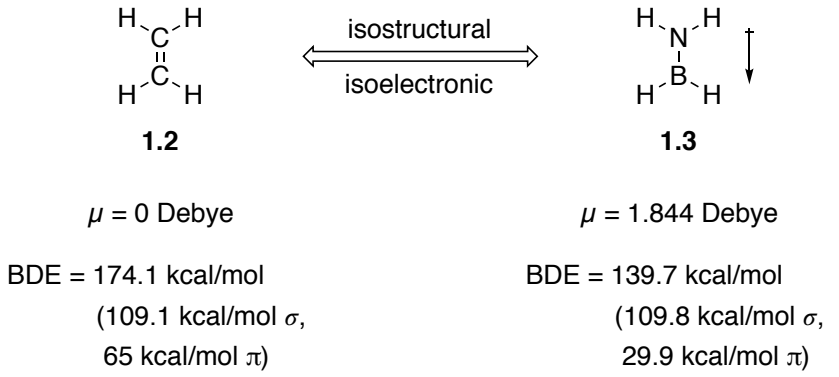

A simple, yet illustrative example of the effects of *BN-CC* isosterism can be found in the comparison of ethene (**1.2**) and its *BN* counterpart, aminoborane (**1.3**) (**Figure 1.1**).

[12] (a) Campbell, P. G.; Zakharov, L. N.; Grant, D.; Dixon, D. A.; Liu, S.-Y. *J. Am. Chem. Soc.* **2010**, *132*, 3289–3291; (b) Abbey, E. R.; Zakharov, L. N.; Liu, S.-Y. *J. Am. Chem. Soc.* **2008**, *130*, 7250–7252.
[13] Morgan, M. M.; Piers, W. E. *Dalton Trans.* **2016**, *45*, 5920–5924.

In the case of ethene, the molecule possesses only nonpolar carbon-carbon and carbon-hydrogen bonds, and the bond dissociation energy of the *C*=*C* linkage is 174.1 kcal/mol. Conversely, the presence of the *B*–*N* bond in the isosteric aminoborane results in the compound having significantly reduced molecular symmetry, a dipole moment of 1.844 Debye, and a lower *B*–*N* bond dissociation energy of 139.7 kcal/mol.[14] Furthermore, the presence of *N*–*H* and *B*–*H* bonds provide the molecule with both protic and hydridic hydrogen atoms, as well the ability to engage in dihydrogen bonding,[15] demonstrating that the *BN* moiety possesses notably different chemical and physical features than its all-carbon counterpart.

In addition to the observable electronic differences between the *BN* and *CC* units, *BN*-*CC* isosterism allows for the expansion of chemical space—that is to say—the generation of molecular diversity and complexity. The substitution of a relatively inert *C*–*C* moiety with a *B*–*N* unit introduces amenable synthetic handles within a molecule. The heightened reactivity of these heteroatomic positions unlocks the potential for site-selective functionalization—a feature that is particularly useful for substrates that possess a high amount of symmetry or that can easily undergo multiple iterations of functionalization, such as arenes.

Regarded as a privileged motif,[16] aromatic compounds have played a pivotal role in biological and physical science, owing to their natural abundance and distinctive biological and optoelectronic properties.[17] In particular, nitrogen-containing heteroarenes

[14] Campbell, P. G.; Marwitz, A. J. V.; Liu, S.-Y. *Angew. Chem. Int. Ed.* **2012**, *51*, 6074–6092.
[15] Demirci, U. B. *Int. J. Hydrogen Energy*, **2017**, *42*, 9978–10013.
[16] (a) Duarte, C. D.; Barreiro, E. J., Fraga, C. A. *Mini Rev Med. Chem.* **2007**, *7*, 1108–1119; (b) Welsch, M. E.; Snyder, S. A.; Stockewell, B. R. *Curr Opin Chem Biol.* **2010**, *14*, 347–361.
[17] (a) Astruc, D. *Modern Arene Chemistry*; Wiley-VCH: Weinheim, Germany, 2002, p 1–19; (b) Suzukia, S.; Yamaguchi, J. *Chem. Commun.* **2017**, *53*, 1568–1582.

(**Figure 1.2**), have found widespread application within the fields of medicinal chemistry,[18] organic synthesis,[19] and materials science.[20]

Figure 1.2 Examples of Prominent Nitrogen Heteroarene Scaffolds[18]

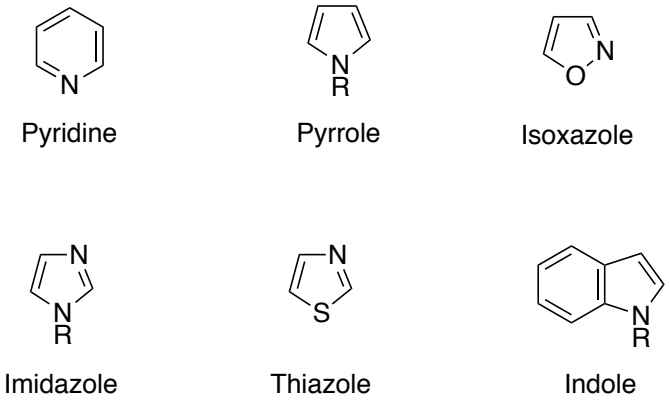

Considering the ubiquity of the heteroarene motif in combination with the chemical diversity offered by *BN*-CC isosterism, *BN*-analogues of benzene have received significant attention, much of which has focused on determining the properties and reactivities of these compounds.[21] Commonly referred to as "inorganic benzene," the earliest-known *BN* heteroarene, borazine (**1.4**), was originally synthesized by Alfred Stock in 1926[22] and has been found to have synthetic and practical applications.[23]

[18] Vitaku, E.; Smith, D. T.; Njardarson, J. T. *J. Med. Chem.* **2014**, *57*, 10257−10274.
[19] Wang, H.; Maiyalagan, T.; Wang, X. *ACS Catal.* **2012**, *2*, 781−794.
[20] Deng, Y.; Xie, Y.; Zoua, K.; Ji, X. *J. Mater. Chem. A*, **2016**, *4*, 1144–1173.
[21] Bélanger-Chabot, G.; Braunschweig, H.; Roy, D. K. *Eur. J. Inorg. Chem.* **2017**, 4353–4368.
[22] Stock, A.; Pohland, E. *Ber. Dtsch. Chem. Ges.* **1926**, *59*, 2210–2215.
[23] (a) Li, J.-S.; Zhang, C.-R.; Bin, L.; Cao, F.; Wang, S.-Q. *Inorg. Chim. Acta* **2011**, *366*, 173–176; (b) Lisovenko, A. S.; Timoshkin, A. Y. *Inorg. Chem.* **2010**, *49*, 10357–10369; (c) Braunschweig, H.; Green, H.; Radacki, K.; Uttinger, K. *Dalton Trans.* **2008**, 3531–3534; (d) Kesharwani, M. K.; Suresh, M.; Das, A.; Ganguly, B. *Tetrahedron Lett.* **2011**, *52*, 3636–3639; (e) Yamamoto Y.; Miyamoto, K.; Umeda, J.; Nakatani, Y.; Yamamoto, T.; Miyaura, N. *J. Organomet. Chem.* **2006**, *691*, 4909–4917.

Since Stock's synthesis of borazine, an assortment of *BN* heteroarenes have been isolated and studied,[21,24] one of which is the azaborine—a *BN* heteroarene that serves as a hybrid between organic benzene (**1.8**) and inorganic borazine (**Figure 1.3**).[25] Varying in the arrangement of the boron and nitrogen atoms within the cyclic structure, three isomeric azaborine structures can exist: the 1,2-azaborine (**1.5**), the 1,3-azaborine (**1.6**), and the 1,4-azaborine (**1.7**), each differing in their reactivities and electronic properties.[26] This capability of the azaborine to undergo isomeric permutations exemplifies *BN*-*CC* isosterism as a viable strategy to generate molecular diversity and expand chemical space.

Figure 1.3 Azaborines as Hybrid Organic/Inorganic Heteroarenes[25–26]

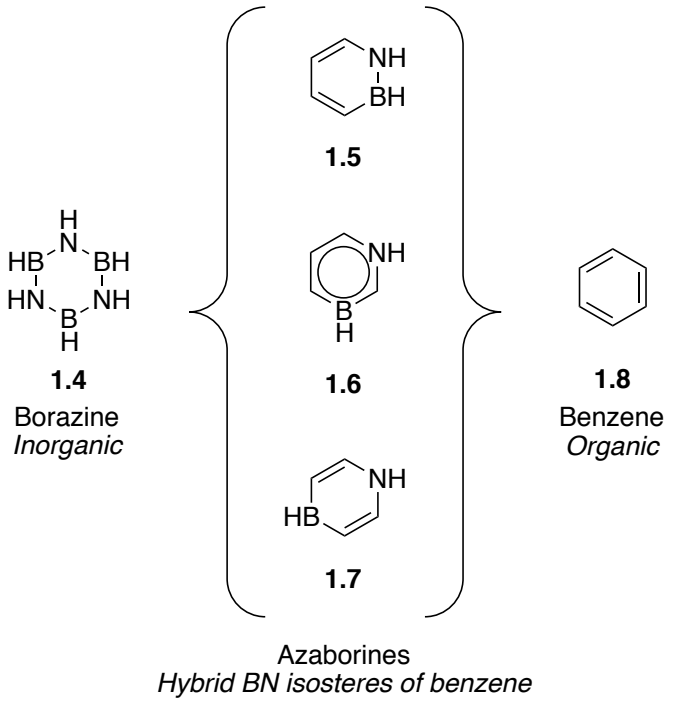

[24] (a) Wang, J.-Y.; Pei, J. *Chin. Chem. Lett.* **2016**, *27*, 1139−1146; (b) Wang, X.-Y.; Wang, J.-Y.; Pei, J. *Chem. Eur. J.* **2015**, *21*, 3528−3539; (c) Wang, S.; Yang, D.-T.; Lu, J.; Shimogawa, H.; Gong, S.; Wang, X.; Mellerup, S. K.; Wakamiya, A.; Chang, Y.-L.; Yang, C.; Lu, Z. H. *Angew. Chem. Int. Ed.* **2015**, *54*, 15074−15078; (d) Yang, D.-T.; Shi, Y.; Peng, T.; Wang, S. *Organmetallics* **2017**, *36*, 2654–2660.

[25] Marwitz, A. J. V.; Matus, M. H.; Zakharov, L. N.; Dixon, D. A.; Liu, S.-Y. *Angew. Chem. Int. Ed.* **2009**, *48*, 973–977.

[26] Giustra, Z. X.; Liu, S.-Y. *J. Am. Chem. Soc.* **2018**, *140*, 1184−1194.

When considering its likeness to the omnipresent benzene moiety, the monocyclic 1,2-azaborine has drawn significant attention in both pure and applied chemistry as an innovative arene mimic.[27] Though the pioneering work on 1,2-azaborines was completed by Dewar[28] and White,[29] a breakthrough in this area of research came from contributions by Ashe[30] and Liu.[25,31] Ashe's synthesis of *N*-Et, *B*-Ph 1,2-azaborine (**1.14**) featured a ring-closing metathesis strategy and allowed for the construction of the cyclic 1,2-azaborine core in five steps (**Scheme 1.1**).

Scheme 1.1 Ashe's Synthesis of *N*-Et, *B*-Ph 1,2-Azaborine[30d]

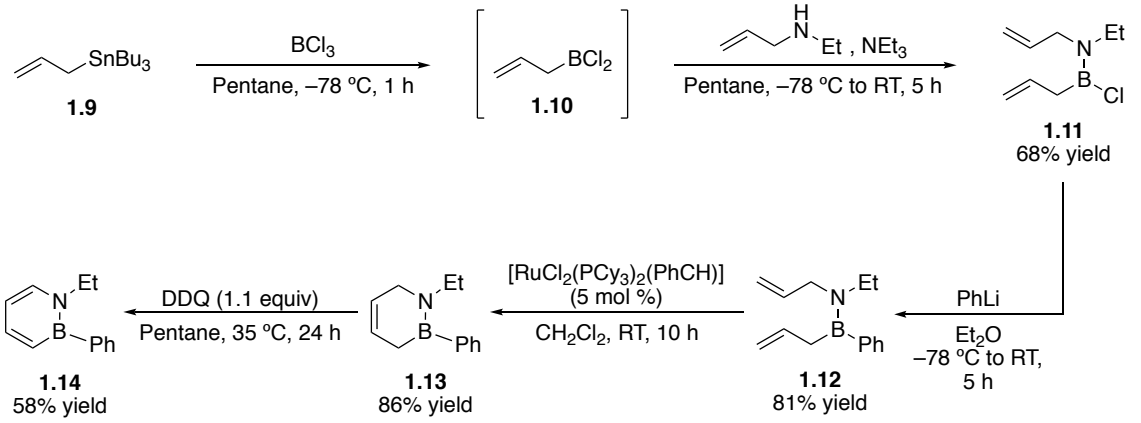

To this end, allyltributyltin (**1.9**) was reacted with boron trichloride to generate allylboron dichloride (**1.10**) *in situ*. Treatment of this species with ethyl allylamine in the presence of triethylamine formed the key *B–N* bond and generated **1.11**, which could then

[27] (a) Liu, L.; Marwitz, A. J. V.; Matthews, B. W.; Liu, S.-Y. *Angew. Chem. Int. Ed.* **2009**, *48*, 6817–6819; (b) Lamm, A. N.; Liu, S.-Y. *Mol. Biosyst.* **2009**, *5*, 1303–1305.
[28] (a) Davies, K. M.; Dewar, M. J. S.; Rona, P. *J. Am. Chem. Soc.* **1967**, *89*, 6294−6297; (b) Culling, G. C.; Dewar, M. J. S.; Marr, P. A. *J. Am. Chem. Soc.* **1964**, *86*, 1125−1127; (c) Dewar, M. J. S.; Kubba, V. P.; Pettit, R. *J. Chem. Soc.* **1958**, 3073–3076.
[29] White, D. G. *J. Am. Chem. Soc.* **1963**, *85*, 3643–3636.
[30] (a) Ashe, A. J., III. *Organometallics* **2009**, *28*, 4236−4248; (b) Pan, J.; Kampf, J. W.; Ashe, A. J., III *J. Organomet. Chem.* **2009**, *694*, 1036−1040; (c) Pan, J.; Kampf, J. W.; Ashe, A. J., III *Organometallics* **2009**, *28*, 506−511; (d) Ashe, A. J., III; Fang, X. *Org. Lett*. **2000**, *2*, 2089–2091.
[31] Marwitz, A. J. V.; Abbey, E. R.; Jenkins, J. T.; Zakharov, L. N.; Liu, S.-Y. *Org. Lett.* **2007**, *9*, 4905–4908.

undergo boron-substitution using phenyllithium to yield adduct **1.12**. The six-membered heterocycle **1.13** was then generated through ring-closing metathesis using Grubb's first-generation catalyst. Lastly, oxidation using DDQ afforded the substituted *N*-Et, *B*-Ph 1,2-azaborine.

Subsequently, Liu reported the synthesis of *N*-TBS, *B*-Cl 1,2-azaborine using a modified version of Ashe's synthetic sequence (**Scheme 1.2**). In addition to shortening the synthetic route to monocyclic azaborines, Liu's synthesis also allowed for the elaboration of the cyclic azaborine core through late-stage functionalization at the boron and nitrogen positions, paving the way for molecular diversity through *BN*-*CC* isosterism.

Scheme 1.2 Liu's Synthesis of *N*-TBS, *B*-Cl 1,2-Azaborine[25]

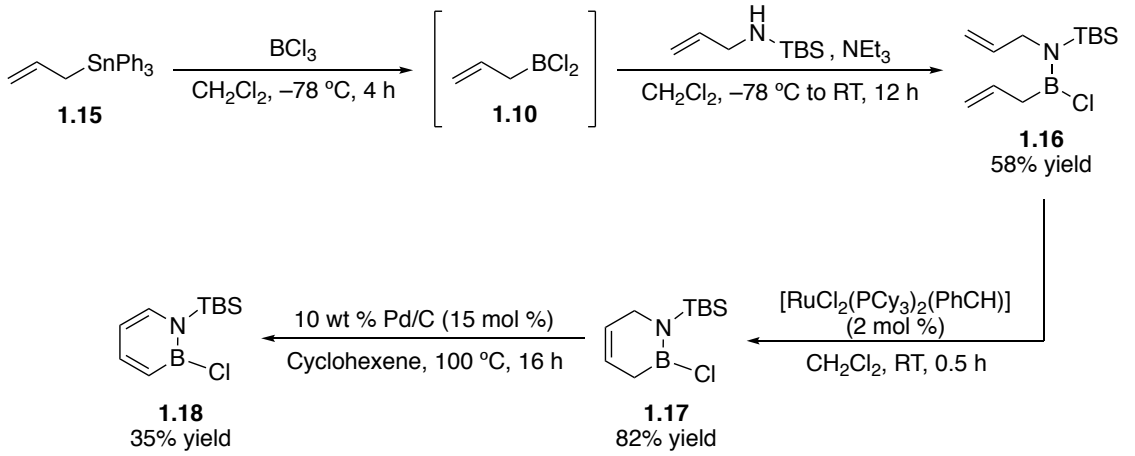

Advancements in *BN*-heteroarene synthesis—like those made by Ashe and Liu—have made these heterocycles drastically more accessible to synthetic chemists. Increased accessibility of these compounds has resulted in a surge of interest in these boron-, nitrogen-, and carbon-containing molecules, and has established *BN*-*CC* isosterism as a new frontier for chemists. Further development of azaborine chemistry—particularly the 1,2 isomer—has the potential to change the way chemists approach chemical diversity and

elaborate upon the themes of isosterism and bioisosterism.[32] Thus, a strong need persists for new functionalization methods to expand the potential applications of the 1,2-azaborine. This work describes methodology aimed at achieving late-stage functionalization of *B*-aryl and *B*-alkyl 1,2-azaborines, as well as the application of these compounds as reagents in organic synthesis and catalysis.

[32] McConnell, C. R.; Liu, S.-Y. *Chem. Soc. Rev.* **2019**, *48*, 3436–3453.

1.2 Aryl and Alkyl Migration Reactions of Brominated *BN*-Heterocycles

1.2.1 Background

Preceding the advances made by Ashe and Liu, the functionalization of monocyclic 1,2-azaborines was limited to substituents that were installed prior to the formation of the cyclic core.[33] Upon the development of these new protocols, methods for the late-stage functionalization of the azaborine core began to arise (**Scheme 1.3**).

Scheme 1.3 Selected Late-stage Functionalizations of the 1,2-Azaborine Core[34–36]

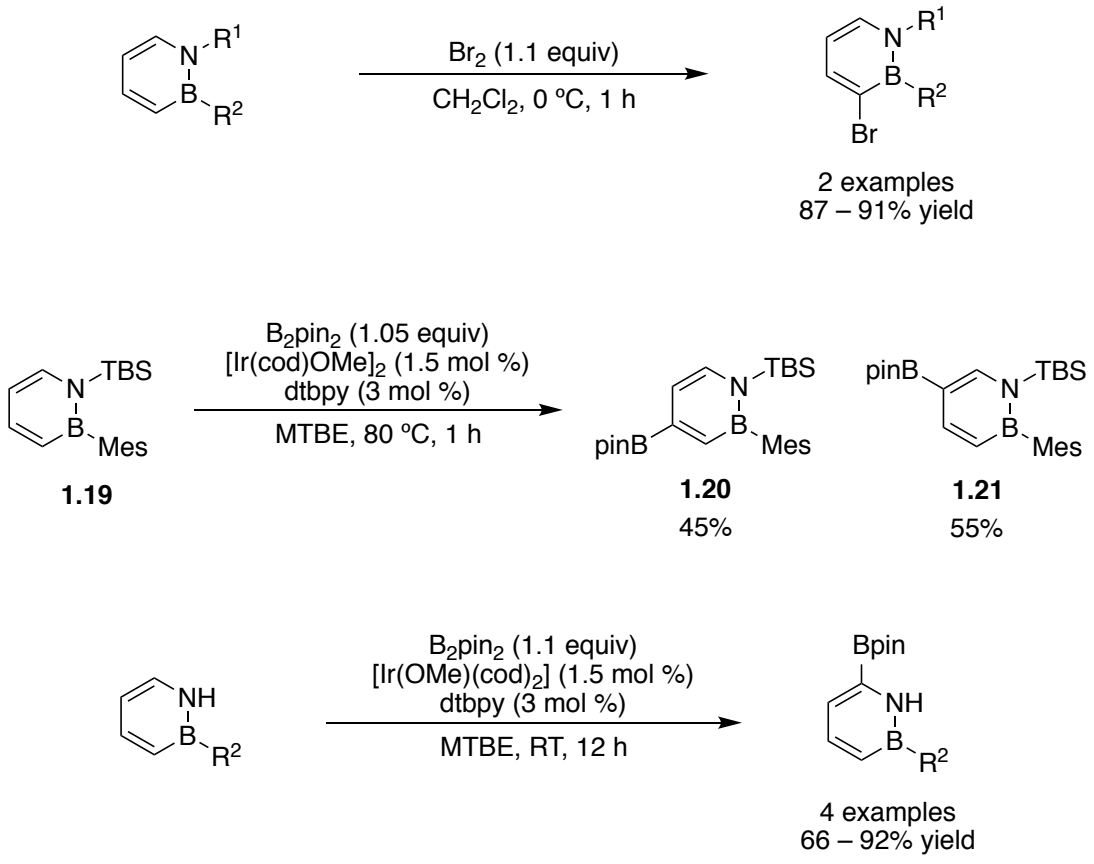

[33] Dewar, M. J. S.; Marr, P. A. *J. Am. Chem. Soc.* **1962**, *84*, 3782.

Of these synthetic methods, *C*3-electrophilic aromatic substitution,[34] *C*4/*C*5-borylation,[35] and *C*6-borylation[36] emerged as modifications that introduce synthetic handles at the azaborine's carbon positions. Furthermore, these synthetic methods allow for further functionalization of the azaborine using well-established methodologies, such as Negishi[37] and Suzuki-Miyaura[36] cross-coupling (**Scheme 1.4**).

Scheme 1.4 Examples of Metal-Catalyzed Functionalizations of 1,2-Azaborines[36–37]

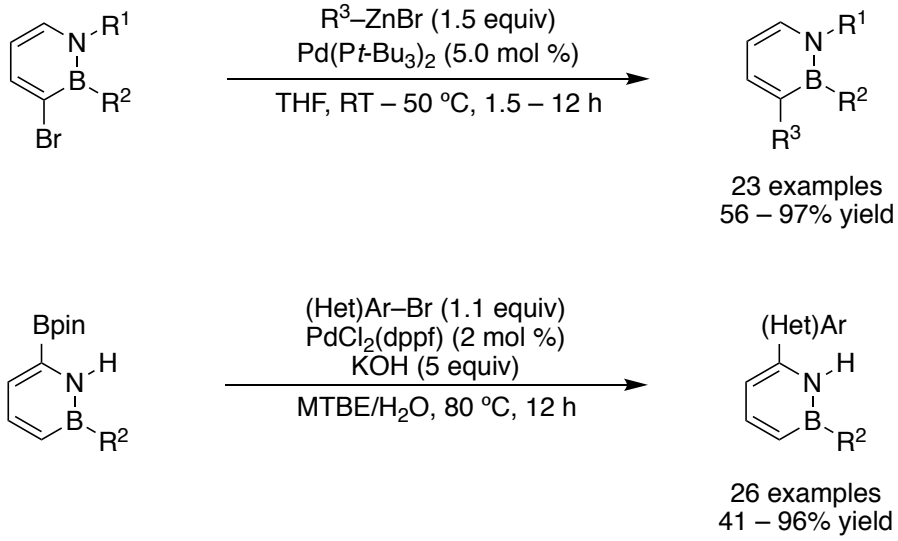

With regard to heteroatomic functionalization, electrophilic and nucleophilic substitution, respectively, allowed for late-stage *B*- and *N*- substitution of 1,2-dihydro-1,2-azaborines (**Scheme 1.5**).[38]

[34] Pan, J.; Kampf, J. K.; Ashe, A. J., III *Org. Lett.* **2007**, *9*, 679–681.
[35] McConnell, C. R.; Haeffner, F.; Baggett, A. W.; Liu, S.-Y. *J. Am. Chem. Soc.* **2019**, *141*, 9072–9078.
[36] Baggett, A. W.; Vasiliu, M.; Li, B.; Dixon, D. A.; Liu, S.-Y. *J. Am. Chem. Soc.* **2015**, *137*, 5536–5541.
[37] (a) Brown, A. N.; Li, B.; Liu, S.-Y. *Tetrahedron* **2019**, *75*, 580–583; (b) Brown, A. N.; Li, B.; Liu, S.-Y. *J. Am. Chem. Soc.* **2015**, *137*, 8932–8935.
[38] Lamm, A. N.; Garner, E. B.; Dixon, D. A.; Liu, S.-Y. *Angew. Chem. Int. Ed.* **2011**, *50*, 8157–8160.

Scheme 1.5 Modular Heteroatomic Reactivity of 1,2-Azaborines[38]

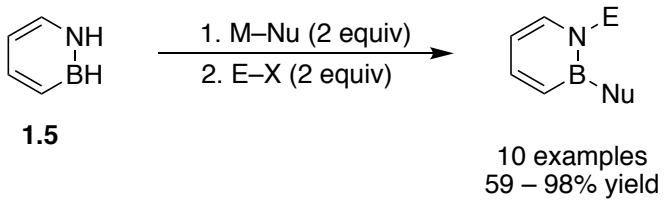

1.5

10 examples
59 – 98% yield

Following Liu's development of an *N*-TBS, *B*-Cl azaborine synthesis protocol, late-stage functionalization of the azaborine's nitrogen and boron positions became much more facile. For example, the rhodium-catalyzed coupling of azaborines with arylstannanes allows for the synthesis of 1,2-azaborine-based biaryl systems that contain a variety of functional groups (**Scheme 1.6**).[39]

Scheme 1.6 Rhodium-Catalyzed Coupling of 1,2-Azaborines with Arylstannanes[39]

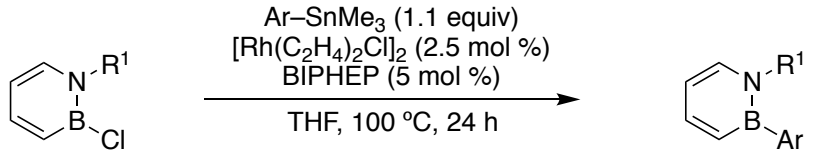

12 examples
40 – 81% yield

In addition to serving as a method for the functionalization of 1,2-azaborines, this cross-coupling protocol raises questions about the ability of *BN*-heterocycles to participate in other metal-catalyzed coupling reactions[40]—in particular—do *BN*-heterocycles have the potential to act as transmetalating reagents in Suzuki-Miyaura coupling reactions?

[39] Rudebusch, G. E.; Zakharov, L. N.; Liu, S.-Y. *Angew. Chem. Int. Ed.* **2013**, *52*, 9316–9319.
[40] (a) Seechurn, C. C. C. J.; Kitching, M. O.; Colacot, T. J.; Snieckus, V. *Angew. Chem. Int. Ed.* **2012**, *51*, 5062–5085; (b) Biffis, A.; Centomo, P.; Del Zotto, A.; Zecca, M. *Chem. Rev.* **2018**, *118*, 2249–2295.

1.2.2 An Overview of Transmetalation in Suzuki-Miyaura Cross-Coupling

Among the wide variety of reactions that feature organoboron reagents, few synthetic strategies match the power and versatility of Suzuki-Miyaura cross-coupling.[41] Since its inception in 1979, the Suzuki-Miyaura reaction has stood as a predominant method for the formation of carbon–carbon bonds,[42] owing to its synthetic efficacy, as well as the accessibility and mild nature of the required organoboron reagents.[43] Since initial reports, technological improvements in the design of novel ligands,[44] unique catalysts,[45] and effective directing groups,[46] have greatly expanded the scope of Suzuki-Miyaura coupling to encompass diverse and highly-functionalized systems.

Generally, the mechanism of Suzuki-Miyaura coupling is comparable to that of other palladium-catalyzed coupling reactions and features three key steps: oxidative addition, transmetalation, and reductive elimination (**Scheme 1.7**).[47] Unique to Suzuki–Miyaura cross-coupling, transmetalation occurs when organic moieties migrate from the organoboron reagent onto the palladium catalyst.

---

[41] (a) Miyaura, N.; Suzuki, A. *Chem. Rev*. **1995**, *95*, 2457−2483; (b) Miyaura, N.; Yamada, K.; Suzuki, A. *Tetrahedron Lett.* **1979**, *20*, 3437−3440.
[42] Brown, D. G.; Boström, J. *J. Med. Chem.* **2016**, *59,* 4443–4458.
[43] Fyfe, J. W. B.; Watson, A. J. B. *Chem*, **2017**, *3*, 31–55.
[44] (a) Tolman, C. *Chem. Rev.* **1977**, *77*, 313–348; (b) Martin, R.; Buchwald, S. L. *Accounts Chem. Res.* **2008**, *41*, 1461–1473; (c) Peris, E. *Chem. Rev.* **2018**, *118*, 9988−10031.
[45] (a) Guram, A. S.; Wang, X.; Bunel, E. E.; Faul, M. M.; Larsen, R. D.; Martinelli, M. J. *J. Org. Chem.* **2007**, *72*, 5104–5112; (b) Rosen, B. M.; Quasdorf, K. W.; Wilson, D. A.; Zhang, N.; Resmerita, A.-M.; Garg, N. K.; Percec, V. *Chem. Rev*. **2011**, *111*, 1346–1416.
[46] (a) Rousseau, G.; Breit, B. *Angew. Chem. Int. Ed.* **2011**, *50*, 2450–2494; (b) Wilsily, A.; Tramutola, F.; Owston, N. A.; Fu, G. C. *J. Am. Chem. Soc.* **2012**, *134*, 5794−5797.
[47] Lennox, A. J. J.; Lloyd-Jones, G. C. *Chem. Soc. Rev.* **2014**, *43*, 412–443.

Scheme 1.7 A Generic Mechanism for Suzuki-Miyaura Cross-Coupling[47]

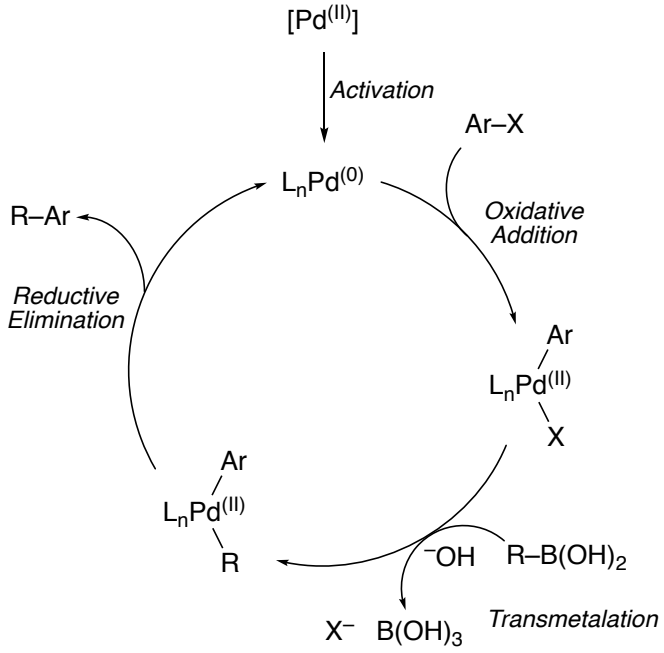

Under Suzuki-Miyaura conditions, transmetalation can occur through two different pathways—the boronate or the oxo-palladium pathway—depending on the organoboron species employed.[48] With Lewis acidic boranes, such as alkylboranes, the boron center is more prone to accepting electron pairs from the present base. As a result, these organoboron reagents tend to form boranate complexes, which then readily transmetalate through the boronate pathway (**Scheme 1.8** equation 1).[49] Conversely, reagents such as alkylboronic esters are prone to reacting through the oxo-palladium pathway (**Scheme 1.8** equation 2). These reagents are less likely to undergo complexation with hydroxy and alkoxy bases; rather, complexation occurs between the base and the palladium catalyst—forming an oxo-palladium species. This oxo-palladium complex then undergoes coordination to the organoboron species, which is followed by transmetalation.[50]

[48] Lennox, A. J. J.; Lloyd-Jones. G. C. *Angew. Chem. Int. Ed.* **2013**, *52*, 7362–7370.
[49] Matos, K.; Soderquist, J. A. *J. Org. Chem.* **1998**, *63*, 461–470.
[50] Miyaura, N.; Yamada, K.; Suginome, H.; Suzuki, A. *J. Am. Chem. Soc.* **1985**, *107*, 972–980.

Scheme 1.8 Boronate (1) and Oxo-Palladium (2) Pathways of Suzuki-Miyaura Transmetalation[48–50]

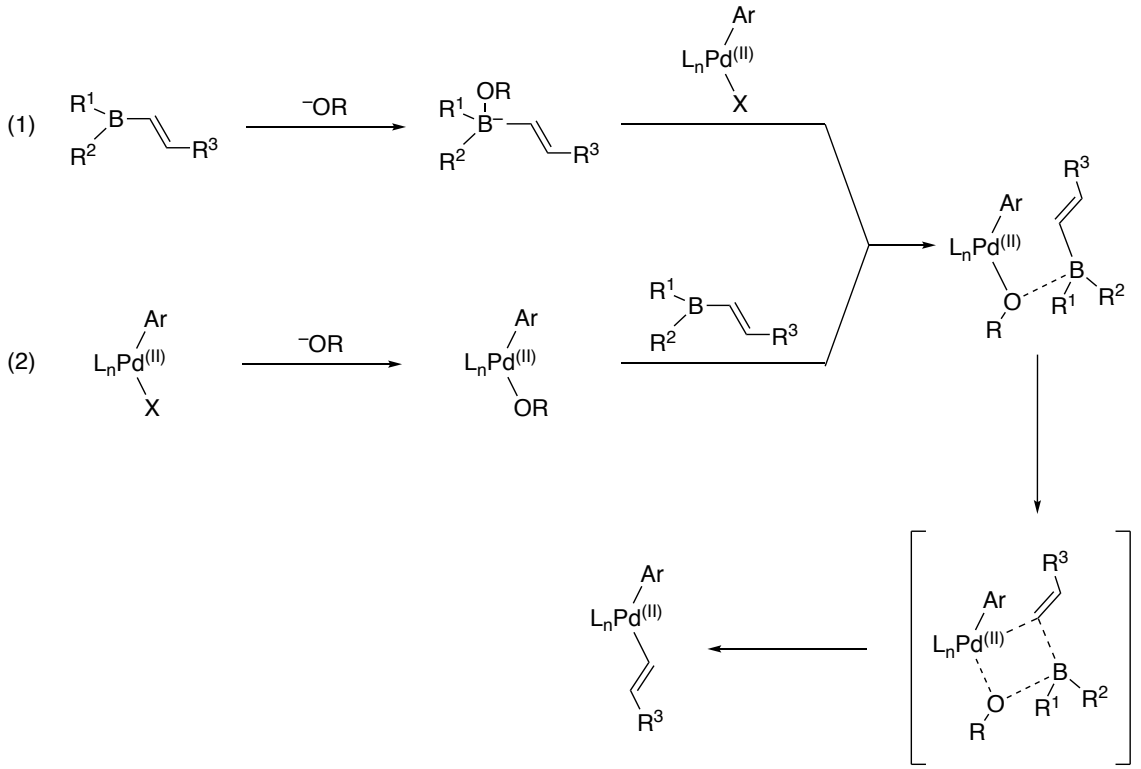

The contrast in transmetalating behaviors of different organoboron species serves as an incentive to investigate the transmetalating abilities of various boron-containing substrates, such as 1,2-azaborines. In addition to shedding light on the properties and reactivities of *BN*-heteroarenes, studying the transmetalating abilities of azaborines may provide further insight into the transmetalation of organometallic species.

To date, *BN*-heterocycles have not been employed as substitutes for organoboron reagents in intermolecular Suzuki-Miyaura cross-coupling reactions. Successfully implementing *BN*-heterocycles in this fashion would not only introduce another strategy to employ azaborines, but also has the potential to unlock Suzuki-Miyaura reactivity that has not been reported using classical organoboron reagents.

1.2.3 Self-Arylation and Self-Alkylation Reactions of 1,2-Azaborines

Molander and co-workers have demonstrated that brominated 1,2-borazaronaphthalenes, *BN*-analogues of naphthalene, are capable of undergoing self-arylation in the presence of base and palladium catalyst (**Scheme 1.9**).[51] Under these Suzuki-Miyaura conditions, borazaronaphthalene substrates serve as both nucleophiles and electrophiles. The migrating aryl substituent is able to displace the bromine substituent at the *C*3 position, resulting in the formation of either a *B–OH* linkage, or a mixture of the boronic acid and borazaronaphthalene dimer.

Scheme 1.9 Self-Arylation of *B*-Aryl, *C*3-Bromo Borazaronaphthalenes[51]

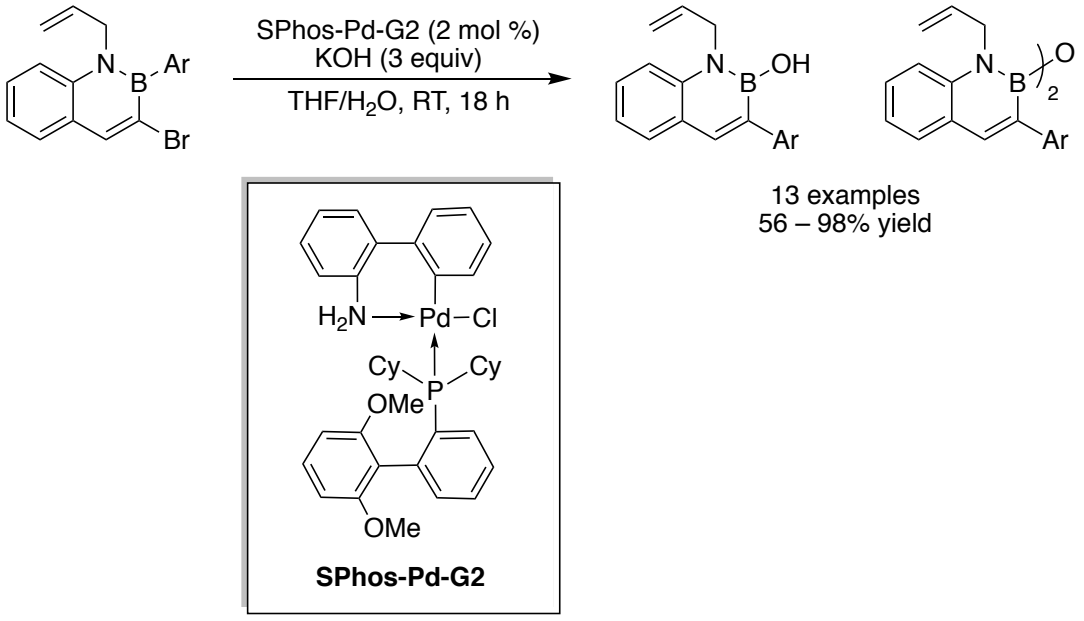

To probe the mechanism of this transformation, the Molander group conducted a double crossover experiment using borazaronaphthalene substrates **1.22** and **1.23**. The formation of four distinct arylated species (**1.24**–**1.27**) suggests that the self-arylation

[51] Molander, G. A.; Wisniewski, S. R. *J. Org. Chem*. **2014**, *79*, 8339–8347.

reaction actually occurs in an intermolecular fashion (**Scheme 1.10**). By demonstrating the borazaronaphthalenes' ability to transmetalate, this study serves as promising evidence that *BN*-arenes can behave similarly to their classical organoboron counterparts, despite possessing distinctively different electronic profiles.

Scheme 1.10 Mechanistic Probe of Borazaronaphthalene Self-Arylation[51]

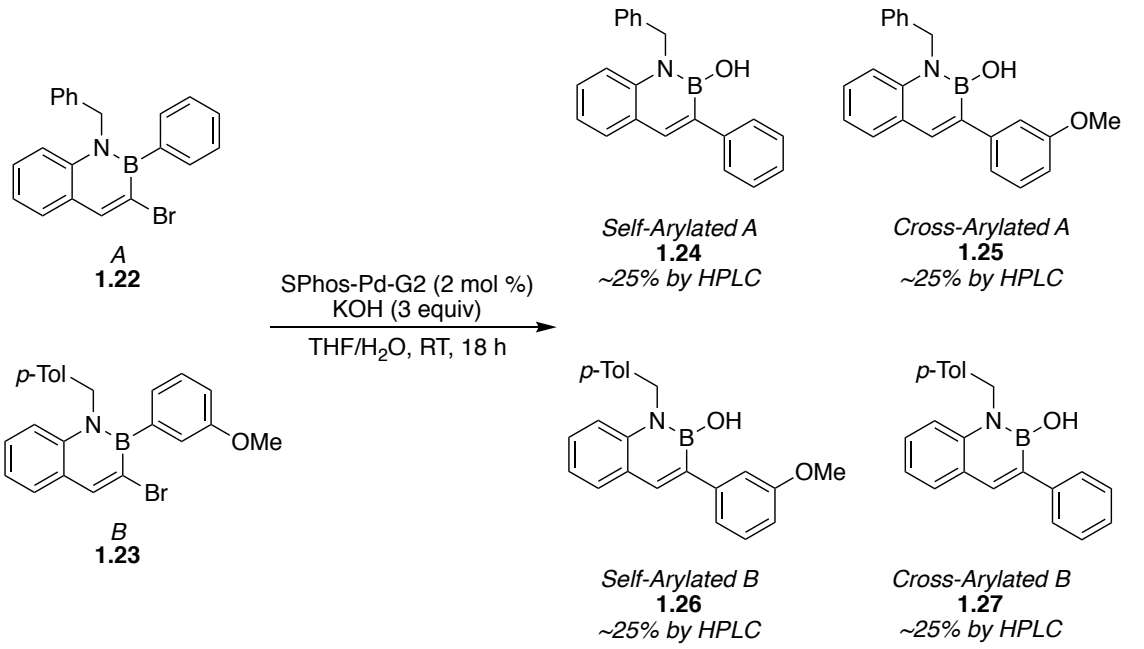

Inspired by these results, as well as our group's previous work on rhodium-catalyzed arylations,[39] we envisioned that 1,2-azaborines could exhibit similar reactivity. We proposed that these heteroarenes could be used as transmetalating reagents in Suzuki-Miyaura cross-coupling reactions, and set out to investigate this potential application of *BN*-*CC* isosterism.

Taking Molander's studies into consideration, our investigation into the transmetalating abilities of 1,2-azaborines began by looking at the ability of *C*3-brominated 1,2-azaborines to undergo self-arylation and self-alkylation reactions. More specifically,

we sought to develop a palladium-catalyzed migration reaction for the synthesis of *C*3-aryl and *C*3-alkyl 1,2-azaborines from brominated *BN*-synthons.

Using previously-developed methodology, the synthesis of substituted *N*-TBS, *B*-R^2, *C*3-bromo 1,2-azaborines could be achieved in three steps from the commercially-available *N*-TBS, *B*-Cl 1,2-azaborine (**1.18**) (**Scheme 1.11**)[25,37]. Following bromination of the *C*3 position with molecular bromine, the *N*-TBS, *B*-Cl, *C*3-bromo azaborine (**1.28**) is susceptible to nucleophilic attack at boron by Grignard and organolithium reagents.

Scheme 1.11 Synthetic Route to *N*-TBS, *B*-R^2, *C*3-Bromo 1,2-Azaborines Followed by Proposed Migration Strategy

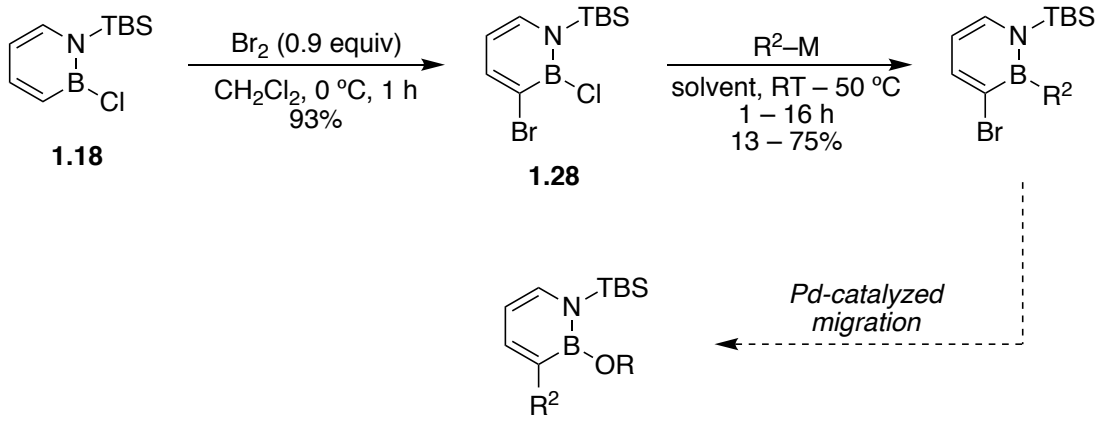

With this general method, a variety of different *B*-aryl and *B*-alkyl azaborines were synthesized. With these azaborines in hand, we could begin testing conditions for the migration of aryl and alkyl groups from boron to *C*3 (**Table 1.3**). Previous reports from our lab indicated that phenyl substituents were able to migrate in the presence of tris(dibenzylideneacetone)dipalladium(0), QPhos, and sodium *tert*-butoxide (entry 1).[52] Upon further investigation, these conditions also allowed for the migration of alkyl moieties (entries 3–4), a reaction that was not possible with Molander's

[52] Lee, H. "Site-Selective Reactions Via Scaffolding Catalysis & Synthesis and Binding Study of 1,2-azaborines" (Doctoral Dissertation). Boston College, 2017, p 671.

borazaronaphthalene substrates. Notably, the *N*-TBS, *B*-Mes, *C*3-bromo 1,2-azaborine displayed no reactivity under these conditions, even for a prolonged period at elevated temperature (entry 2), likely due to interfering steric interactions.

Table 1.3 Self-Arylation and Self-Alkylation of *B*-R^2, *C*3-Bromo 1,2-Azaborines

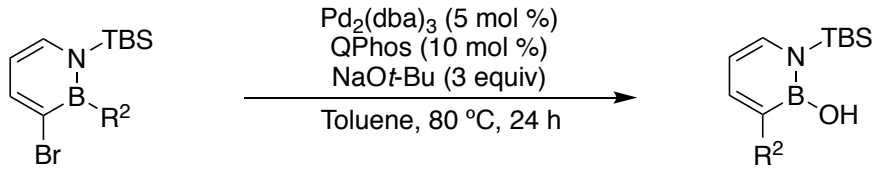

entry	R^2	starting material	product	yield (%)[a]
1	Ph	**1.29**	**1.33**	60[b]
2	Mes	**1.30**	**1.34**	0[c]
3	Et	**1.31**	**1.35**	79
4	*i*-Pr	**1.32**	**1.36**	33

[a] isolated yield. [b] previously reported.[52] [c] no conversion of starting material observed after 48 h at 100° C.

In addition to serving as a novel method for the functionalization of *BN* heterocycles, these self-arylation and self-alkylation experiments served as proof of concept that the transmetalation of aryl and alkyl species from the azaborine's boron site is possible. Ultimately, these results encouraged the pursuit of reaction parameters that could allow for the development of 1,2-azaborines as unique transmetalating reagents.

1.3 Studies toward the Application of 1,2-Azaborines as Transmetalation Reagents in Suzuki-Miyaura Cross-Coupling Reactions

1.3.1 Background

While recent advances in synthetic methodology have reinforced the profound importance of Suzuki-Miyaura cross-coupling, this progress also highlights the lasting limitations of the reaction. The formation of $C(sp^3)$–$C(sp^2)$ bonds under Suzuki-Miyaura conditions, for example, remains largely underdeveloped compared to the construction of $C(sp^2)$–$C(sp^2)$ linkages.[53] Considering the widespread use of Suzuki-Miyaura cross-coupling in both academic and industrial settings, as well as the overabundance of flat, aromatic molecules in pharmaceutical libraries,[54] a facile and adaptable protocol for the coupling of stereogenic carbon centers would serve as an invaluable resource to the scientific community at large.

Within the last decade, significant efforts have been made to develop protocols for the coupling of $C(sp^3)$–$C(sp^2)$ centers;[55] however, stereospecific Suzuki-Miyaura cross-couplings remain underexplored and pose a number of challenges to researchers.[56] First, the sensitivity of Suzuki-Miyaura cross-coupling to steric factors favors transmetalation with primary alkyl boron reagents, whereas secondary alkyl boron reagents exhibit notably slower transmetalation. In the event of successful transmetalation, chiral alkyl-palladium

[53] St. Denis, J. D.; Scully, C. C. G.; Lee, F.; Yudin, A. K. *Org. Lett.* **2014**, *16*, 1338–1341.
[54] (a) Lovering, F.; Bikker, J.; Humblet, C. *J. Med. Chem.* **2009**, *52*, 6752–6756.
[55] Rygus, J. P. G.; Crudden, C. M. *J. Am. Chem. Soc.* **2017**, *139*, 18124-18137.
[56] (a) Cammidge, A. N.; Crépy, K. V. L. *Chem. Commun.* **2000**, 1723–1724; (b) Thompson, W. J.; Gaudino, J. *J. Org. Chem.* **1984**, *49*, 5237–5243.

complexes are still amenable to ß-hydride elimination and reinsertion, which can result in the racemization of stereogenic centers (**Scheme 1.12**).[57]

Scheme 1.12 Potential Racemization Pathway and Formation of Byproducts Using Chiral Alkyl-Palladium Complexes

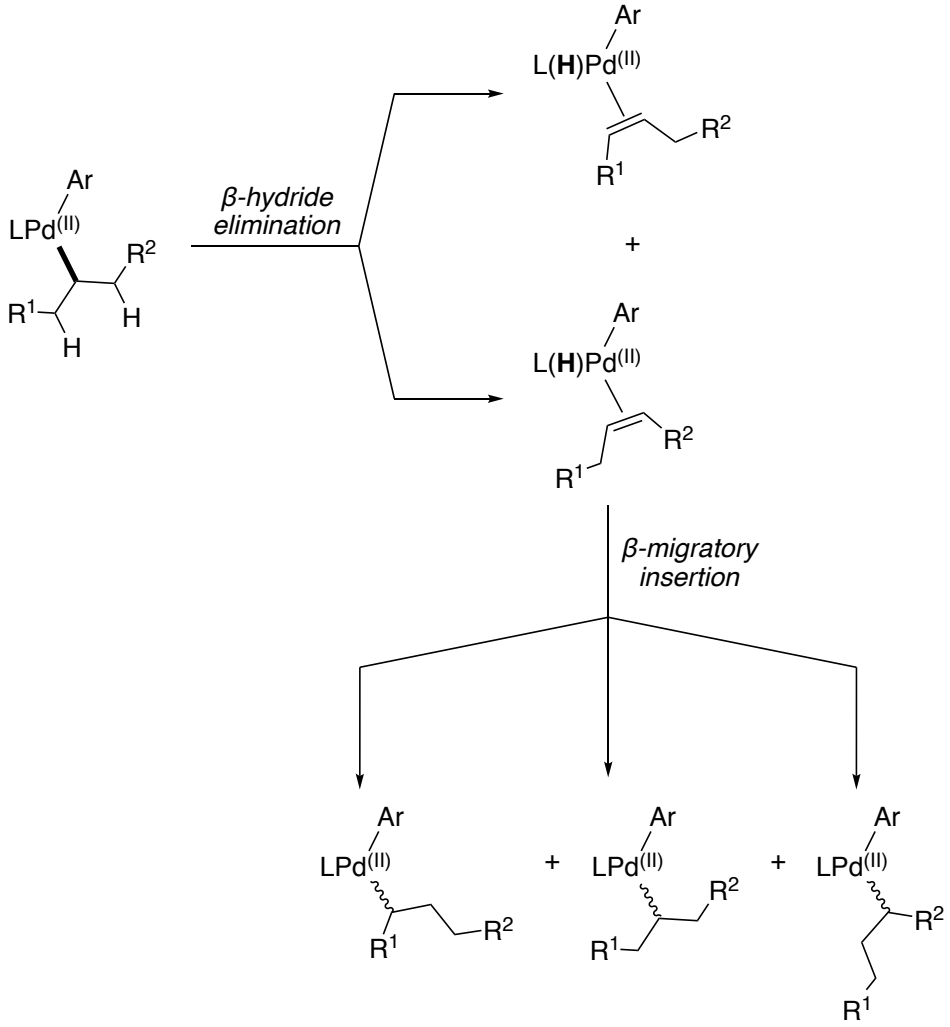

Though the factors affecting the mechanism of transmetalation with chiral substrates are still poorly understood, a number of procedures have been established for iterative enantiospecific Suzuki-Miyaura reactions—all but two examples of which rely on

[57] (a) Hartwig, J. F., *Organotransition Metal Chemistry: From Bonding to Catalysis*; University Science Books: Sausalito, 2010, p 349–416; (b) Dreher, S. P.; Dormer, P. G.; Sandrock, D. L.; Molander, G. A. *J. Am. Chem. Soc.* **2008**, *130*, 9257–9259.

the use of directing groups. The incorporation of directing groups adjacent to sites of transmetalation have shown to facilitate transmetalation (*vide infra)*, likely due to a weakening of the boron-carbon bond.[58] Moreover, the directing ability of these groups allows for control over the stereochemical outcome of the reaction.

Following advances in the syntheses of chiral boronic esters, boronic acids, and potassium trifluorborates as readily available reagents,[59] significant work has been done in the area of π-directed enantiospecific $C(sp^3)$–$C(sp^2)$ bond construction, primarily by the Crudden group (**Scheme 1.13**).[60] When cross-coupling reactions featuring chiral secondary organoboron reagents were investigated, sites with π-systems adjacent to the B–$C(sp^3)$ bond, such as benzylic and allylic positions, displayed notably faster rates of transmetalation.[60b] As a result, these Suzuki-Miyaura protocols could be used for the synthesis of diarylethanes and triarylmethanes with an effective transfer of chirality.

[58] (a) Imao, D.; Glasspoole, B. W.; Laberge, V. S.; Crudden, C. M. *J. Am. Chem. Soc*. **2009**, *131*, 5024−5025.
[59] (a) Littke, A. F.; Dai, C. Y.; Fu, G. C. *J. Am. Chem. Soc.* **2000**, *122*, 4020−4028; (b) Dreher, S. D.; Dormer, P. G.; Sandrock, D. L.; Molander, G. A. *J. Am. Chem. Soc.* **2008**, *130*, 9257−9259; (c) van den Hoogenband, A.; Lange, J. H. M.; Terpstra, J. W.; Koch, M.; Visser, G. M.; Visser, M.; Korstanje, T. J.; Jastrzebski, J. T. B. H. *Tetrahedron Lett.* **2008**, *49*, 4122–4124.
[60] (a) Glasspoole, B. W.; Ghozati, K.; Moir, J.; Crudden, C. M. *Chem. Commun*. **2012**, *48*, 1230−1232; (b) Matthew, S. C.; Glasspoole, B. W.; Eisenberger, P.; Crudden, C. M. *J. Am. Chem. Soc.* **2014**, *136*, 5828–5831. (c) Partridge, B. M.; Chausset-Boissarie, L.; Burns, M.; Pulis, A. P.; Aggarwal, V. K. *Angew. Chem. Int. Ed.* **2012**, *51*, 11795−11799; (d) Molander, G. A.; Wisniewski, S. R. *J. Am. Chem. Soc.* **2012**, *134*, 16856−16868; (e) Lou, Y.; Cao, P.; Jia, T.; Zhang, Y.; Wang, M.; Liao, J. *Angew. Chem. Int. Ed.* **2015**, *54*, 12134–12138.

Scheme 1.13 Enantiospecific π-Directed Couplings of Secondary Organoboron Reagents[60]

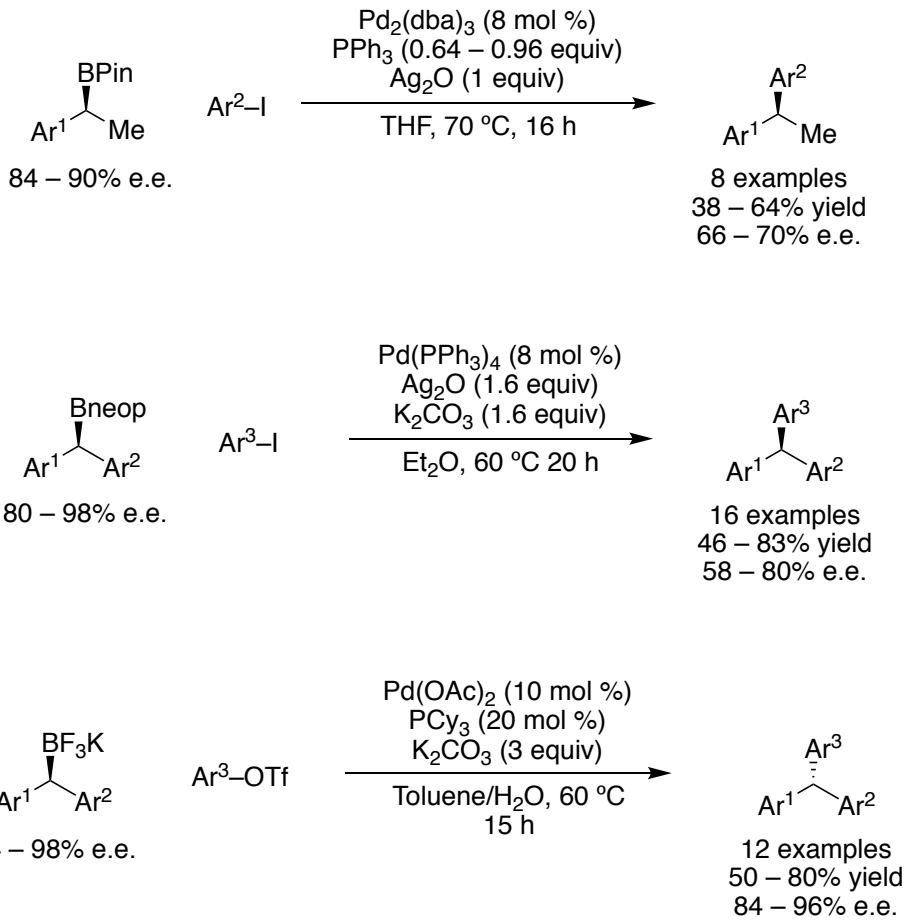

For the coupling of some benzylic chiral organoboron reagents (**1.37**) with aryl iodides, the reaction stalls in the absence of silver (I) oxide. Based on prior work by Kishi,[61] it is proposed that silver may facilitate the transmetalation step by complexation to adjacent π-systems present in transmetalating agents (**Figure 1.4**).

[61] Uenishi, J.-i.; Beau, J. M.; Armstrong, R. W.; Kishi, Y. *J. Am. Chem. Soc.* **1987,** *109*, 4756–4758.

Figure 1.4 Proposed Silver Oxide Effect on π-Directed Couplings[55,61]

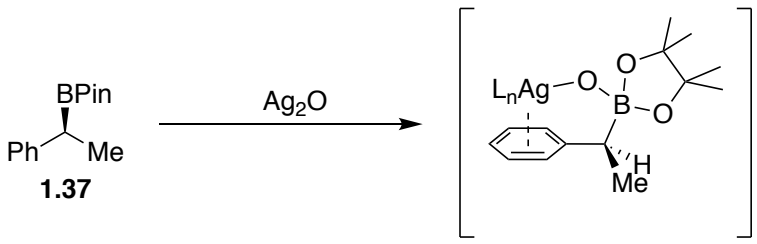

Similarly, proximal carbonyl substituents have been shown to engage in Lewis acid-base interactions that also aid transmetalation within secondary alkyl boron compounds. For example, chiral borates and boronic esters have been shown to participate in stereospecific cross-coupling reactions with amide- and ester-containing substrates, furnishing arylated products in both high yield and high enantiospecificity (**Scheme 1.14**).[62]

[62] (a) Ohmura, T.; Awano, T.; Suginome, M. *Chem. Lett.* **2009**, *38*, 664−665; (b) Sandrock, D. L.; Jean-Geŕard, L.; Chen, C.-y.; Dreher, S. D.; Molander, G. A. *J. Am. Chem. Soc.* **2010**, *132*, 17108−17110.

Scheme 1.14 Selected Carbonyl-Directed Enantiospecific Cross-Couplings[62,63]

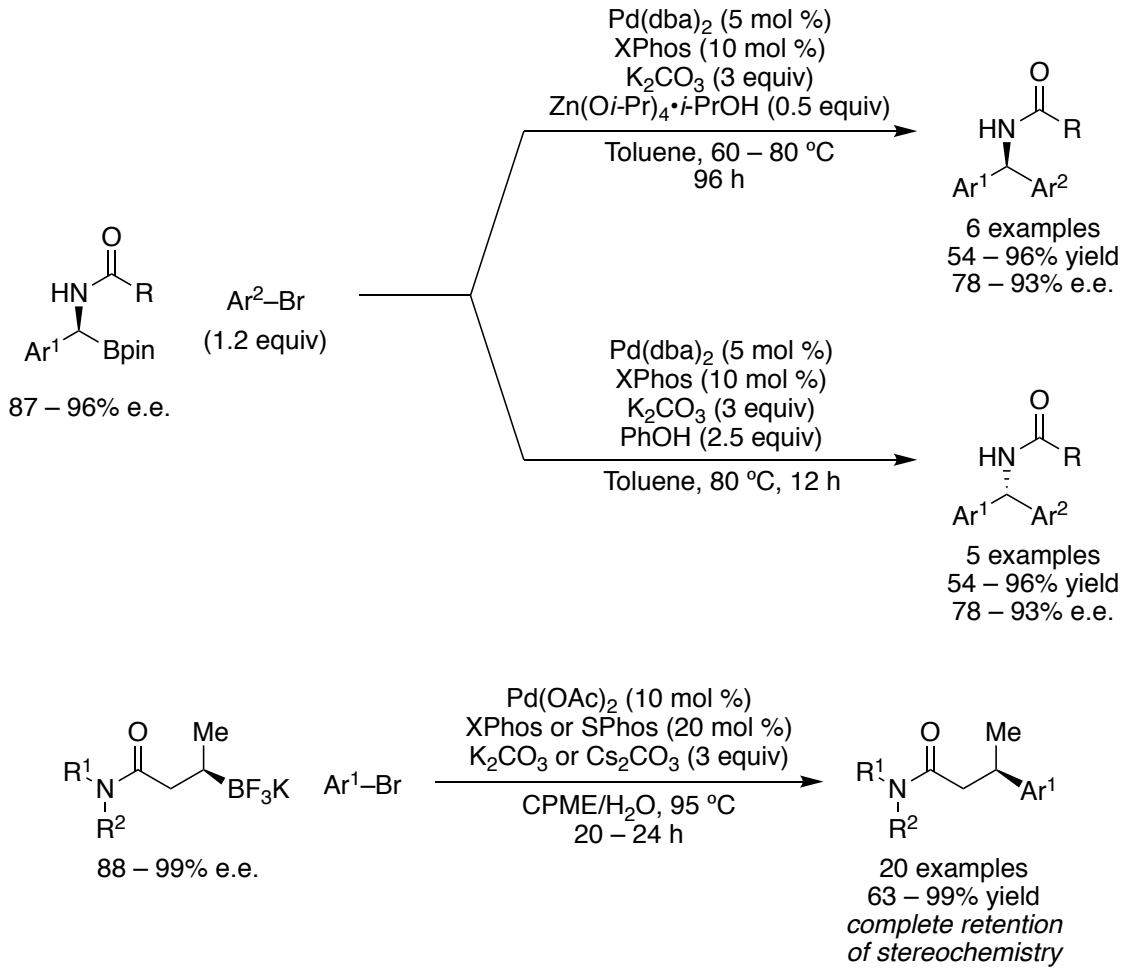

Notably, Ohmura and Suginome found that the presence of an acid additive was pivotal in determining whether stereochemistry was inverted or retained following these reaction sequences.[63] In addition, these cross-coupling reactions gave the best results when bulky groups, such as *tert*-butyl, were affixed to the carbonyl-containing species.

As demonstrated by the Morken group, hydroxyl groups are also capable of serving as internal activating groups for the enantiospecific coupling of secondary *C–B* centers with aryl and vinyl bromides (**Scheme 1.15**).[64] In particular, diborated substrates that

[63] Awano, T.; Ohmura, T.; Suginome, M. *J. Am. Chem. Soc.* **2011**, *133*, 20738–20741.
[64] Blaisdell, T. P.; Morken, J. P. *J. Am. Chem. Soc.* **2015**, *137*, 8712–8715.

contain free hydroxyl moieties β to the Bpin moieties were found to undergo stereoretentive cross-coupling exclusively at the secondary position. Additional studies concluded that the hydroxyl group is directly responsible for this unexpected reactivity.

Scheme 1.15 Hydroxyl-Directed Cross-Couplings by Morken[64]

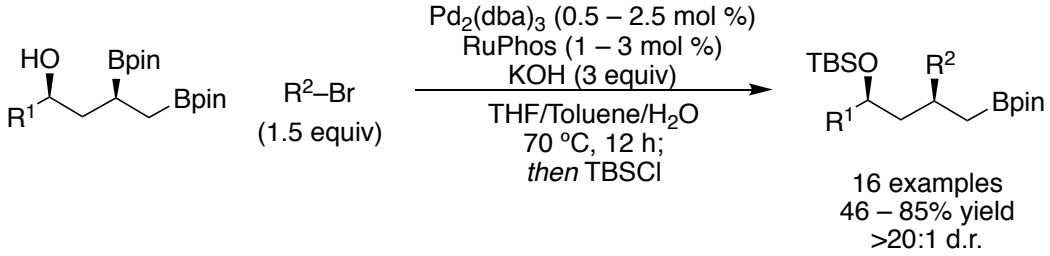

Although π-, carbonyl-, and hydroxyl-directed Suzuki-Miyaura reactions allow for the stereocontrolled construction of $C(sp^3)$–$C(sp^2)$ bonds, the reliance on specific, ancillary directing groups limits the broader application of these methods to other systems. To date, the only reports of stereospecific Suzuki-Miyaura cross-coupling reactions featuring nonactivated chiral secondary alkyl boron substrates come from the Biscoe group,[65] whose recent reports highlight stereodivergent Suzuki-Miyaura cross-coupling reactions. In this work, Biscoe demonstrates that sterically-demanding phosphine ligands are able to promote transmetalation and minimize the undesired isomerization of the active alkyl palladium species, selectively resulting in either retention or inversion of stereochemistry (**Scheme 1.16**).[66] More specifically, it was found that the electronic properties of the ligands dictate the stereochemical outcome of the transmetalation step—the use of

[65] For some of Biscoe's previous work on catalytic systems, see: (a) Wang, C.-Y.; Ralph, G.; Derosa, J.; Biscoe, M. R. *Angew. Chem. Int. Ed.* **2017**, *56*, 856–860; (b) Li, L.; Zhao, S.; Joshi-Pangu, A.; Diane, M.; Biscoe, M. R. *J. Am. Chem. Soc.* **2014**, *136*, 14027−14030; (c) Li, L.; Wang, C.-Y.; Huang, R.; Biscoe, M. R. *Nature Chemistry* **2013**, *5*, 607–612.

[66] (a) Zhao, S.; Gensch, T.; Murray, B.; Niemeyer, Z. L.; Sigman, M. S.; Biscoe, M. R. *Science* **2018**, *362*, 670–674.

electron-rich trialkylphosphines resulted in the inversion of stereochemistry, while electron-poor triarylphosphines promoted a stereoretentive reaction pathway. As an incipient display of non-directed, stereocontrollable cross-coupling, this study offers a promising result for future work in the field of enantioselective cross-coupling.

Scheme 1.16 Biscoe's Enantiodivergent Non-Directed Cross-Coupling of Aryl Halides and Aryl Triflates with Secondary Alkylboron Reagents[66]

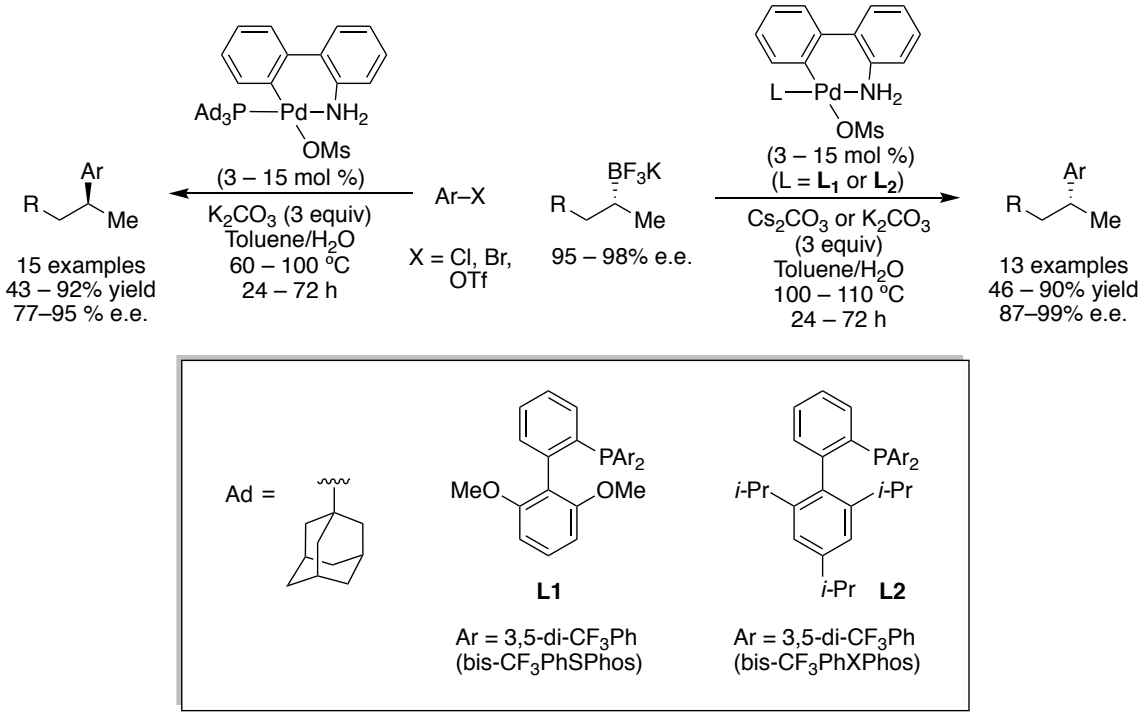

1.3.2 Survey of Conditions for the Arylation and Alkylation of Aryl Halides Using 1,2-Azaborines as Transmetalating Reagents

Evidenced by Biscoe's work, as well as earlier reports on asymmetric hydroboration,[67] minor modifications to boron-containing systems are capable of having large effects on the reactivities and stereochemical outcomes of encompassing reactions.[68] In the context of Suzuki-Miyaura coupling reactions, the characteristics of the 1,2-azaborine heterocycle offer potential advantages[69] when compared to other transmetalation-resistant organoboron reagents, such as secondary alkyl species.[55,56,60b] Most notably, the aromatic nature of the 1,2-azaborine provides the boron atom with an electron-rich environment, which may increase the nucleophilicity of organic boron substituents. Furthermore, we hypothesize that the aromatic backbone of the 1,2-azaborine may also be subject to Kishi's silver oxide effect[61] and engage in π interactions that increase the rate of transmetalation. In this vein, we sought to investigate the potential of *BN*-functionalized molecules to act as transmetalating reagents for Suzuki-Miyaura cross-coupling reactions.

The results from our previous migration studies indicate that 1,2-azaborines have the potential to transmetalate aryl, primary alkyl, and secondary alkyl substituents from boron onto halogen-substituted *C*(sp^2) centers—a result we sought to apply to cross-coupling reactions (**Scheme 1.17**). Overall, the goal of investigating this methodology was to probe the unique reactivity of *BN* heterocycles further and provide additional methods

[67] (a) Brown, H. C.; Zweifel, G. *J. Am. Chem. Soc.* **1961**, *83*, 486–487; (b) Zweifel, G.; Brown, H. C. *J. Am. Chem. Soc.* **1964**, *86*, 393–397; (c) Brown, H. C.; Desai, M. C.; Jadhav, P. K. *J. Org. Chem.* **1982**, *47*, 5065–5069.
[68] Sandford, C.; Aggarwal, V. K. *Chem. Commun.* **2017**, *53*, 5481–5494.
[69] Campbell, P. G.; Marwitz, A. J. V.; Liu, S.-Y. *Angew. Chem. Int. Ed.* **2012**, *51*, 6074–6092.

for azaborine functionalization, with the broader aim of contributing to the field of asymmetric catalysis.

Scheme 1.17 Potential Application of 1,2-Azaborines in Suzuki-Miyaura Cross-Coupling Reactions

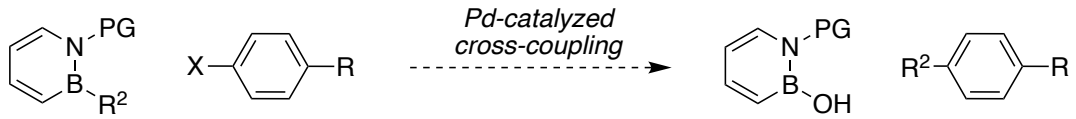

Our studies began by surveying conditions for the transfer of aryl and alkyl groups from the boron of *N*-TBS 1,2-azaborines to the halogen-substituted $C(sp^2)$ center of 4-bromotoluene and 4-iodotoluene. In the case of *N*-TBS, *B*-aryl 1,2-azaborines, no transmetalation was observed under the self-arylation/alkylation conditions previously employed, even after varying the electronic properties of the aryl substituent (**Scheme 1.18**). For each substrate, the dominant species detected by GC-MS were unreacted azaborine and 4,4'-dimethylbiphenyl (**1.41**) as the major byproduct—the result of homo-coupling between two molecules of 4-bromotoluene—indicative of sluggish or disfavored transmetalation.

Scheme 1.18 Cross-Arylation Studies of 4-Bromotoluene Using *N*-TBS, *B*-Aryl 1,2-Azaborines

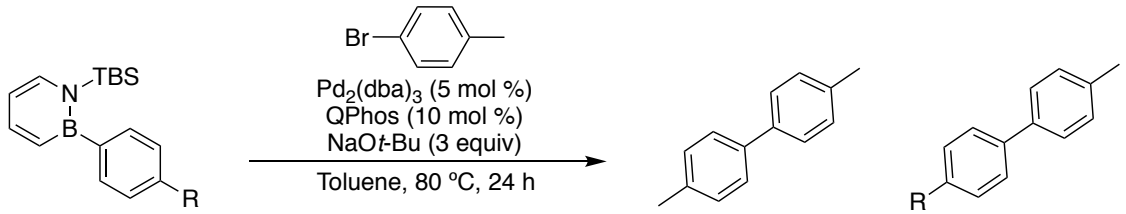

Primarily, we looked to assess our reaction parameters in an effort to promote transmetalation using secondary alkyl substrates; thus, reaction parameter screening was performed using *N*-TBS, *B*-*i*-Pr 1,2-azaborine (**1.42**) (**Table 1.4**). Our focus was to

establish a catalytic system that would allow for the coupling of symmetric secondary alkyl centers with sp^2-hybridized carbons, with the hope that this system could be later adapted and optimized for asymmetric substrates.

Table 1.4 Parameter Screen for the Cross-Coupling of *N*-TBS, *B*-*i*-Pr 1,2-Azaborine with 4-Halotoluene

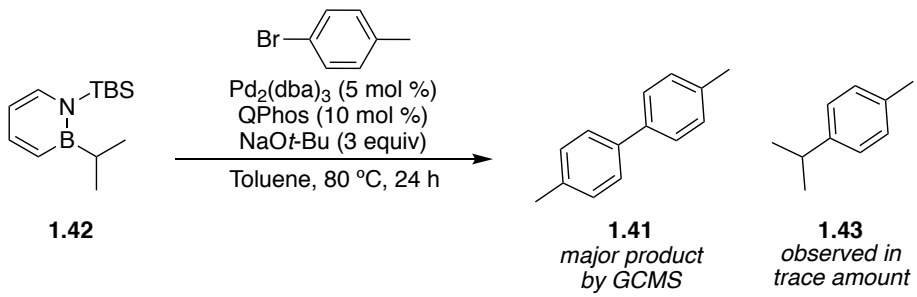

1.42 | **1.41** *major product by GCMS* | **1.43** *observed in trace amount*

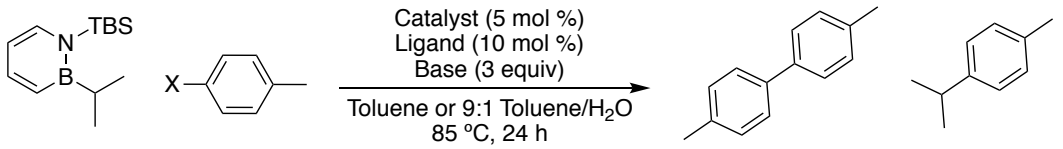

1.42 | X = Br or I | **1.41** *major product by GCMS* | **1.43** *observed in ≤ trace amount*

Reagents employed:

catalysts	ligands	bases
$Pd_2(dba)_3$	QPhos	Ag_2O
$Pd(dppf)Cl_2$	PPh_3	KOH
$Pd(OAc)_2$	XPhos	NaO*t*-Bu
$NiCl_2(PCy_3)_2$	dppp	Cs_2CO_3
$PdCl_2[P(o\text{-Tol})_3]_2$	dppb	K_3PO_4
SPhos-Pd-G2	JohnPhos	
	IPr	

Using our previous conditions, the cross-coupled product **1.43** was detected by GC-MS in trace amounts; however, despite surveying over 60 reaction conditions, varying in the metal catalysts, ligands, and bases employed, no more than a trace amount of desired

product was observed, with the major byproduct continuing to be the homo-coupled product **1.41**.

With regard to the substrates used, *N*-TBS 1,2-azaborines provided a valuable starting point for our investigation not only because of their relative molecular simplicity, but more so because of their modularity at the nitrogen position.[38] A set of diverse *N*-substituted azaborine products can be accessed, which enables the fine-tuning of the azaborine's steric and electronic properties as a cross-coupling partner.[21,26]

Considering the results of our previous studies, we suspected that steric interference from the bulky TBS protecting group could limit the azaborine's ability to interact with the metal catalyst. This notion of sterics playing a role in the transmetalating abilities of the azaborine is consistent with the observed inability of *N*-TBS, *B*-Mes, *C*3-bromo 1,2-azaborine to undergo self-arylation.

Thus, we began to look at the transmetalating abilities of 1,2-azaborines with reduced steric profiles compared to those previously studied. The first substrate used in these studies was *N*-TBS, *B*-Bn 1,2-azaborine (**1.44**)—a molecule that not only possesses reduced steric bulk around the boron center, but also is expected to undergo more facile transmetalation due to its inability to undergo β-hydride elimination.[70] Using this substrate, the desired cross-coupling product was detected by GC-MS, with the homo-coupled species persisting as a major byproduct (**Scheme 1.19**). The detection of cross-coupled

[70] (a) Crudden, C. M.; Ziebenhaus, C.; Rygus, J. P. G.; Ghozati, K.; Unsworth, P. J.; Nambo, M.; Voth, S.; Hutchinson, M.; Laberge, V. S.; Maekawa, Y.; Imao, D. *Nat. Commun.* **2016**, *7*, 11065; (b) Glasspoole, B. W.; Oderinde, M. S.; Moore, B. D.; Antoft-Finch, A.; Crudden, C. M. *Synthesis* **2013**, *45*, 1759–1763; (c) Farina, V.; Krishnamurthy, V.; Scott, W. J. in *Organic Reactions,* Vol. 50, John Wiley & Sons, Inc.: Hoboken, 1997.

product **1.45** validated our hypothesis that 1,2-azaborines have the potential to serve as transmetalating reagents in cross-coupling reactions.

Scheme 1.19 Successful Benzyl Migration Using *N*-TBS, *B*-Bn 1,2-Azaborine

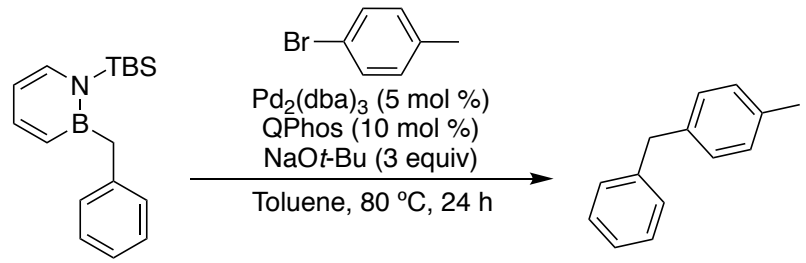

1.44 **1.45** *detected by GCMS*

Following this result, we sought to employ a modified 1,2-azaborine scaffold in our cross-coupling studies. As previously described, methodology has been established for the functionalization of the 1,2-azaborine at each position, which enables the modification of the azaborine's steric and electronic properties.[71] Aiming to reduce the steric profile of our potential transmetalating reagent, we synthesized *N*-Me, *B*-*i*-Pr 1,2-azaborine (**1.46**) to use as a secondary alkyl-substituted substrate in this cross-coupling protocol (**Scheme 1.20**).

Scheme 1.20 Successful Isopropyl Migration Using *N*-Me, *B*-*i*-Pr 1,2-Azaborine

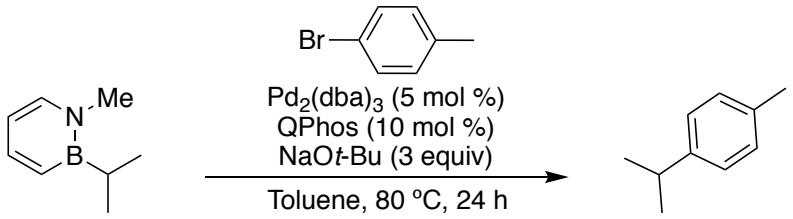

1.46 **1.43** *detected by GCMS*

Using this substrate, the cross-coupled product **1.43** was also detected by GC-MS, leading us to conclude that steric interference at boron-adjacent sites may in fact play a role

[71] Boknevitz, K.; Italia, J. S.; Li, B.; Chatterjee, A.; Liu, S.-Y. *Chem. Sci.* **2019**, *10*, 4994–4998.

in the efficacy of transmetalation. To see if further reduction of the steric profile of the azaborine would continue to promote transmetalation, *N*-H, *B*-*i*-Pr 1,2-azaborine (**1.47**) was synthesized and tested under the same cross-coupling conditions (**Scheme 1.21**). In this case, rather than detecting transmetalation of the isopropyl fragment, a GC-MS trace with a *m*/*z* corresponding to the Buchwald-Hartwig amination product **1.48** was observed in addition to the homo-coupled byproduct **1.41**. This amination product was not isolated, but this result is in accordance with previous methodology developed by our lab.[72]

Scheme 1.21 Formation of Buchwald-Hartwig Byproduct Using *N*-H *B*-*i*-Pr 1,2-Azaborine

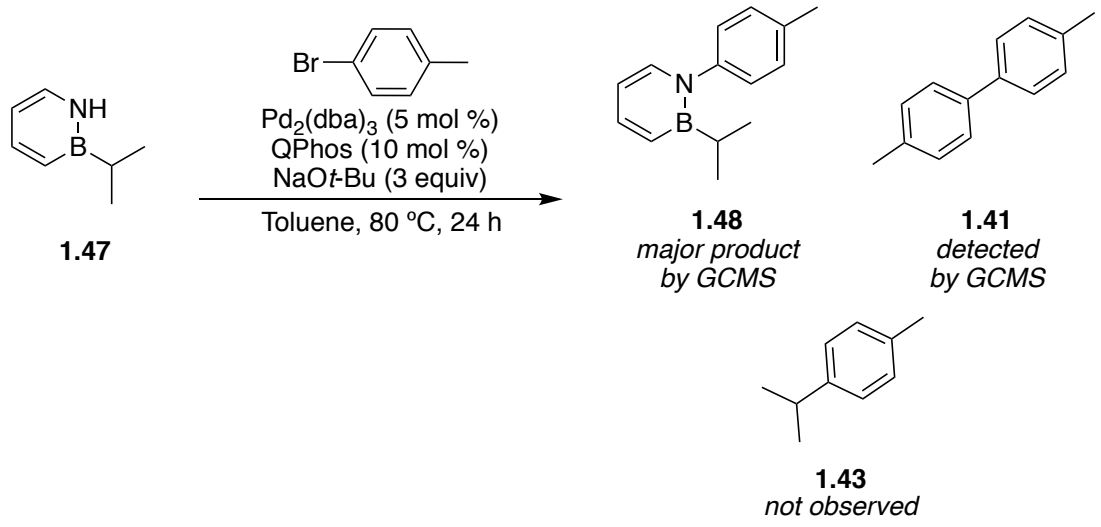

[72] Lee, H. "Site-Selective Reactions Via Scaffolding Catalysis & Synthesis and Binding Study of 1,2-azaborines" (Doctoral Dissertation). Boston College, 2017, p 664–668.

1.4 Conclusions

Considering the previously-established methodologies featuring *BN*-heterocycles, such as the rhodium-catalyzed arylation of *N*-TBS, *B*-Cl 1,2-azaborines and self-arylation reaction of borazaronaphthalenes, our group sought to investigate the ability of 1,2-azaborines to transmetalate aryl and alkyl substituents under Suzuki-Miyaura cross-coupling conditions. By developing a variant of the self-arylation reaction for monocyclic 1,2-azaborines, we expanded the reaction scope to encompass alkyl migrations with primary and secondary alkyl groups—a transformation that was not achieved using *BN*-naphthalene analogues. This method contributes to the growing collection of *BN*-heterocycle methodology, and also serves as a novel method for the functionalization of 1,2-azaborines.

Additionally, *N*-TBS, *B*-Bn and *N*-Me, *B*-*i*-Pr azaborines demonstrated the ability to transmetalate under cross-coupling conditions with 4-bromotoluene. While the precise yields of these transformations remain to be determined, these preliminary results demonstrate that 1,2-azaborines are capable of serving as transmetalating reagents, and suggest that future studies towards developing enantiospecific protocols may be worthwhile.

CHAPTER 2
Experimental Section

2.1 General Information

Unless otherwise noted, all reactions were carried out in flame- or oven-dried glassware under an atmosphere of nitrogen using either standard Schlenk technique or a nitrogen-filled glove box. THF, Et_2O, CH_2Cl_2, toluene, pentane, and acetonitrile were dried using a Brady® solvent purification system, which consisted of columnar molecular sieves under argon atmosphere. All reagents were purchased from commercial vendors (Acros Organics®, Millipore Sigma®, Oakwood Chemical®, TCI®, or Combi-Blocks®) and used as received unless otherwise stated.

All NMR spectra were recorded on a Varian VNMRS 600 MHz, VNMRS 500 MHz, INOVA 500 MHz, or VNMRS 400 MHz spectrometer at ambient temperature in the Michael Gerson Magnetic Resonance and Instrumentation Laboratory at Boston College. ^{11}B NMR spectra were externally referenced to $BF_3 \bullet Et_2O$ (δ 0.0 ppm). ^1H NMR spectra were internally referenced to either chloroform-d (δ 7.26 ppm) or methylene chloride-d2 (δ 5.32 ppm). Infrared spectroscopy was performed on a Bruker ALPHA-Platinum FT-IR Spectrometer with an ATR-sampling module. High-resolution mass spectra were collected by Marek Domin on a JEOL AccuTOF instrument equipped with a DART ion source in positive ion mode at the Boston College Center for Mass Spectrometry.

2.2 Synthesis of 1,2-Azaborines

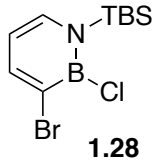

1.28

Compound **1.28** (3.62 g, 67% yield) was synthesized as a colorless oil from compound **1.18** (4.00 g, 17.6 mmol) and a solution of molecular bromine in CH_2Cl_2 (0.85 mL, 1.10 M, 16.7 mmol). Under nitrogen atmosphere, compound **1.18** was dissolved in 20 mL CH_2Cl_2 and cooled to –30 ºC using a dry ice/acetone bath. Upon cooling, the solution of molecular bromine was added dropwise to the reaction mixture. The solution turned red-orange shortly after the addition of bromine. The reaction was allowed to stir for 1 hour while warming to room temperature, at which point 11B NMR analysis deemed the reaction to be complete. The solution was concentrated under reduced pressure, and the crude material was purified by vacuum distillation (170 ºC, 300 mTorr). Spectra of the isolated compound matched previously published records.[37b]

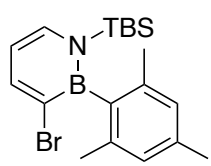

1.30

Compound **1.30** (9.00 g, 57% yield) was synthesized as a white solid from **1.28** (12.4 g, 40.3 mmol) and 2-mesityllithium (13.2 g, 105 mmol). In a nitrogen glove box, compound **1.28** was dissolved in 85 mL THF at room temperature. Solid 2-mesityllithium was added in portions to the stirred solution at room temperature. The solution turned orange shortly after addition of the lithiated species. The reaction mixture was allowed to stir for 1 hour at room temperature, at which point 11B NMR analysis deemed the reaction to be complete. The solution was concentrated under reduced pressure and 40 mL pentane was added. The resulting suspension was filtered through a fritted funnel to remove salts. The filtrate was concentrated under reduced pressure, and the crude material was purified inside a nitrogen glove box by silica gel chromatography using 97:3 pentane/Et_2O as eluent. Spectra of the isolated compound matched previously published records.[73]

[73] Baggett, A. W.; Guo, F.; Li, B.; Liu, S.-Y.; Jakle, F. *Angew. Chem. Int. Ed.* **2015**, *54*, 11191–11195.

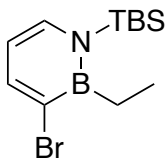

1.31

Compound **1.31** (0.45 g, 13% yield) was synthesized as a tan solid from **1.28** (3.71 g, 12.1 mmol) and a solution of ethylmagnesium bromide in Et_2O (13.3 mL, 1.00 M, 13.3 mmol). Under nitrogen atmosphere, compound **1.28** was dissolved in 10mL Et_2O and cooled to –30 ºC using a dry ice/acetone bath. The solution of ethylmagnesium bromide was then added dropwise to the reaction mixture. The reaction mixture was allowed to stir for 14 hours while warming room temperature, at which point 11B NMR analysis deemed the reaction to be complete. The solution was concentrated under reduced pressure and 25 mL pentane was added. The resulting suspension was filtered through a fritted funnel to remove salts. The yellow filtrate was concentrated under reduced pressure, and the crude material was purified inside a nitrogen glove box by silica gel chromatography using pentane as eluent. ^{1}H NMR (500 MHz, $CDCl_3$) δ 7.84–7.71 (m, 1H), 7.24 (d, J = 6.6 Hz, 1H), 6.19–6.04 (m, 1H), 1.44–1.29 (m, 2H), 1.09 (td, J = 7.9, 2.0 Hz, 3H), 0.91 (dd, J = 4.1, 2.5 Hz, 9H), 0.60–0.44 (m, 6H). ^{11}B NMR (160 MHz, $CDCl_3$): δ 40.3 ^{13}C NMR (151 MHz, $CDCl_3$): δ 144.5, 137.8, 132.3 (br), 110.8, 26.4, 19.6, 12.9 (br), 10.1, –1.4. FTIR (thin film): 2931, 1606, 1497, 1463, 1339, 1263, 1150, 996, 841, 822, 791, 760, 707 cm^{-1}. HRMS (DART-TOF) calculated for $C_{12}H_{24}BNSiBr$ ($[M+H]^+$): 300.09490, found: 300.09480.

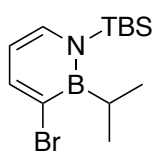

1.32

Compound **1.32** (0.355 g, 35% yield) was synthesized as a white crystalline solid from **1.28** (1.00g, 3.26 mmol) and a solution of isopropylmagnesium chloride in THF (6.50 mL, 2.00 M, 13.0 mmol). Under nitrogen atmosphere, compound **1.28** was dissolved in 10 mL THF at room temperature. The solution of isopropylmagnesium chloride was then added dropwise to the reaction mixture. The reaction mixture was then allowed to stir for 16 hours at 50 ºC, at which point 11B NMR analysis deemed the reaction to be complete. The solution was concentrated under reduced pressure and 75 mL pentane was added. The resulting suspension was filtered through a fritted funnel to remove salts. The yellow filtrate was concentrated under reduced pressure, and the crude material was purified inside a nitrogen glove box by silica gel chromatography using pentane as eluent. ^{1}H NMR (600 MHz, $CDCl_3$): δ 7.87–7.69 (m, 1H), 7.23 (dq, J = 6.8, 3.6 Hz, 1H), 6.07 (dd, J = 7.1, 3.3 Hz, 1H), 1.64 (qd, J = 8.2, 7.7, 3.6 Hz, 1H), 1.31–1.20 (m, 6H), 1.01–0.91 (m, 9H), 0.53–0.43 (m, 6H). ^{11}B NMR (160 MHz, $CDCl_3$): δ 40.3. ^{13}C NMR (151 MHz, $CDCl_3$): δ 146.8, 138.2, 136.1 (br), 110.8, 27.1, 19.1 (br), 18.9, 14.2, –0.2. FTIR (thin film): 2930, 1606, 1463, 1339, 1262, 1149, 996, 842, 822, 790, 746, 707, 577, 506 cm^{-1}. HRMS (DART-TOF) calculated for $C_{13}H_{26}BNSiBr$ ($[M+H]^+$): 314.11055, found: 314.10989.

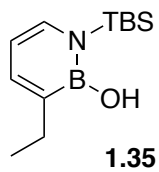

1.35

Compound **1.35** (0.025 g, 79% yield) was synthesized as a tan oil from compound **1.31** (0.040 g, 0.133 mmol), tris(dibenzylideneacetone)-dipalladium(0) (0.004 g, 0.003 mmol), QPhos (0.005 g, 0.007 mmol), and sodium *tert*-butoxide (0.013 g, 0.133 mmol). In a nitrogen glove box, compound **1.31**, tris(dibenzylideneacetone)dipalladium(0), QPhos, and sodium *tert*-butoxide were dissolved in 3 mL toluene at room temperature. The reaction mixture was allowed to stir for 24 hours at 80 ºC and judged to be complete by 11B NMR. The solution was concentrated under reduced pressure, and the crude material was purified inside a nitrogen glove box by silica gel chromatography using 98:2 hexane/dichloromethane as eluent. ^{1}H NMR (600 MHz, CD_2Cl_2): δ 7.14 (d, J = 6.2 Hz, 1H), 6.87 (d, J = 6.8 Hz, 1H), 5.84 (d, J = 1.8 Hz, 1H), 3.89 (d, J = 1.5 Hz, 1H), 2.46–2.28 (m, 2H), 1.14 (d, J = 2.0 Hz, 3H), 0.95 (d, J = 2.1 Hz, 9H), 0.44 (d, J = 2.1 Hz, 6H). ^{11}B NMR (160 MHz, $CDCl_3$): δ 31.0 ^{13}C NMR (151 MHz, CD_2Cl_2): δ 140.8, 136.4 (br), 135.8, 107.2, 26.8, 26.1, 19.4, 15.1, –2.9. FTIR (thin film): 2924, 2854, 1609, 1489, 1461, 1259, 838, 785 cm^{-1}. HRMS (DART-TOF) calculated for $C_{12}H_{25}BNOSi$ ($[M+H]^+$): 238.17930, found: 238.17918.

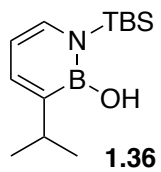

1.36

Compound **1.36** (0.019 g, 33% yield) was synthesized as a yellow oil from compound **1.32** (0.068 g, 0.216 mmol), tris(dibenzylideneacetone)-dipalladium(0) (0.010 g, 0.011 mmol), QPhos (0.015 g, 0.022 mmol), and sodium *tert*-butoxide (0.062 g, 0.649 mmol). In a nitrogen glove box, compound **1.32**, tris(dibenzylideneacetone)dipalladium(0), QPhos, and sodium *tert*-butoxide were dissolved in 5 mL toluene at room temperature. The reaction mixture was allowed to stir for 24 hours at 80 ºC and judged to be complete by 11B NMR. The solution was concentrated under reduced pressure, and the crude material was purified inside a nitrogen glove box by silica gel chromatography using pentane as eluent. ^{1}H NMR (400 MHz, CD_2Cl_2): δ 7.14 (d, J = 6.4 Hz, 1H), 6.84 (d, J = 6.9 Hz, 1H), 5.83 (t, J = 6.6 Hz, 1H), 3.90 (s, 1H), 2.66 (hept, J = 7.1, 6.7 Hz, 1H), 1.14 (d, J = 6.8 Hz, 6H), 0.91 (s, 9H), 0.41 (s, 6H). ^{11}B NMR (160 MHz, $CDCl_3$): δ 31.2 ^{13}C NMR (151 MHz, $CDCl_3$): δ 138.5, 137.1 (br), 134.5, 106.4, 30.4, 26.4, 20.7, 18.7, –3.8. FTIR (thin film): 2926, 2856, 1609, 1492, 1462, 1261, 839, 786, 739 cm^{-1}. HRMS (DART-TOF) calculated for $C_{13}H_{27}BNOSi$ ($[M+H]^+$): 252.19495, found: 252.19504.

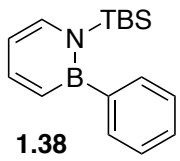

1.38

Compound **1.38** (2.08 g, 59% yield) was synthesized as a clear oil from compound **1.18** (3.00 g, 13.2 mmol) and a solution of phenylmagnesium bromide in THF (5.00 mL, 3.00 M, 15.0 mmol). In a nitrogen glovebox, compound **1.18** was dissolved in 35 mL THF. The solution of phenylmagnesium bromide was then added dropwise to the reaction mixture, and the solution turned grey shortly after the addition of the Grignard reagent. The reaction was allowed to stir at room temperature for 9.5 hours, at which point 11B NMR analysis deemed the reaction to be complete. The solution was concentrated under reduced pressure and 30 mL pentane was added. The resulting suspension was filtered through a fritted funnel to remove salts. The filtrate was concentrated under reduced pressure, and the crude material was purified by vacuum distillation (180 ºC, 300 mTorr). Spectra of the isolated compound matched previously published records.[39]

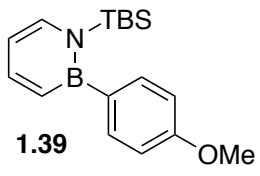

1.39

Compound **1.39** (1.84 g, 70% yield) was synthesized as a white solid from compound **1.18** (2.00 g, 8.79 mmol) and a solution of 4-methoxyphenylmagnesium bromide in THF (19.3 mL, 0.500 M, 9.67 mmol). In a nitrogen glovebox, compound **1.18** was dissolved in 15 mL of THF at room temperature. The solution of 4-methoxyphenylmagnesium bromide was then added dropwise to the reaction mixture, and the solution turned yellow shortly after addition of the Grignard reagent. The reaction mixture was allowed to stir at room temperature for 4.5 hours, at which point 11B NMR deemed the reaction to be complete. The solution was concentrated under reduced pressure and the crude material was purified inside a nitrogen glove box by silica gel chromatography using 97:3 pentane/Et_2O as eluent. Spectra of the isolated compound matched previously published records.[74]

[74] Baggett, A.W.; Liu, S.-Y. *J. Am. Chem. Soc.* **2017**, *139*, 15259–15264.

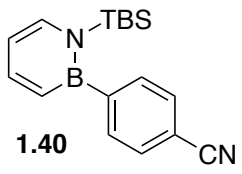

1.40

Compound **1.40** (0.90 g, 97%) was synthesized as a white solid from compound **1.18**, compound **S1** (0.92 g, 3.46 mmol), chlorobis(ethylene)rhodium dimer (30.6 mg, 78.6 μmol), and BIPHEP (82.2 mg, 0.157 mmol). In a nitrogen glove box, chlorobis(ethylene)rhodium dimer and BIPHEP were dissolved in 5 mL THF at room temperature. The solution was allowed to stir for 0.5 hours before being added to a pressure vessel containing a solution of compound **1.18** and compound **S1** in 5 mL THF. The reaction mixture was then allowed to stir for 24 hours at 100 ºC, at which point 11B NMR deemed the reaction to be complete. The solution was concentrated under reduced pressure and the crude material was purified inside a nitrogen glove box by silica gel chromatography using 97:3 pentane/Et_2O as eluent. ^{1}H NMR (500 MHz, $CDCl_3$): δ 7.63 (dd, *J* = 11.0, 6.6 Hz, 1H), 7.56 (dd, *J* = 8.2, 2.3 Hz, 2H), 7.52–7.44 (m, 2H), 7.42 (d, *J* = 6.8 Hz, 1H), 6.60 (d, *J* = 10.9 Hz, 1H), 6.53–6.42 (m, 1H), 0.88 (d, *J* = 2.4 Hz, 9H), 0.04 (d, *J* = 2.3 Hz, 6H). ^{11}B NMR (160 MHz, $CDCl_3$): δ 38.1. ^{13}C NMR (151 MHz, $CDCl_3$): δ 143.8, 138.5, 137.2 (br), 132.7, 130.4, 119.8, 116.4 (br), 112.8, 110.5, 27.0, 19.1, –1.8. FTIR (thin film): 3364, 2226, 1604, 1505, 1454, 1390, 1270, 1096, 998, 957, 810, 786, 745, 709, 562 cm^{-1}. HRMS (DART-TOF) calculated for $C_{17}H_{24}BN_2Si$ ($[M+H]^+$): 295.17963, found: 295.17959.

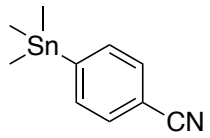

S1

Compound **S1** (0.92 g, 85% yield) was synthesized as a yellow oil from 4-iodocyanobenzene (0.933 g, 4.07 mmol), trimethyltin chloride (0.98 g, 4.92 mmol), and a solution of isopropylmagnesium chloride (2.25 mL, 2.00 M, 4.50 mmol). Under nitrogen atmosphere, 4-iodocyanobenzene was dissolved in 15 mL THF and cooled to –40 ºC using a dry ice/acetonitrile bath. The solution of isopropylmagnesium chloride was added dropwise to the reaction mixture, and the solution turned yellow shortly after the addition of the Grignard reagent. The reaction mixture was allowed to stir at –40 ºC for 1 hour. Subsequently, trimethyltin chloride was added to the solution, and the reaction mixture was allowed to stir for an additional 1 hour while warming to room temperature. The reaction was then quenched with a saturated ammonium chloride solution and extracted with Et_2O. The combined organic extracts were washed with brine and dried over magnesium sulfate, prior to concentration under reduced pressure. The crude material was purified by silica gel chromatography using 5:1 hexane/ethyl acetate as eluent. Spectra of the isolated compound matched previously published records.[39]

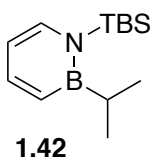

1.42

Compound **1.42** (3.44 g, 89% yield) was synthesized as a colorless oil from compound **1.18** (3.75 g, 16.5 mmol) and a solution of isopropylmagnesium chloride in THF (12 mL, 2.00 M, 24.0 mmol). In a nitrogen glove box, compound **1.18** was dissolved in 20 mL THF in a pressure vessel at room temperature. The solution of isopropylmagnesium chloride was then added to the solution, and the solution turned yellow shortly after addition of the Grignard reagent. The reaction mixture was then allowed to stir for 7 hours at 100 ºC, at which point 11B NMR deemed the reaction to be complete. The solution was concentrated under reduced pressure and the crude material was purified inside a nitrogen glove box by silica gel chromatography using pentane as eluent. ^{1}H NMR (500 MHz, $CDCl_3$): δ 7.59–7.45 (m, 1H), 7.26–7.15 (m, 1H), 6.88–6.73 (m, 1H), 6.20 (ddt, J = 8.2, 5.5, 1.4 Hz, 1H), 1.60–1.48 (m, 1H), 1.05 (d, J = 7.0 Hz, 6H), 0.93 (d, J = 1.3 Hz, 9H), 0.48 (s, 6H). ^{11}B NMR (160 MHz, $CDCl_3$): δ 42.8. ^{13}C NMR (126 MHz, $CDCl_3$): δ 141.7, 137.8, 128.1 (br), 110.8, 26.5, 21.7, 19.2, 18.1 (br), –1.3. FTIR (thin film): 2954, 2931, 2886, 2856, 1610, 1511, 1463, 1393, 1362, 1292, 1264, 1188, 1177, 1156, 1136, 1054, 1017, 1005, 963, 841, 822, 811, 784, 739, 725, 707, 685, 406 cm^{-1}. HRMS (DART-TOF) calculated for $C_{13}H_{27}BNSi$ ($[M+H]^+$): 236.20003, found: 236.19954.

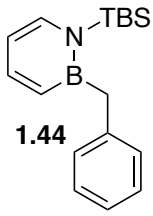

1.44

Compound **1.44** (0.72 g, 21% yield) was synthesized as a yellow oil from compound **1.18** (2.82 g, 12.4 mmol) and a solution of benzylmagnesium chloride in THF (13.4 mL, 1.40 M, 18.8 mmol). In a nitrogen glove box, compound **1.18** was dissolved in 25 mL THF, and the solution of benzylmagnesium chloride was then added dropwise to the solution. The reaction mixture was allowed to stir at room temperature for 1 hour, at which point 11B NMR analysis deemed the reaction to be complete. The solution was concentrated under reduced pressure and 20 mL pentane was added. The resulting suspension was filtered through a fritted funnel to remove salts. The filtrate was concentrated under reduced pressure, and the crude material was purified inside a nitrogen glove box by silica gel chromatography using 98:2 pentane/Et_2O as eluent. Spectra of the isolated compound matched previously published records.[74]

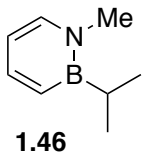

1.46

Compound **1.46** (0.022 g, 13% yield) was synthesized as a clear oil from compound **1.47** (0.150 g, 1.24 mmol), a solution of KHMDS in toluene (1.82 mL, 0.500 M, 1.36 mmol), and iodomethane (0.155 mL, 2.48 mmol). Inside a nitrogen glove box, compound **1.47** was dissolved in 5 mL THF, and the solution of KHMDS in toluene was added dropwise to the solution. The mixture was allowed to stir for 3 hours at room temperature. Subsequently, iodomethane was added dropwise to the reaction mixture, which was allowed to stir for an additional 4h, at which point 11B NMR analysis deemed the reaction to be complete. The solution was concentrated under reduced pressure, and the crude material was purified inside a nitrogen glove box by silica gel chromatography using pentane as eluent. ^{1}H NMR (600 MHz, $CDCl_3$): δ 7.68–7.41 (m, 1H), 7.10 (dd, J = 7.0, 3.2 Hz, 1H), 6.74 (dd, J = 11.1, 3.2 Hz, 1H), 6.27–6.09 (m, 1H), 3.54 (d, J = 3.4 Hz, 3H), 1.63–1.49 (m, 1H), 1.09 (dd, J = 7.3, 3.4 Hz, 6H). ^{11}B NMR (160 MHz, $CDCl_3$): δ 39.2. ^{13}C NMR (151 MHz, $CDCl_3$): δ 143.7, 136.3, 136.0 (br), 126.4, 30.1, 20.2 (br). FTIR (thin film): 2924, 1616, 1518, 1464, 1411, 1259, 1085, 802, 736 cm^{-1}. HRMS (DART-TOF) calculated for $C_8H_{15}BN$ ($[M+H]^+$): 136.12921, found: 136.12983.

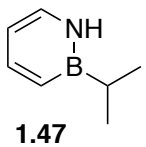

1.47

Compound **1.47** (1.24 g, 70% yield) was synthesized as a yellow oil from compound **1.42** (3.44 g, 14.6 mmol) and a solution of tetrabutylammonium fluoride in THF (19.0 mL, 1.00 M, 19.0 mmol). Inside a nitrogen glove box, compound **1.42** was dissolved in 15 mL THF at room temperature, and the solution of tetrabutylammonium fluoride was then added to the solution. The solution turned dark brown after addition of the fluoride source. The reaction mixture was allowed to stir at room temperature for 4 hours, at which point 11B NMR analysis deemed the reaction to be complete. The solution was concentrated under reduced pressure and the crude material was purified inside a nitrogen glove box by silica gel chromatography using 99:1 pentane/Et_2O as eluent. ^{1}H NMR (500 MHz, $CDCl_3$): δ 7.84 (d, J = 46.1 Hz, 1H), 7.62 (dd, J = 11.3, 6.6 Hz, 1H), 7.26 (t, J = 7.1 Hz, 1H), 6.80 (d, J = 11.3 Hz, 1H), 6.24 (t, J = 6.7 Hz, 1H), 1.43 (h, J = 6.8, 5.9 Hz, 1H), 1.11 (dd, J = 7.4, 2.4 Hz, 6H). ^{11}B NMR (160 MHz, $CDCl_3$): δ 38.2. ^{13}C NMR (151 MHz, $CDCl_3$): δ 143.9, 133.8, 129.0 (br), 110.2, 20.4, 15.5 (br). FTIR (thin film): 3413, 2942, 2930, 1536, 1462, 1422, 1072, 988, 726, 519 cm^{-1}. HRMS (DART-TOF) calculated for $C_7H_{13}BN$ ($[M+H]^+$): 122.11356, found: 122.11416.

2.3 Screening Experiment Data

GC-MS analysis was performed at Boston College using an Agilent 7890B GC equipped with an Agilent 5977B MSD. The screening experiment was performed on 0.100 mmol scale, and a variety of arylhalide, catalyst, ligand, base, and solvent mixture combinations were employed. All reactions were allowed to stir at 80 ºC for 24h. Thereafter, 0.45 μmol of hexadecane (0.100 mL of a 0.045 M solution in toluene) was added to each reaction as an internal standard. The reaction mixtures were then filtered through silica gel prior to analysis by GC-MS. The GC-MS parameters are displayed below.

Table 2.1 GC-MS Instrument Parameters

Parameter	Description
GC Column	HP-5ms Ultra Inert
Column Dimensions	30 m x 250 μm x 0.25 μm
Initial Oven Temperature	100 ºC
Initial Time	4 min
Oven Ramp Rate	15 ºC/min
Oven Final after Ramp	280 ºC
Final Time after Ramp	16 min
Total Run Time	25 min
Inlet Temperature	290 ºC
Inlet Mode	Split
Injection Volume	1.5 μL
Carrier Gas	Helium
Flow Mode	Constant
Flow Rate	1.0 mL/min
Nominal Initial Pressure	10.52 psi
Split Ratio	10:1
Split Flow	10 mL/min
GC Outlet	MSD
Outlet Pressure	6.69 x 10^{-6} Torr
MSD Transfer Line Temperature	300 ºC
Ion Source Temperature	230 ºC
Quadrupole Temperature	150 ºC
MSD Solvent Delay	2.40 min

The peak areas for the hexadecane internal standard (IS), desired product (P), and undesired byproduct (BP) obtained under various conditions are shown in the tables below. Ratios of P:IS and BP:IS were measured to semi-quantitatively compare the reaction

outcomes under various reaction conditions. Higher P:IS ratios indicated greater success in the desired reaction. In certain cases, non-integrable amounts of product were detected using the GC-MS. Because these peaks were observed, though in minuscule amounts, the area of product is denoted as: *trace*. **Table 2.2** details the outcomes of the screening using *N*-TBS, *B*-*i*-Pr 1,2-azaborine.

Table 2.2 GC-MS Analysis of *N*-TBS, *B*-*i*-Pr 1,2-Azaborine Screen

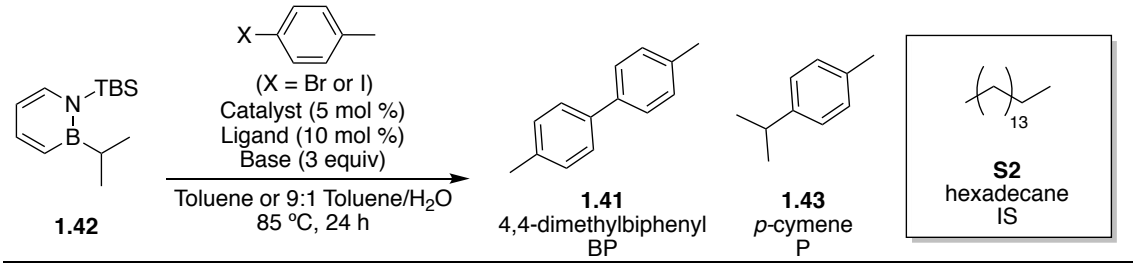

1.42

1.41 4,4-dimethylbiphenyl BP

1.43 *p*-cymene P

S2 hexadecane IS

X	Catalyst	Ligand	Base	Solvent Mixture	IS Area	P Area	BP Area	P/IS	BP/IS
I	$Pd(OAc)_2$	XPhos	KOH	Tol	6.42E+08	*trace*	1.06E+09	-	1.66
I	$Pd(OAc)_2$	PPh_3	Ag_2O	Tol	5.20E+08	*trace*	4.63E+08	-	0.89
I	$Pd(dppf)Cl_2$	PPh_3	Cs_2CO_3	Tol	5.61E+08	*trace*	4.04E+08	-	0.72
I	$Pd_2(dba)_3$	XPhos	Ag_2O	Tol	6.21E+08	*trace*	3.35E+08	-	0.54
I	SPhos-Pd-G2	-	KOH	Tol	6.56E+08	0	1.67E+09	0	2.54
I	$Pd(OAc)_2$	IPr	NaO-*t*Bu	Tol	7.49E+08	0	1.68E+09	0	2.24
I	$Pd(OAc)_2$	dppp	NaO-*t*Bu	Tol	4.11E+08	0	6.92E+08	0	1.68
I	$Pd(OAc)_2$	XPhos	NaO-*t*Bu	Tol	5.98E+08	0	9.60E+08	0	1.61
I	SPhos-Pd-G2	-	Cs_2CO_3	Tol	5.51E+08	0	7.76E+08	0	1.41
I	$Pd_2(dba)_3$	XPhos	Cs_2CO_3	Tol	6.32E+08	0	8.88E+08	0	1.40
I	$Pd_2(dba)_3$	XPhos	NaO-*t*Bu	Tol	5.73E+08	0	7.39E+08	0	1.29
I	$Pd_2(dba)_3$	IPr	NaO-*t*Bu	Tol	7.91E+08	0	9.93E+08	0	1.26
I	$Pd_2(dba)_3$	XPhos	KOH	Tol	4.73E+08	0	5.17E+08	0	1.09
I	$Pd(OAc)_2$	QPhos	NaO-*t*Bu	Tol	7.33E+08	0	7.51E+08	0	1.02
I	$Pd(OAc)_2$	QPhos	KOH	Tol	1.07E+08	0	9.32E+08	0	0.87
I	$Pd(dppf)Cl_2$	PPh_3	KOH	Tol	7.21E+08	0	4.25E+08	0	0.59
I	$Pd(OAc)_2$	JohnPhos	NaO-*t*Bu	Tol	8.02E+08	0	4.71E+08	0	0.59
I	$Pd_2(dba)_3$	dppp	NaO-*t*Bu	Tol	9.52E+08	0	5.56E+08	0	0.58
Br	$Pd(OAc)_2$	QPhos	NaO-*t*Bu	Tol	3.09E+08	0	1.79E+08	0	0.58
I	$Pd(OAc)_2$	XPhos	Ag_2O	Tol	5.75E+08	0	2.99E+08	0	0.52
Br	$Pd_2(dba)_3$	QPhos	NaO-*t*Bu	Tol/H_2O	3.77E+08	0	1.90E+08	0	0.50
I	$Pd(dppf)Cl_2$	PPh_3	NaO-*t*Bu	Tol	5.48E+08	0	2.26E+08	0	0.41
Br	$Pd(dppf)Cl_2$	QPhos	NaO-*t*Bu	Tol	3.05E+08	0	1.21E+08	0	0.40
I	$Pd(dppf)Cl_2$	QPhos	KOH	Tol	4.24E+08	0	1.63E+08	0	0.38
I	$NiCl_2(PCy_3)_2$	QPhos	NaO-*t*Bu	Tol	6.58E+08	0	2.22E+08	0	0.34
Br	$PdCl_2[P(o\text{-Tol})_3]_2$	QPhos	NaO-*t*Bu	Tol	2.90E+08	0	9.47E+07	0	0.33
Br	$Pd_2(dba)_3$	QPhos	KOH	Tol	8.35E+08	0	2.62E+08	0	0.32
I	$Pd(OAc)_2$	dppb	NaO-*t*Bu	Tol	4.43E+08	0	1.34E+08	0	0.30
I	$Pd_2(dba)_3$	QPhos	NaO-*t*Bu	Tol	6.52E+08	0	1.90E+08	0	0.29
I	$Pd_2(dba)_3$	QPhos	NaO-*t*Bu	Tol/H_2O	7.74E+08	0	2.26E+08	0	0.29
I	$Pd_2(dba)_3$	JohnPhos	NaO-*t*Bu	Tol	7.86E+08	0	2.20E+08	0	0.28
I	$Pd_2(dba)_3$	PPh_3	Cs_2CO_3	Tol	5.34E+08	0	1.48E+08	0	0.28
I	SPhos-Pd-G2	-	NaO-*t*Bu	Tol	6.23E+08	0	1.67E+08	0	0.27
Br	SPhos-Pd-G2	QPhos	NaO-*t*Bu	Tol	2.82E+08	0	6.97E+07	0	0.25
Br	$Pd_2(dba)_3$	QPhos	Ag_2O	Tol	6.92E+08	0	1.71E+08	0	0.25
Br	$Pd_2(dba)_3$	QPhos	K_3PO_4	Tol	8.26E+08	0	1.69E+08	0	0.20
I	$Pd_2(dba)_3$	QPhos	KOH	Tol/H_2O	6.99E+08	0	1.10E+08	0	0.16
I	$NiCl_2(PCy_3)_2$	QPhos	KOH	Tol	6.00E+08	0	7.63E+07	0	0.13
Br	$Pd_2(dba)_3$	QPhos	Cs_2CO_3	Tol	7.47E+08	0	7.23E+07	0	0.10
Br	$Pd_2(dba)_3$	QPhos	NaO-*t*Bu	Tol	3.84E+08	0	3.48E+07	0	0.09
I	$Pd_2(dba)_3$	QPhos	KOH	Tol	5.92E+08	0	4.84E+07	0	0.08
I	$Pd_2(dba)_3$	QPhos	Cs_2CO_3	Tol/H_2O	5.80E+08	0	3.77E+07	0	0.07
I	$Pd_2(dba)_3$	dppb	NaO-*t*Bu	Tol	4.75E+08	0	2.85E+07	0	0.06
I	$NiCl_2(PCy_3)_2$	XPhos	KOH	Tol	6.63E+08	0	3.64E+07	0	0.05
I	$NiCl_2(PCy_3)_2$	XPhos	NaO-*t*Bu	Tol	6.46E+08	0	2.54E+07	0	0.04
Br	$NiCl_2(PCy_3)_2$	QPhos	NaO-*t*Bu	Tol	2.78E+08	0	0	0	0
I	$Pd(dppf)Cl_2$	PPh_3	Ag_2O	Tol	6.71E+08	0	0	0	0
I	$Pd(OAc)_2$	PPh_3	NaO-*t*Bu	Tol	5.28E+08	0	0	0	0
I	$Pd(OAc)_2$	PPh_3	KOH	Tol	7.67E+08	0	0	0	0
I	$Pd(OAc)_2$	PPh_3	Cs_2CO_3	Tol	8.15E+08	0	0	0	0
I	SPhos-Pd-G2	-	Ag_2O	Tol	5.72E+08	0	0	0	0

Table 2.3 and **Table 2.4** show the results of the cross-coupling reactions using *N*-TBS, *B*-Bn 1,2-azaborine and *N*-Me, *B*-*i*-Pr 1,2-azaborine, respectively.

Table 2.3 GC-MS Analysis of *N*-TBS, *B*-Bn 1,2-Azaborine Cross-Coupling

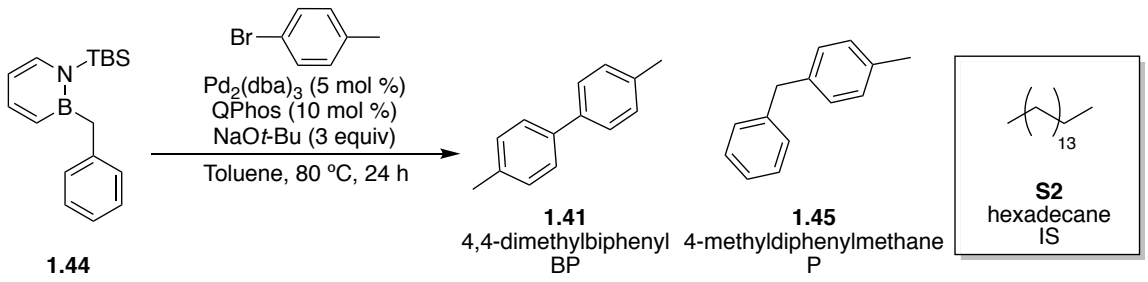

1.44

1.41
4,4-dimethylbiphenyl
BP

1.45
4-methyldiphenylmethane
P

S2
hexadecane
IS

IS Area	P Area	BP Area	P/IS	BP/IS
6.05E+08	4.90E+07	4.62E+08	0.08	0.76

Table 2.4 GC-MS Analysis of *N*-Me, *B*-*i*-Pr 1,2-Azaborine Cross-Coupling

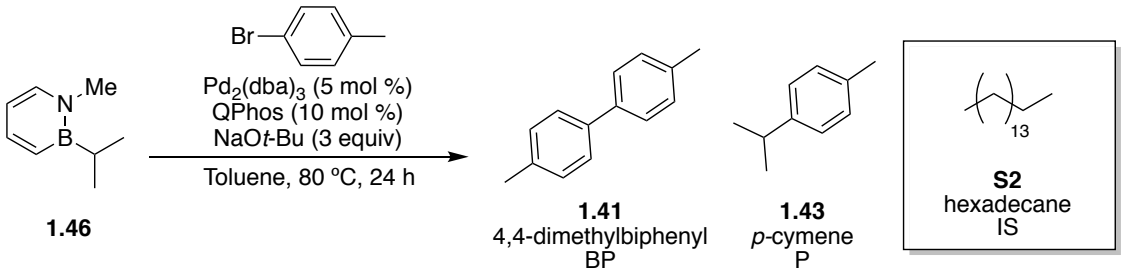

1.46

1.41
4,4-dimethylbiphenyl
BP

1.43
p-cymene
P

S2
hexadecane
IS

IS Area	P Area	BP Area	P/IS	BP/IS
6.94E+08	2.54E+08	3.55E+08	0.37	0.51

Lastly, **Table 2.5** shows the observed formation of the Buchwald-Hartwig amination product (BH) using *N*-H, *B*-*i*-Pr 1,2-azaborine with a variety of metal catalysts.

Table 2.5 GC-MS Analysis of *N*-H *B*-*i*-Pr 1,2-Azaborine Cross-Coupling

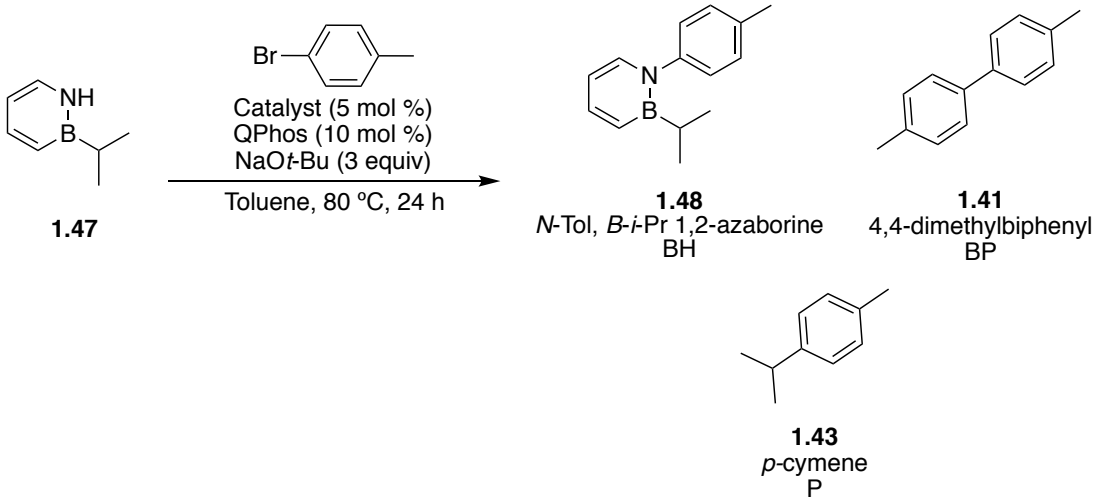

1.47

1.48
N-Tol, *B*-*i*-Pr 1,2-azaborine
BH

1.41
4,4-dimethylbiphenyl
BP

1.43
p-cymene
P

Catalyst	IS Area	P Area	BP Area	BH Area	P/IS	BP/IS	BH/IS
$Pd_2(dba)_3$	1.53E+08	0	1.77E+07	1.04E+09	0	0.12	6.80
SPhos Pd G2	1.41E+08	0	1.83E+07	8.78E+08	0	0.13	6.23
$Pd(OAc)_2$	1.49E+08	0	3.49E+07	9.09E+08	0	0.23	6.11
$PdCl_2(P(o\text{-tolyl})_3)_2$	1.41E+08	0	4.03E+07	8.44E+08	0	0.28	5.97
$NiCl_2(PCy_3)_2$	1.50E+08	0	0	0	0	0	0

2.4 Spectral Data

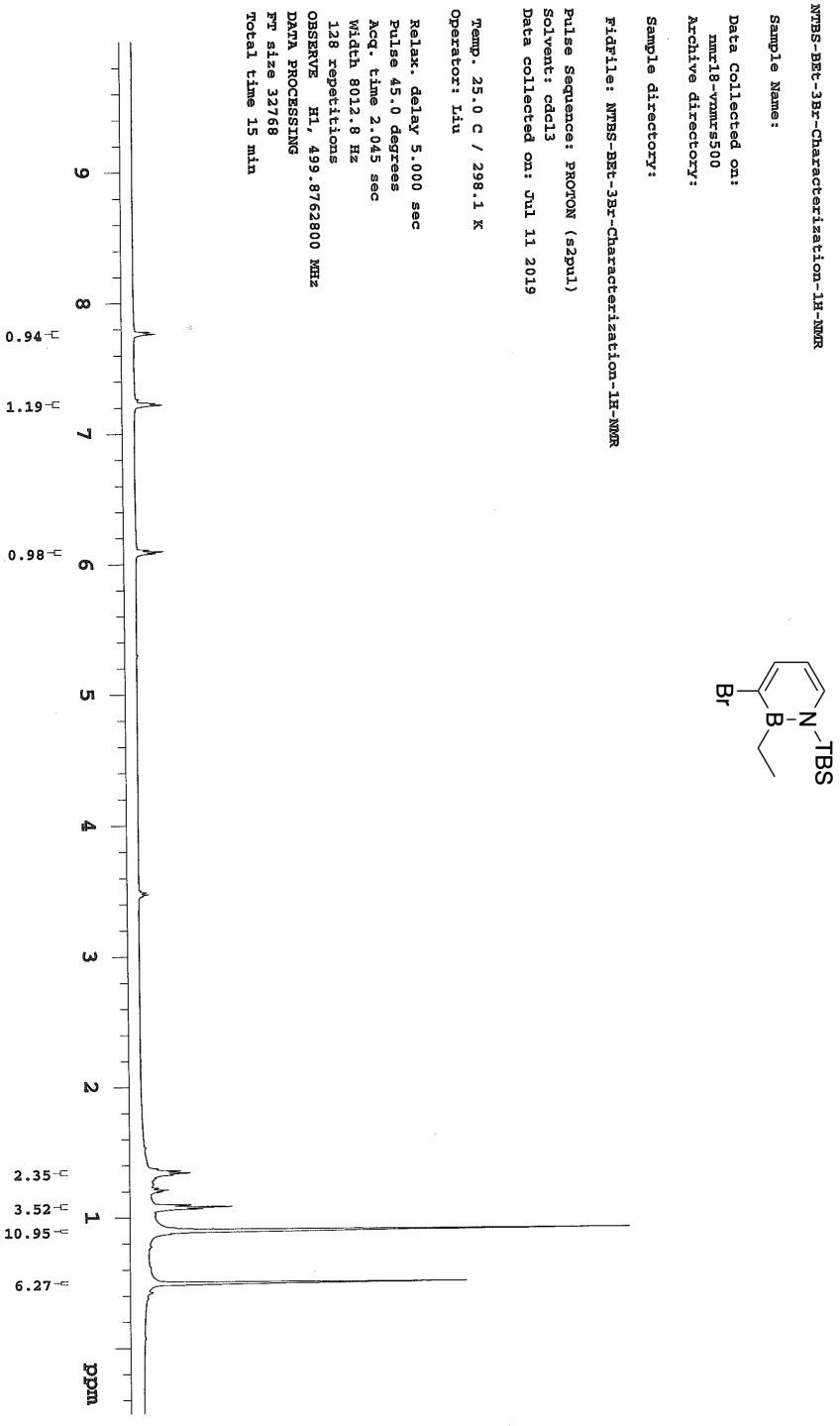

NTBS-BEt-C3Br-Characterization-11B-NMR

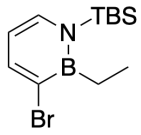

Sample Name:

Data Collected on:
nmr11-inova500
Archive directory:

Sample directory:

FidFile: NTBS-BEt-C3Br-Characterization-11B-NMR

Pulse Sequence: s2pul
Solvent: cdcl3
Data collected on: Jul 11 2019

Temp. 25.0 C / 298.1 K
Operator: Liu

Relax. delay 0.100 sec
Pulse 22.2 degrees
Acq. time 0.064 sec
Width 32064.1 Hz
1000 repetitions
OBSERVE B11, 160.3466286 MHz
DATA PROCESSING
Line broadening 0.5 Hz
FT size 4096
Total time 4 min 24 sec

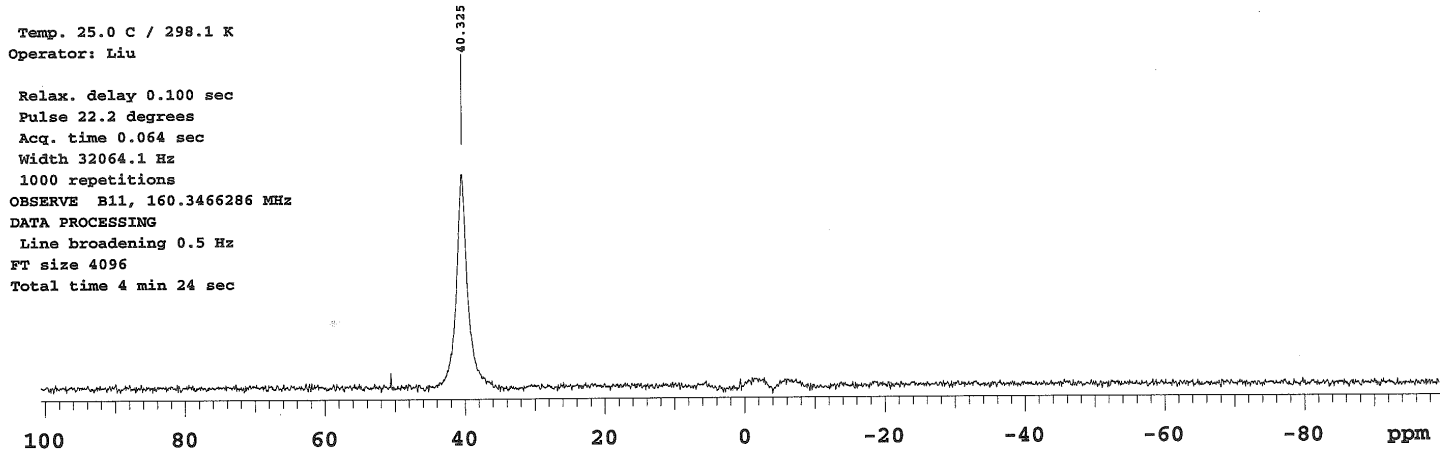

NTBS-BEt-3Br-Characterization-13C-NMR

Sample Name:

Data Collected on:
nmr19-vnmrs600
Archive directory:

Sample directory:

FidFile: NTBS-BEt-3Br-Characterization-13C-NMR

Pulse Sequence: CARBON (s2pul)
Solvent: cdcl3
Data collected on: Jul 16 2019

Temp. 25.0 C / 298.1 K
Operator: Liu

Relax. delay 1.000 sec
Pulse 45.0 degrees
Acq. time 0.865 sec
Width 37878.8 Hz
2000 repetitions
OBSERVE C13, 150.7898486 MHz
DECOUPLE H1, 599.6839027 MHz
Power 42 dB
continuously on
WALTZ-16 modulated
DATA PROCESSING
Line broadening 0.5 Hz
FT size 65536
Total time 1 hr, 2 min

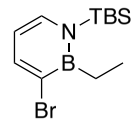

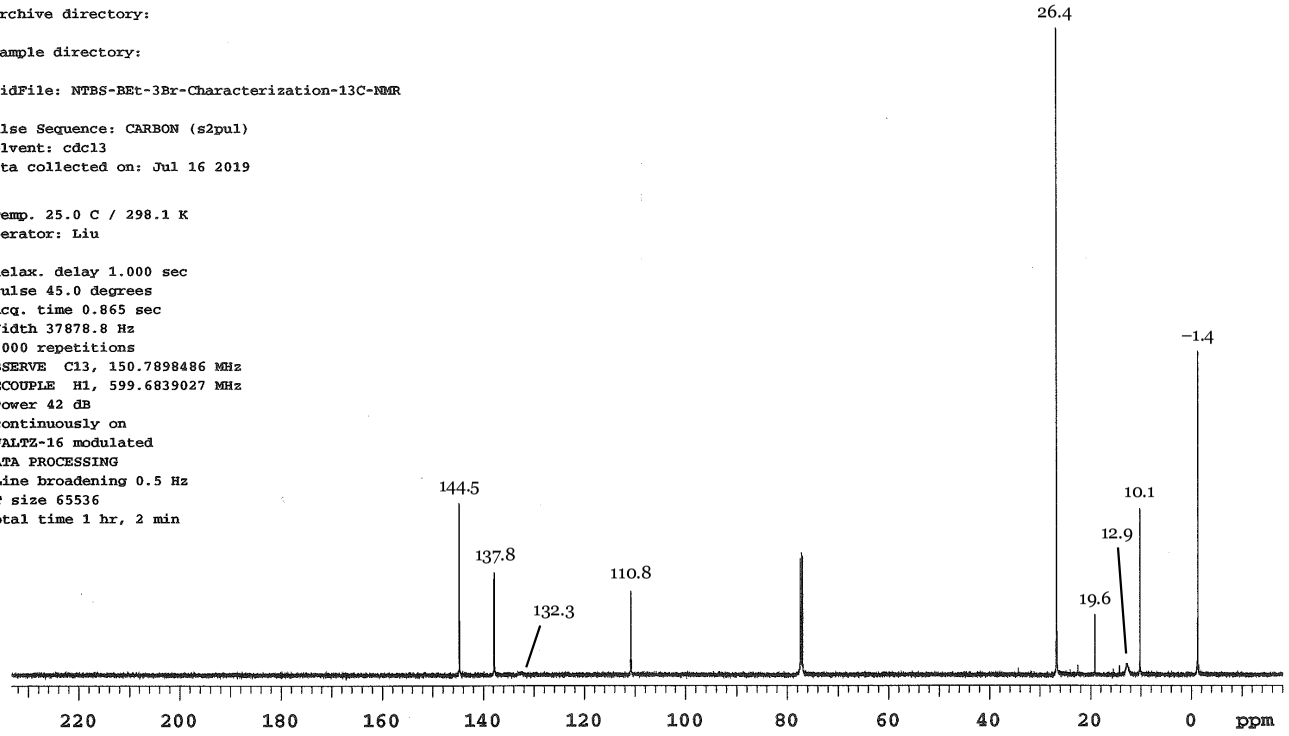

NTBS-BiPr-C3Br-Characterization-1H-NMR

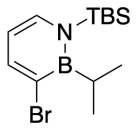

Sample Name:

Data Collected on:
nmr19-vnmrs600
Archive directory:

Sample directory:

FidFile: NTBS-BiPr-C3Br-Characterization-1H-NMR

Pulse Sequence: PROTON (s2pul)
Solvent: cdcl3
Data collected on: Jul 11 2019

Temp. 25.0 C / 298.1 K
Operator: Liu

Relax. delay 5.000 sec
Pulse 45.0 degrees
Acq. time 1.704 sec
Width 9615.4 Hz
128 repetitions
OBSERVE H1, 599.6809043 MHz
DATA PROCESSING
FT size 32768
Total time 14 min

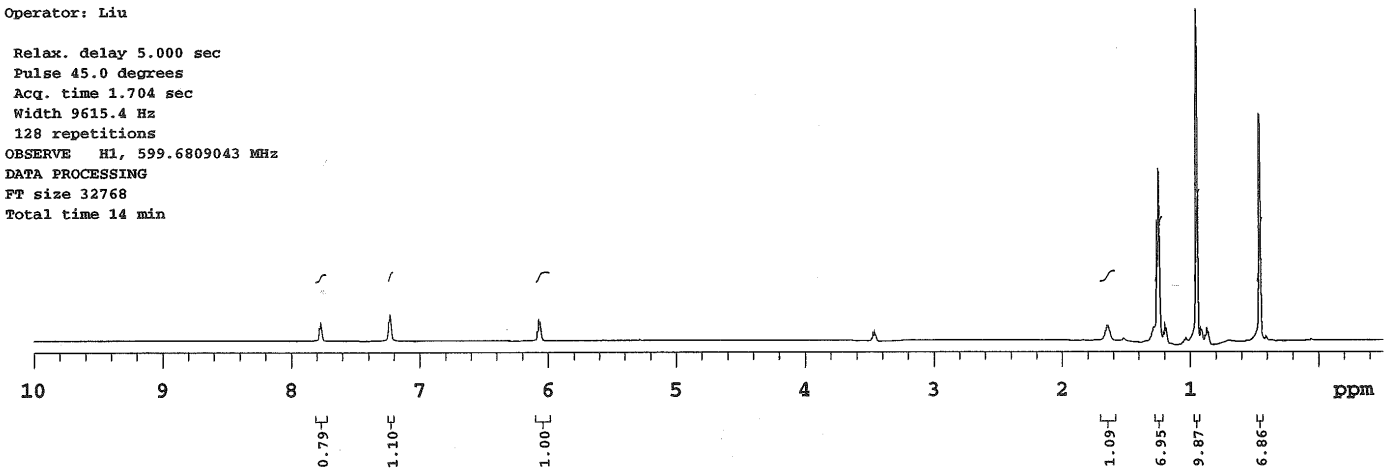

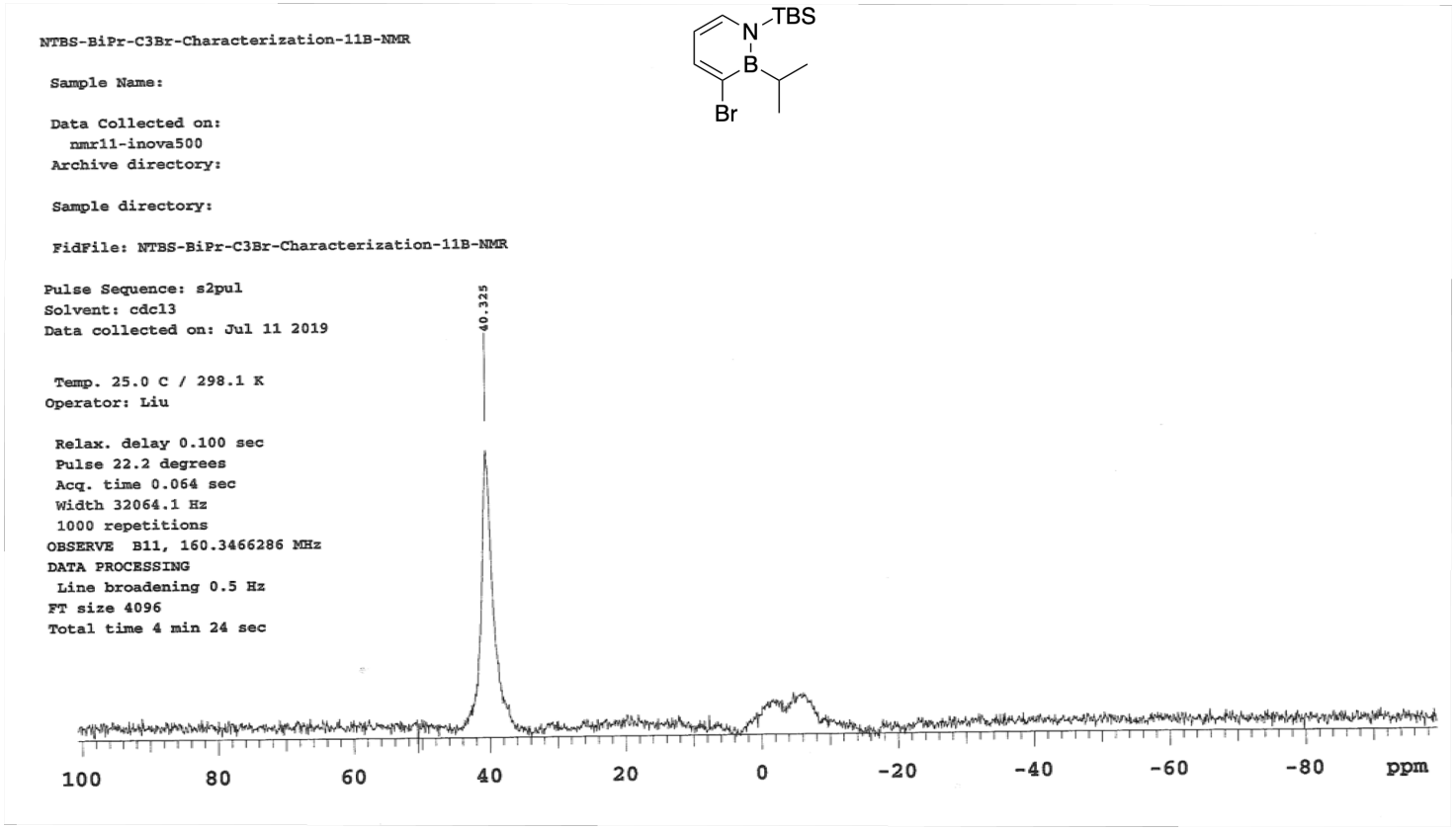
NTBS-BiPr-C3Br-Characterization-11B-NMR
Sample Name:
Data Collected on:
nmr11-inova500
Archive directory:
Sample directory:
FidFile: NTBS-BiPr-C3Br-Characterization-11B-NMR
Pulse Sequence: s2pul
Solvent: cdcl3
Data collected on: Jul 11 2019
Temp. 25.0 C / 298.1 K
Operator: Liu
Relax. delay 0.100 sec
Pulse 22.2 degrees
Acq. time 0.064 sec
Width 32064.1 Hz
1000 repetitions
OBSERVE B11, 160.3466286 MHz
DATA PROCESSING
Line broadening 0.5 Hz
FT size 4096
Total time 4 min 24 sec
40.325
TBS
N
B
Br
100
80
60
40
20
0
-20
-40
-60
-80
ppm

NTBS-BiPr-3Br-Characterization-13C-NMR

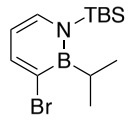

Sample Name:

Data Collected on:
nmr19-vnmrs600
Archive directory:

Sample directory:

FidFile: NTBS-BiPr-3Br-Characterization-13C-NMR

Pulse Sequence: CARBON (s2pul)
Solvent: cdcl3
Data collected on: Jul 16 2019

Temp. 25.0 C / 298.1 K
Operator: Liu

Relax. delay 1.000 sec
Pulse 45.0 degrees
Acq. time 0.865 sec
Width 37878.8 Hz
2000 repetitions
OBSERVE C13, 150.7898151 MHz
DECOUPLE H1, 599.6839027 MHz
Power 42 dB
continuously on
WALTZ-16 modulated
DATA PROCESSING
Line broadening 0.5 Hz
FT size 65536
Total time 1 hr, 2 min

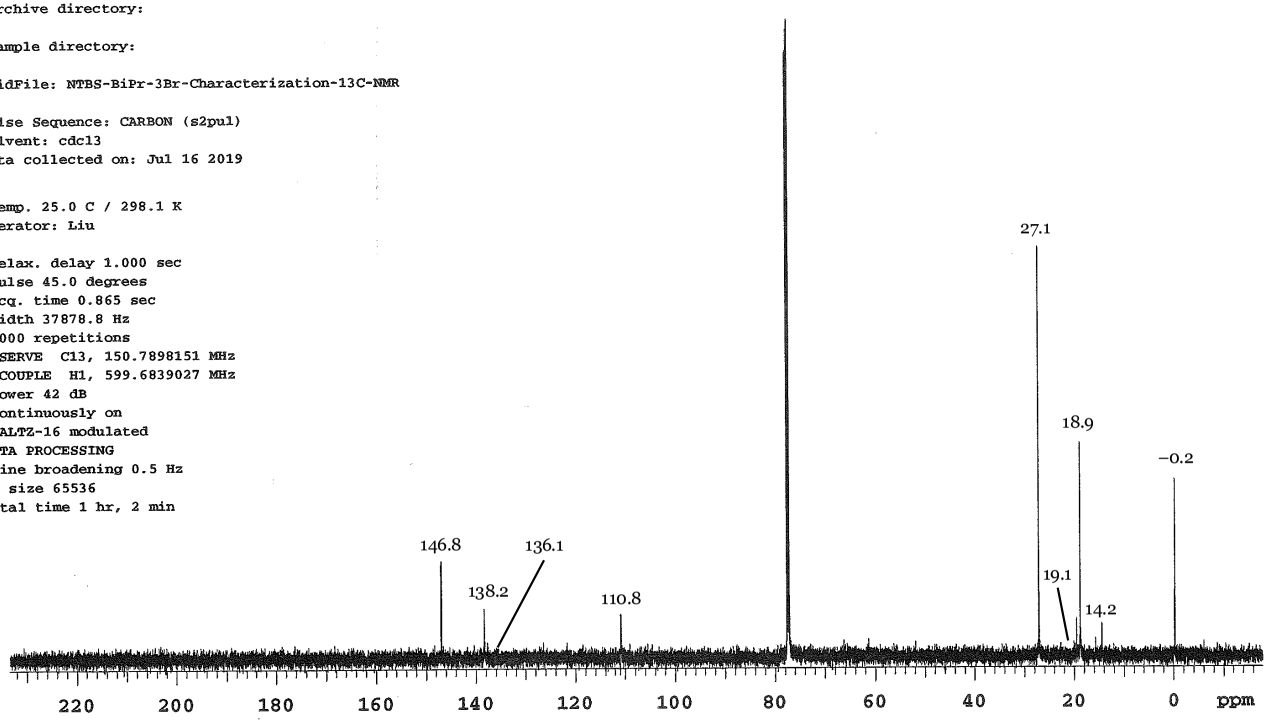

NTBS-BOH-3Et Characterization 1H NMR

Sample Name:

Data Collected on:
nmr19-vnmrs600
Archive directory:

Sample directory:

FidFile: PROTON

Pulse Sequence: PROTON (s2pul)
Solvent: cd2cl2
Data collected on: Apr 9 2018

Temp. 25.0 C / 298.1 K
Operator: Liu

Relax. delay 10.000 sec
Pulse 45.0 degrees
Acq. time 1.704 sec
Width 9615.4 Hz
17 repetitions
OBSERVE H1, 599.6876984 MHz
DECOUPLE C13, 150.8058827 MHz
Power 46 dB
on during acquisition
off during delay
single frequency
DATA PROCESSING
FT size 32768
Total time 6 min 15 sec

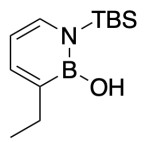

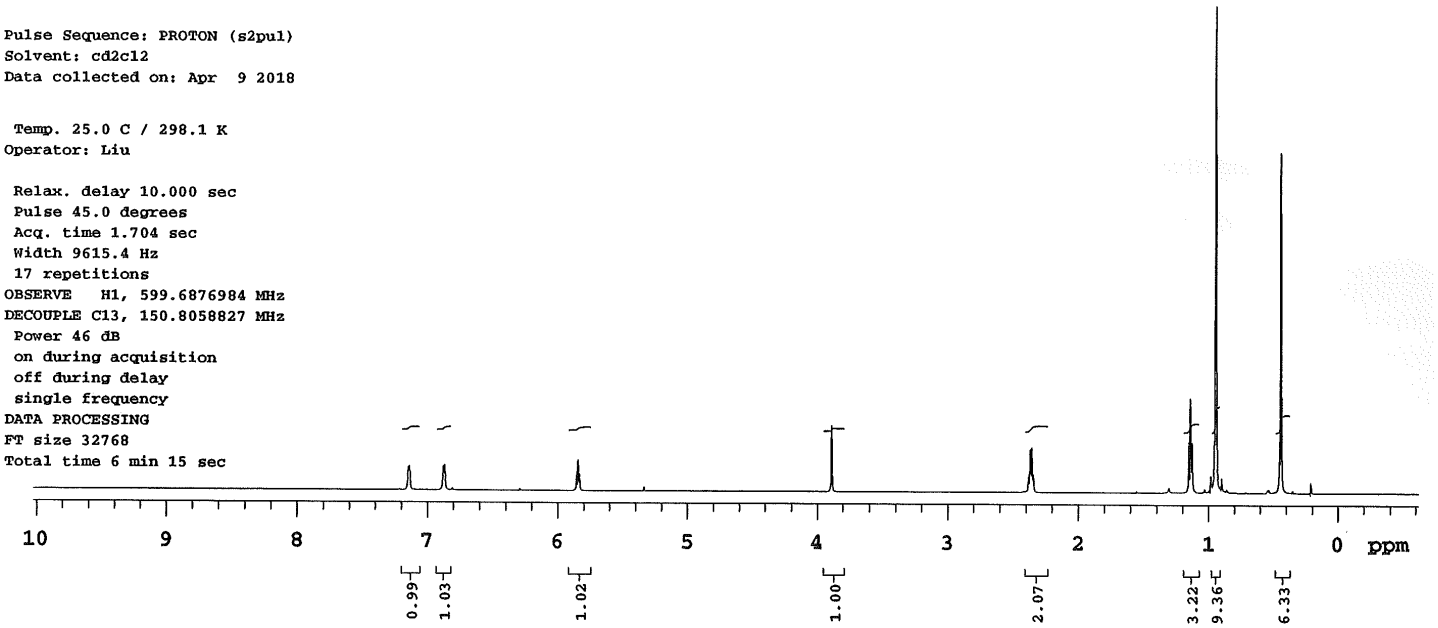

NTBS-BOH-3Et Characterization 11B NMR

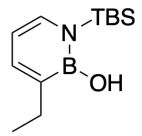

Sample Name:

Data Collected on:
nmr11-inova500
Archive directory:

Sample directory:

FidFile: B11

Pulse Sequence: s2pul
Solvent: cd2cl2
Data collected on: Apr 9 2018

Temp. 25.0 C / 298.1 K
Operator: Liu

Relax. delay 0.010 sec
Pulse 45.0 degrees
Acq. time 0.064 sec
Width 32064.1 Hz
960 repetitions
OBSERVE B11, 160.3472245 MHz
DATA PROCESSING
Line broadening 0.5 Hz
FT size 4096
Total time 1 min 16 sec

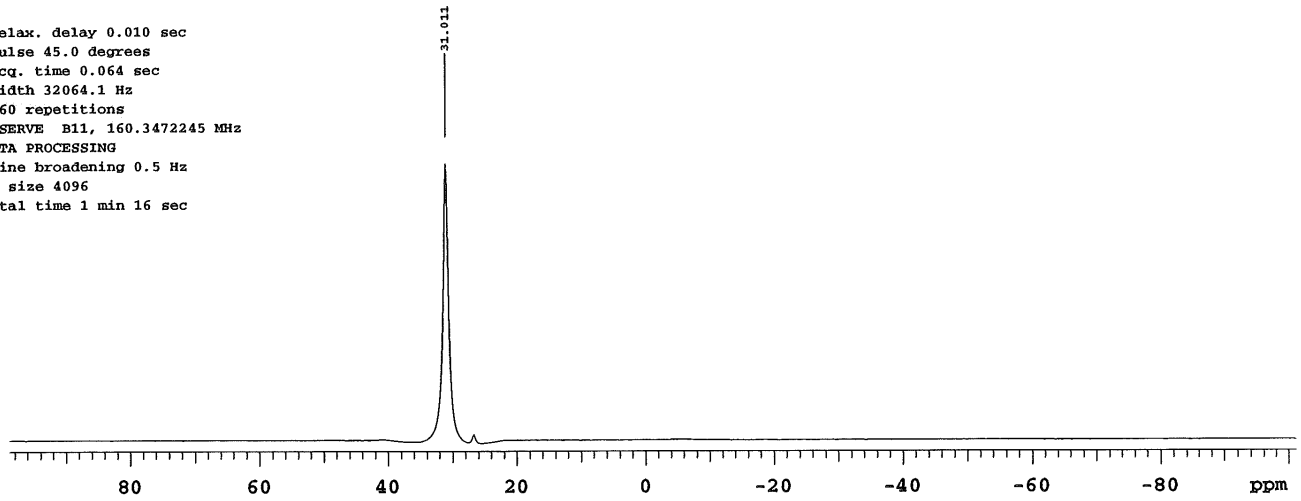

NTBS BOH 3Et Characterization 13C NMR

Sample Name:

Data Collected on:
nmr19-vnmrs600
Archive directory:

Sample directory:

FidFile: CARBON

Pulse Sequence: CARBON (s2pul)
Solvent: cd2cl2
Data collected on: Apr 9 2018

Temp. 25.0 C / 298.1 K
Operator: Liu

Relax. delay 1.000 sec
Pulse 45.0 degrees
Acq. time 0.865 sec
Width 37878.8 Hz
251 repetitions
OBSERVE C13, 150.7914950 MHz
DECOUPLE H1, 599.6906968 MHz
Power 45 dB
continuously on
WALTZ-16 modulated
DATA PROCESSING
Line broadening 0.5 Hz
FT size 65536
Total time 7 min 57 sec

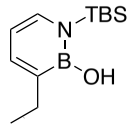

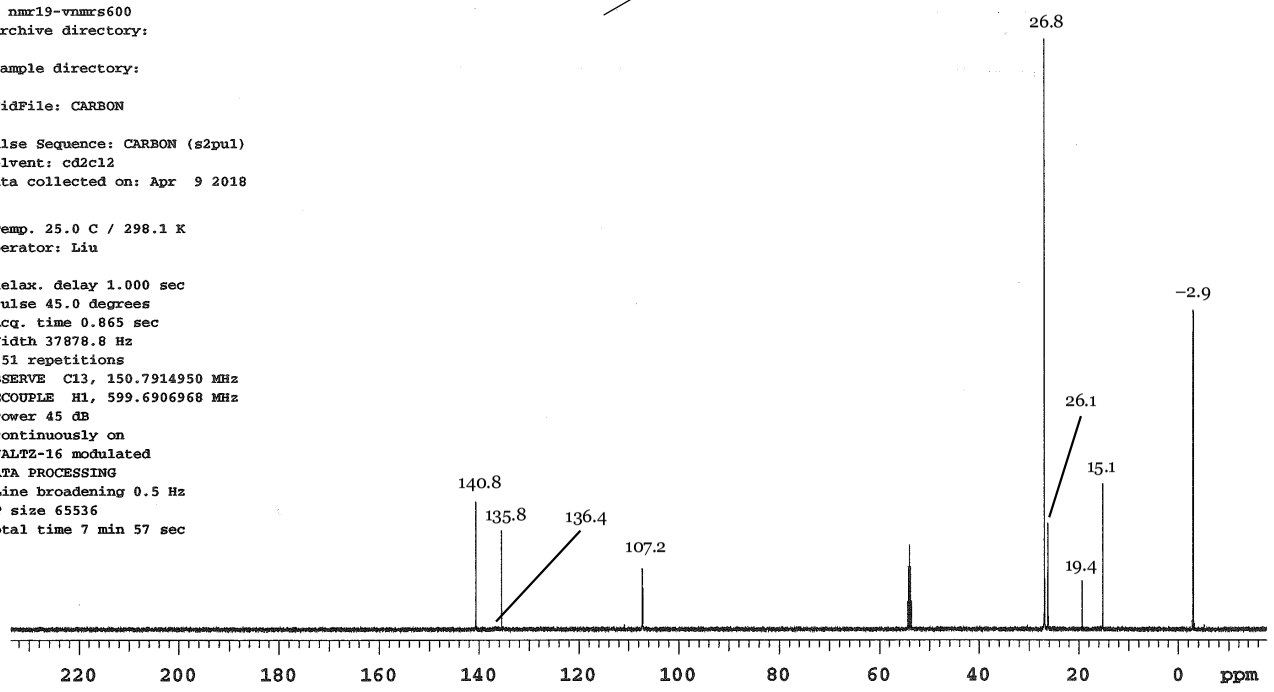

NTBS-BOH-C3iPr-Characterization-1H-NMR

Sample Name:

Data Collected on:
nmr14-vnmrs400
Archive directory:

Sample directory:

FidFile: PROTON

Pulse Sequence: PROTON (s2pul)
Solvent: cd2cl2
Data collected on: Jun 21 2018

Temp. 25.0 C / 298.1 K
Operator: Liu

Relax. delay 10.000 sec
Pulse 45.0 degrees
Acq. time 2.556 sec
Width 6410.3 Hz
8 repetitions
OBSERVE H1, 399.7670443 MHz
DATA PROCESSING
FT size 32768
Total time 6 min 42 sec

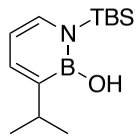

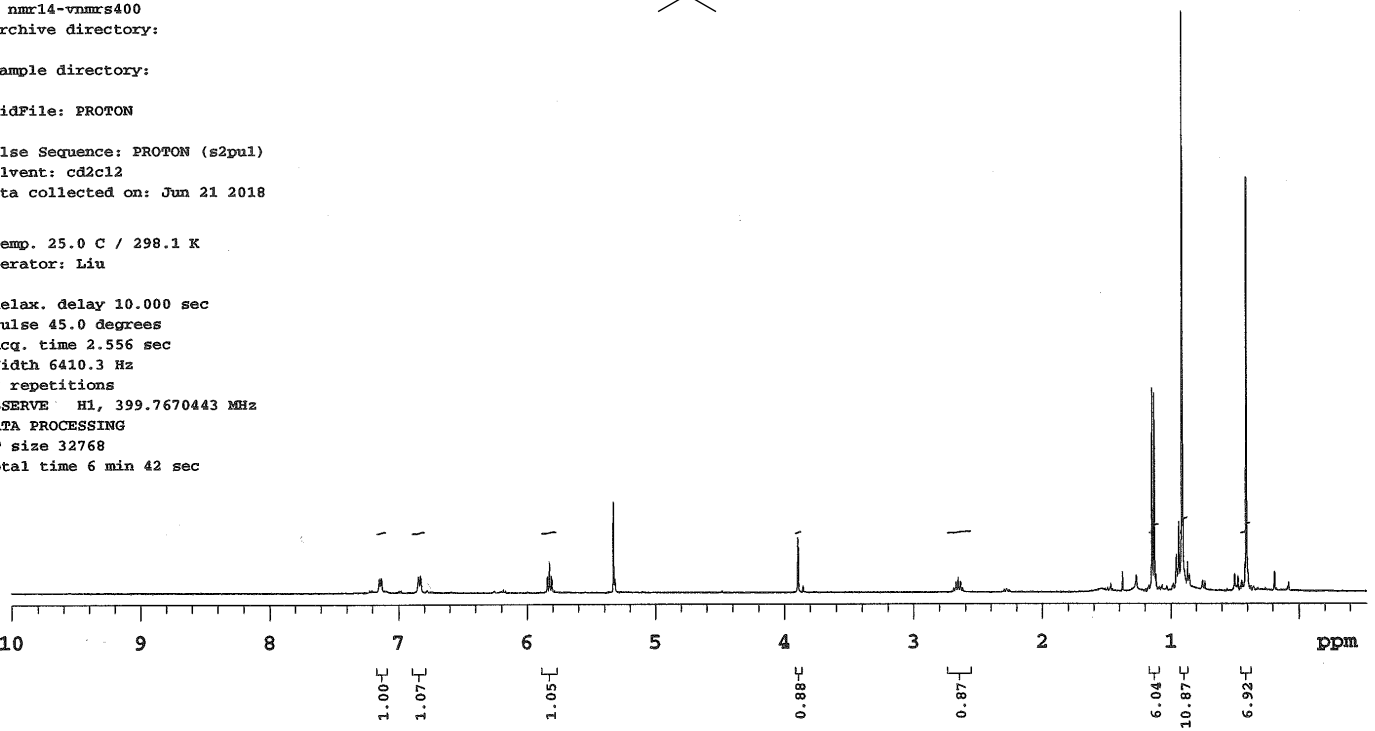

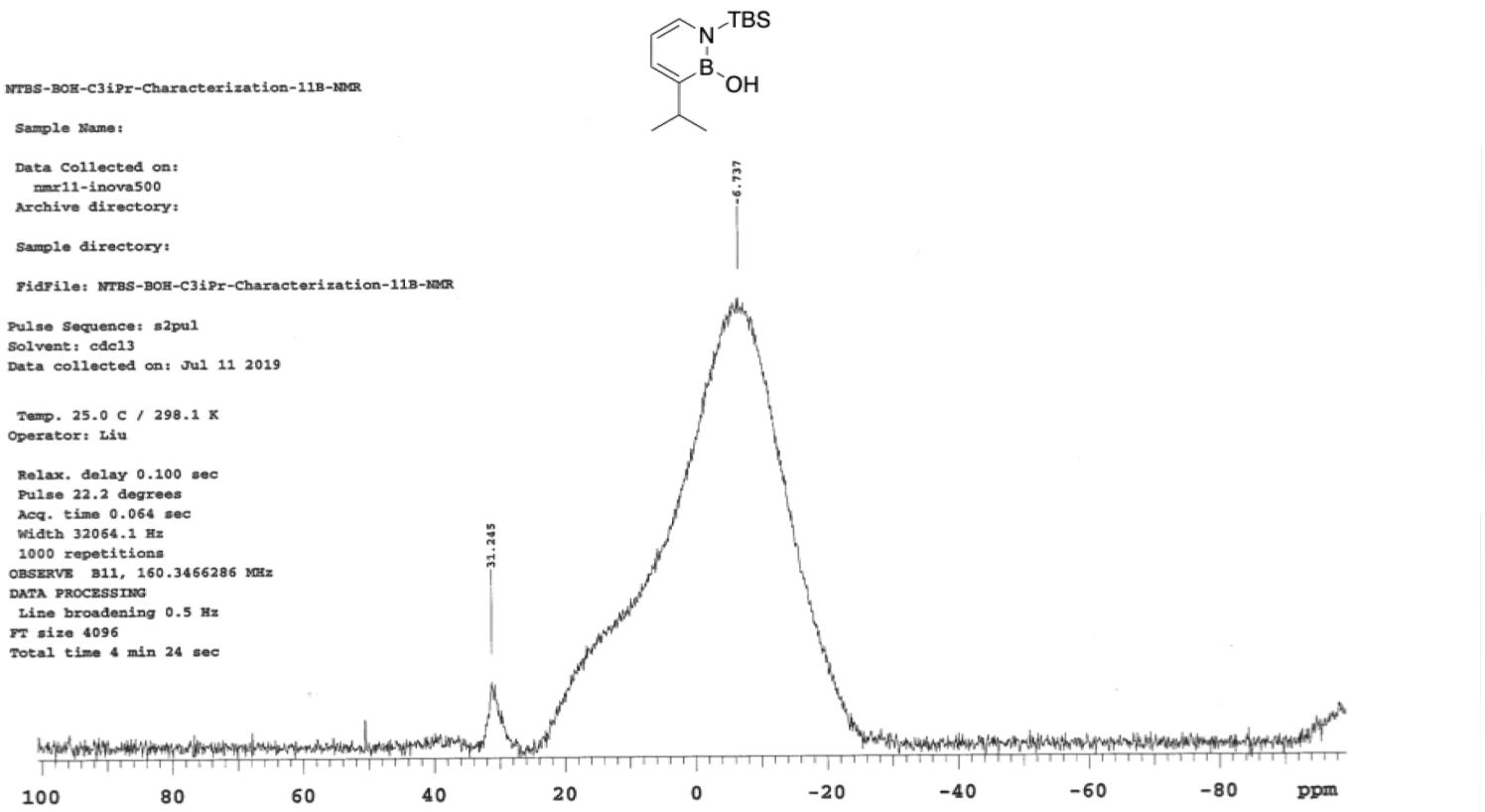
TBS
N
B
OH
NTBS-BOH-C3iPr-Characterization-11B-NMR
Sample Name:
Data Collected on:
nmr11-inova500
Archive directory:
Sample directory:
FidFile: NTBS-BOH-C3iPr-Characterization-11B-NMR
Pulse Sequence: s2pul
Solvent: cdcl3
Data collected on: Jul 11 2019
Temp. 25.0 C / 298.1 K
Operator: Liu
Relax. delay 0.100 sec
Pulse 22.2 degrees
Acq. time 0.064 sec
Width 32064.1 Hz
1000 repetitions
OBSERVE B11, 160.3466286 MHz
DATA PROCESSING
Line broadening 0.5 Hz
FT size 4096
Total time 4 min 24 sec
31.245
6.737
100
80
60
40
20
0
-20
-40
-60
-80
ppm

NTBS-BOH-3iPr-Characterization-13C-NMR

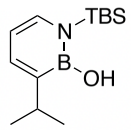

Sample Name:

Data Collected on:
nmr19-vnmrs600
Archive directory:

Sample directory:

FidFile: NTBS-BOH-3iPr-Characterization-13C-NMR

Pulse Sequence: CARBON (s2pul)
Solvent: cdcl3
Data collected on: Jul 21 2019

Temp. 25.0 C / 298.1 K
Operator: Liu

Relax. delay 1.000 sec
Pulse 45.0 degrees
Acq. time 0.865 sec
Width 37878.8 Hz
2000 repetitions
OBSERVE C13, 150.7899146 MHz
DECOUPLE H1, 599.6839027 MHz
Power 42 dB
continuously on
WALTZ-16 modulated
DATA PROCESSING
Line broadening 0.5 Hz
FT size 65536
Total time 2 hr, 35 min

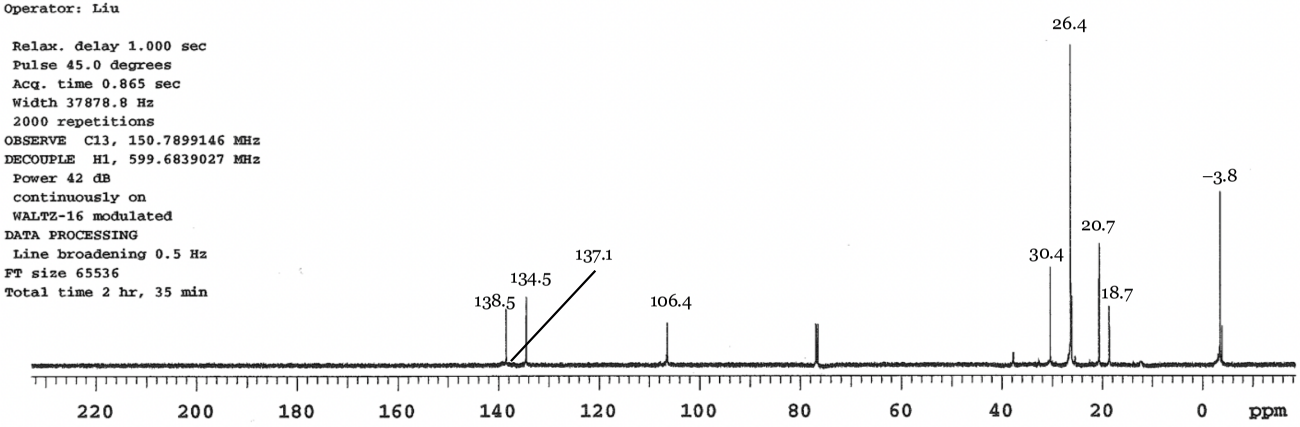

NTBS-BpCNPh-Characterization-1H-NMR

Sample Name:

Data Collected on:
nmr18-vnmrs500
Archive directory:

Sample directory:

FidFile: NTBS-BpCNPh-Characterization-1H-NMR

Pulse Sequence: PROTON (s2pul)
Solvent: cdcl3
Data collected on: May 27 2019

Temp. 25.0 C / 298.1 K
Operator: Liu

Relax. delay 4.000 sec
Pulse 45.0 degrees
Acq. time 2.045 sec
Width 8012.8 Hz
64 repetitions
OBSERVE H1, 499.8762812 MHz
DATA PROCESSING
FT size 32768
Total time 6 min 27 sec

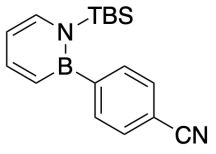

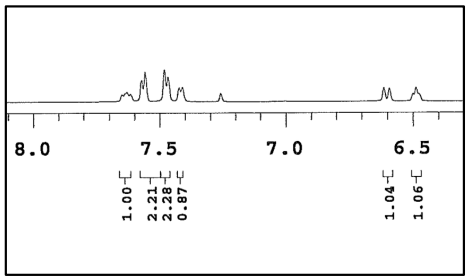

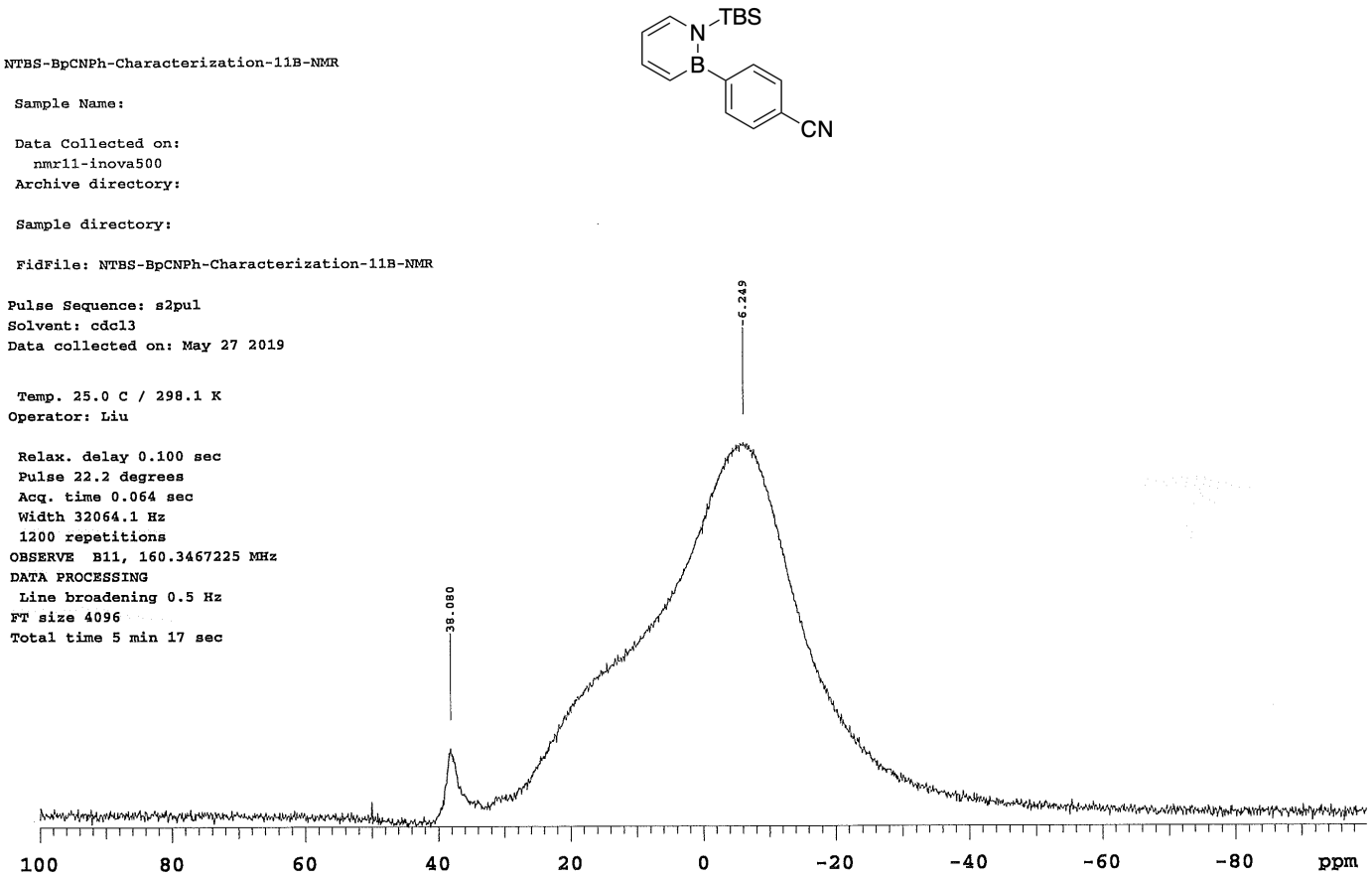
NTBS-BpCNPh-Characterization-11B-NMR
Sample Name:
Data Collected on:
nmr11-inova500
Archive directory:
Sample directory:
FidFile: NTBS-BpCNPh-Characterization-11B-NMR
Pulse Sequence: s2pul
Solvent: cdcl3
Data collected on: May 27 2019
Temp. 25.0 C / 298.1 K
Operator: Liu
Relax. delay 0.100 sec
Pulse 22.2 degrees
Acq. time 0.064 sec
Width 32064.1 Hz
1200 repetitions
OBSERVE B11, 160.3467225 MHz
DATA PROCESSING
Line broadening 0.5 Hz
FT size 4096
Total time 5 min 17 sec
N
TBS
B
CN
6.249
38.080
100
80
60
40
20
0
-20
-40
-60
-80
ppm

NTBS-BpCNPh-Characterization-13C-NMR

Sample Name:

Data Collected on:
nmr19-vnmrs600
Archive directory:

Sample directory:

FidFile: NTBS-BpCNPh-Characterization-13C-NMR

Pulse Sequence: CARBON (s2pul)
Solvent: cdcl3
Data collected on: May 27 2019

Temp. 25.0 C / 298.1 K
Operator: Liu

Relax. delay 1.000 sec
Pulse 45.0 degrees
Acq. time 0.865 sec
Width 37878.8 Hz
550 repetitions
OBSERVE C13, 150.7898441 MHz
DECOUPLE H1, 599.6839027 MHz
Power 42 dB
continuously on
WALTZ-16 modulated
DATA PROCESSING
Line broadening 0.5 Hz
FT size 65536
Total time 17 min

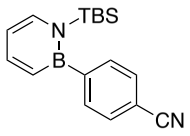

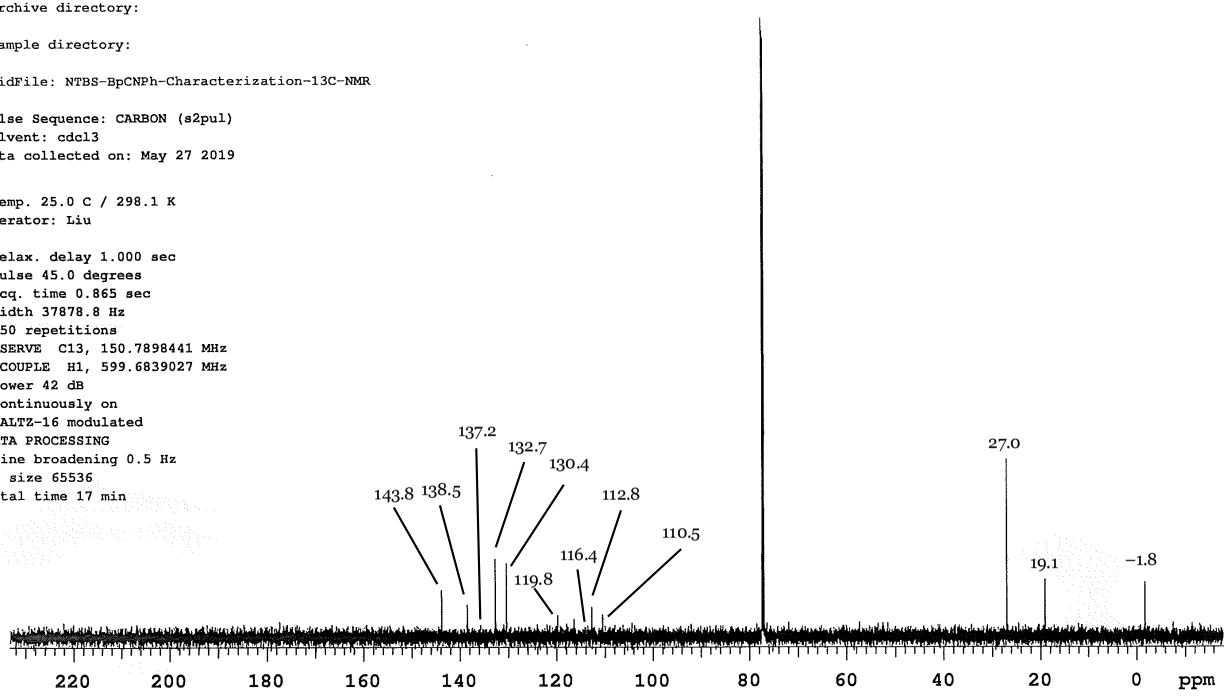

NTBS-BiPr Characterization 1H NMR

Sample Name:

Data Collected on:
nmr18-vnmrs500
Archive directory:

Sample directory:

FidFile: PROTON

Pulse Sequence: PROTON (s2pul)
Solvent: cdcl3
Data collected on: May 21 2019

Temp. 25.0 C / 298.1 K
Operator: Liu

Relax. delay 2.000 sec
Pulse 45.0 degrees
Acq. time 2.045 sec
Width 8012.8 Hz
75 repetitions
OBSERVE H1, 499.8762807 MHz
DATA PROCESSING
FT size 32768
Total time 5 min 3 sec

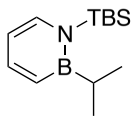

Agilent Technologies

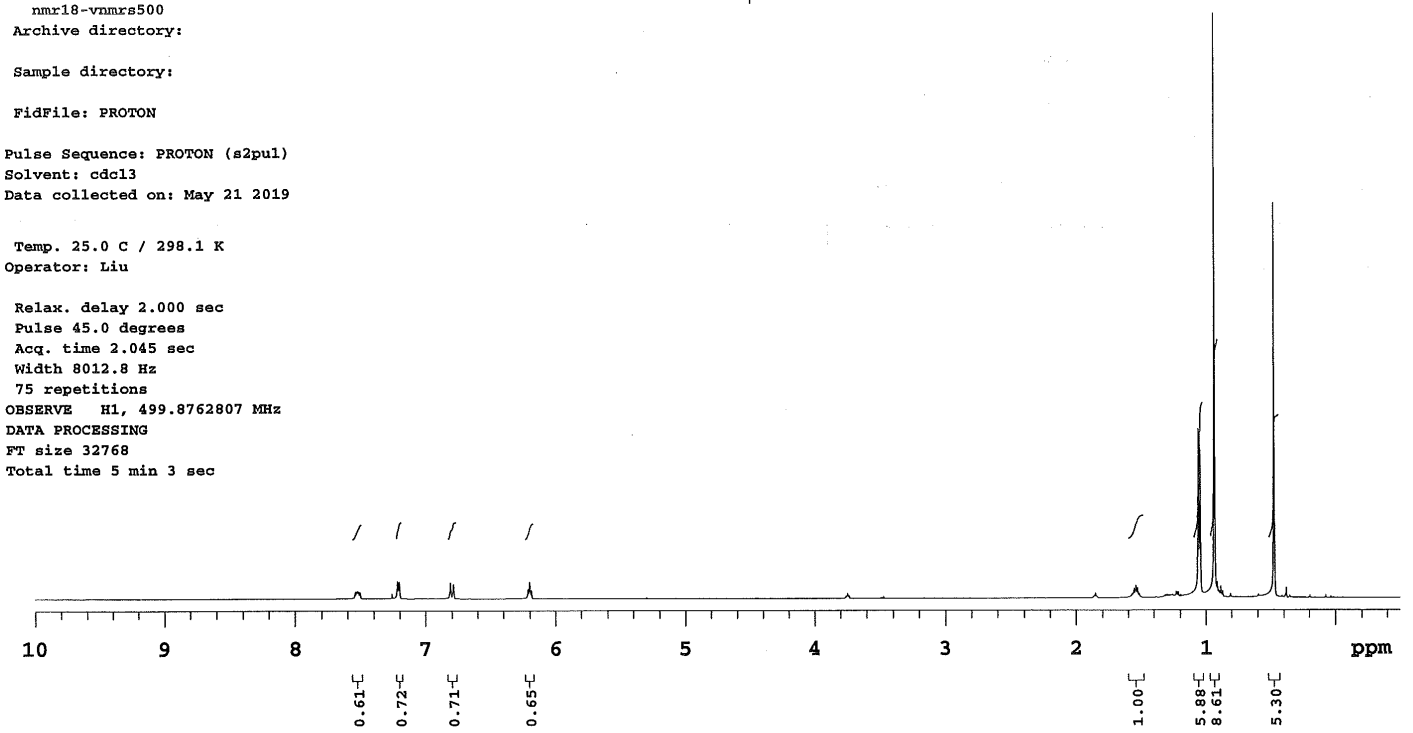

NTBS-BiPr Characterization 11B NMR

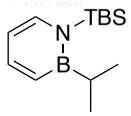

Agilent Technologies

Sample Name:

Data Collected on:
nmr11-inova500
Archive directory:

Sample directory:

FidFile: B11

Pulse Sequence: s2pul
Solvent: cdcl3
Data collected on: May 21 2019

Temp. 25.0 C / 298.1 K
Operator: Liu

Relax. delay 0.100 sec
Pulse 22.2 degrees
Acq. time 0.064 sec
Width 32064.1 Hz
500 repetitions
OBSERVE B11, 160.3467225 MHz
DATA PROCESSING
Line broadening 0.5 Hz
FT size 4096
Total time 2 min 16 sec

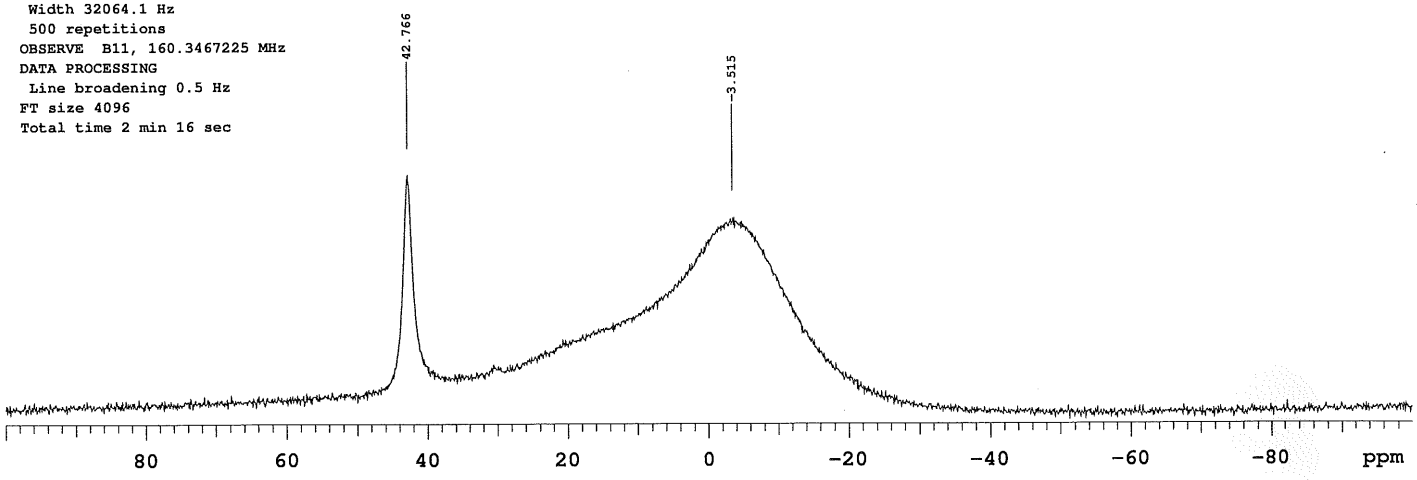

NTBS-BiPr Characterization 13C NMR

Sample Name:

Data Collected on:
nmr18-vnmrs500
Archive directory:

Sample directory:

FidFile: CARBON

Pulse Sequence: CARBON (s2pul)
Solvent: cdcl3
Data collected on: May 21 2019

Temp. 25.0 C / 298.1 K
Operator: Liu

Relax. delay 1.000 sec
Pulse 45.0 degrees
Acq. time 1.049 sec
Width 31250.0 Hz
256 repetitions
OBSERVE C13, 125.6939894 MHz
DECOUPLE H1, 499.8787746 MHz
Power 43 dB
continuously on
WALTZ-16 modulated
DATA PROCESSING
Line broadening 0.5 Hz
FT size 65536
Total time 25 min

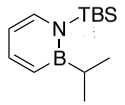

Agilent Technologies

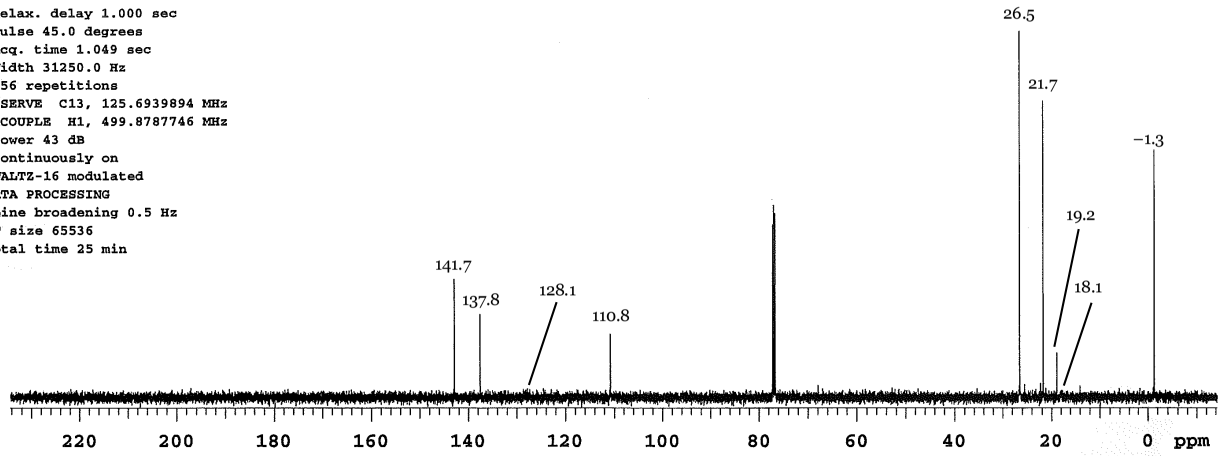

NMe-BiPr-Characterization-1H-NMR

Sample Name:

Data Collected on:
nmr19-vnmrs600
Archive directory:

Sample directory:

FidFile: NMe-BiPr-Characterization-1H-NMR

Pulse Sequence: PROTON (s2pul)
Solvent: cdcl3
Data collected on: Jul 11 2019

Temp. 25.0 C / 298.1 K
Operator: Liu

Relax. delay 5.000 sec
Pulse 45.0 degrees
Acq. time 1.704 sec
Width 9615.4 Hz
128 repetitions
OBSERVE H1, 599.6808978 MHz
DATA PROCESSING
FT size 32768
Total time 14 min

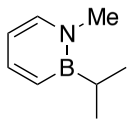

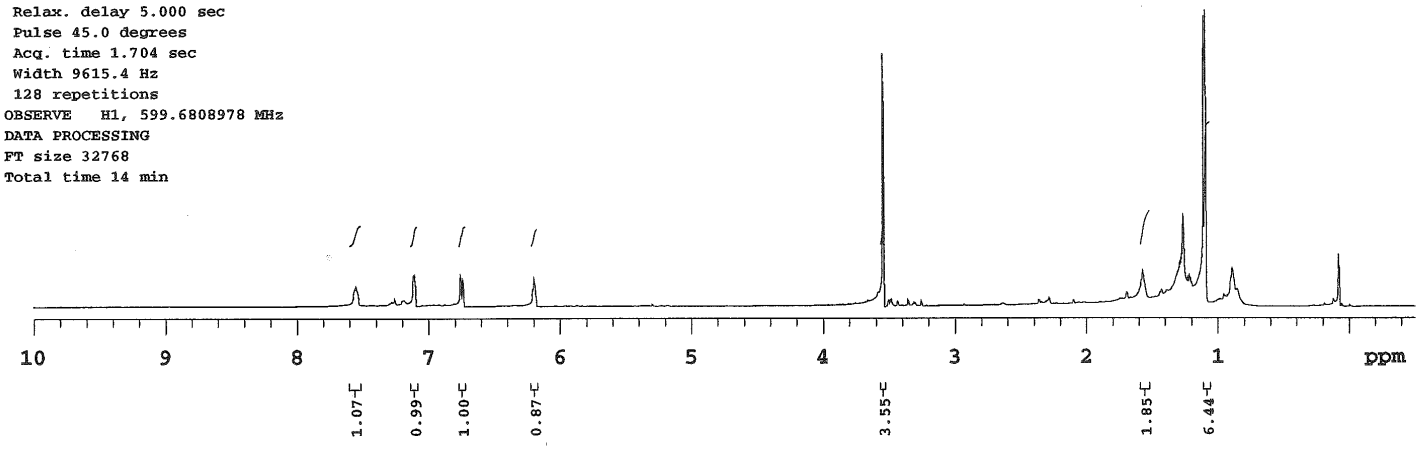

NMe-BiPr-Characterization-11B-NMR

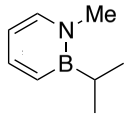

Sample Name:

Data Collected on:
nmr11-inova500
Archive directory:

Sample directory:

FidFile: NMe-BiPr-Characterization-11B-NMR

Pulse Sequence: s2pul
Solvent: cdcl3
Data collected on: Jul 11 2019

Temp. 25.0 C / 298.1 K
Operator: Liu

Relax. delay 0.100 sec
Pulse 22.2 degrees
Acq. time 0.064 sec
Width 32064.1 Hz
800 repetitions
OBSERVE B11, 160.3466286 MHz
DATA PROCESSING
Line broadening 0.5 Hz
FT size 4096
Total time 3 min 31 sec

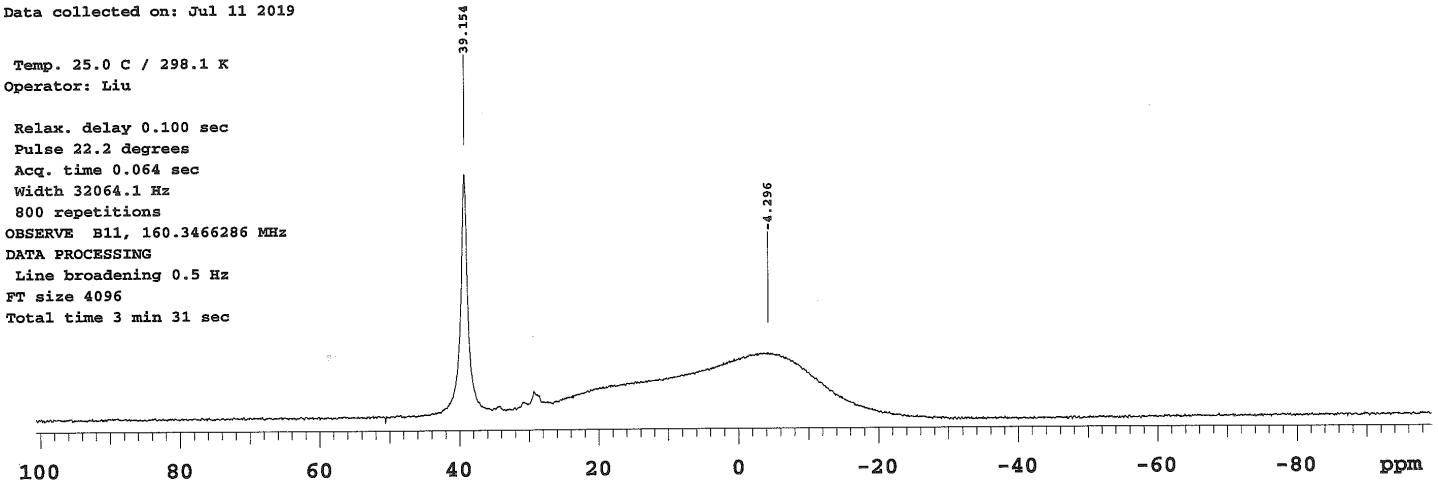

NMe-BiPr-Characterization-13C-NMR

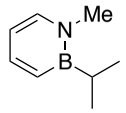

Sample Name:

Data Collected on:
nmr19-vnmrs600
Archive directory:

Sample directory:

FidFile: NMe-BiPr-Characterization-13C-NMR

Pulse Sequence: CARBON (s2pul)
Solvent: cdcl3
Data collected on: Jul 21 2019

Temp. 25.0 C / 298.1 K
Operator: Liu

Relax. delay 1.000 sec
Pulse 45.0 degrees
Acq. time 0.865 sec
Width 37878.8 Hz
2500 repetitions
OBSERVE C13, 150.7898464 MHz
DECOUPLE H1, 599.6839027 MHz
Power 42 dB
continuously on
WALTZ-16 modulated
DATA PROCESSING
Line broadening 0.5 Hz
FT size 65536
Total time 1 hr, 17 min

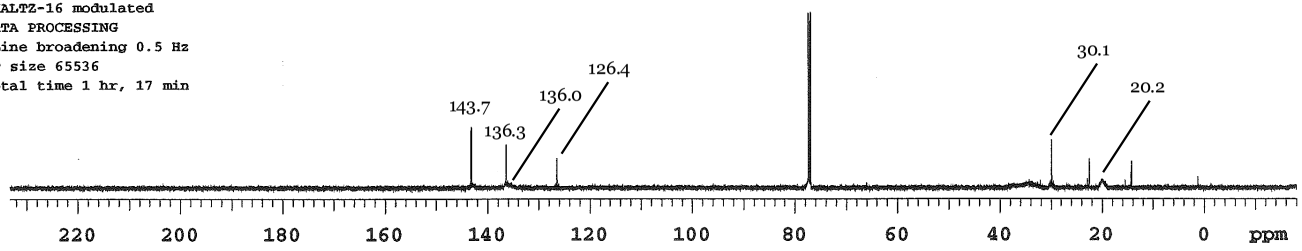

NH-BiPr-Characterization-1H-NMR

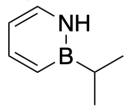

Sample Name:

Data Collected on:
nmr18-vnmrs500
Archive directory:

Sample directory:

FidFile: NH-BiPr-Characterization-1H-NMR

Pulse Sequence: PROTON (s2pul)
Solvent: cdcl3
Data collected on: May 27 2019

Temp. 25.0 C / 298.1 K
Operator: Liu

Relax. delay 3.000 sec
Pulse 45.0 degrees
Acq. time 2.045 sec
Width 8012.8 Hz
65 repetitions
OBSERVE H1, 499.8762807 MHz
DATA PROCESSING
FT size 32768
Total time 5 min 28 sec

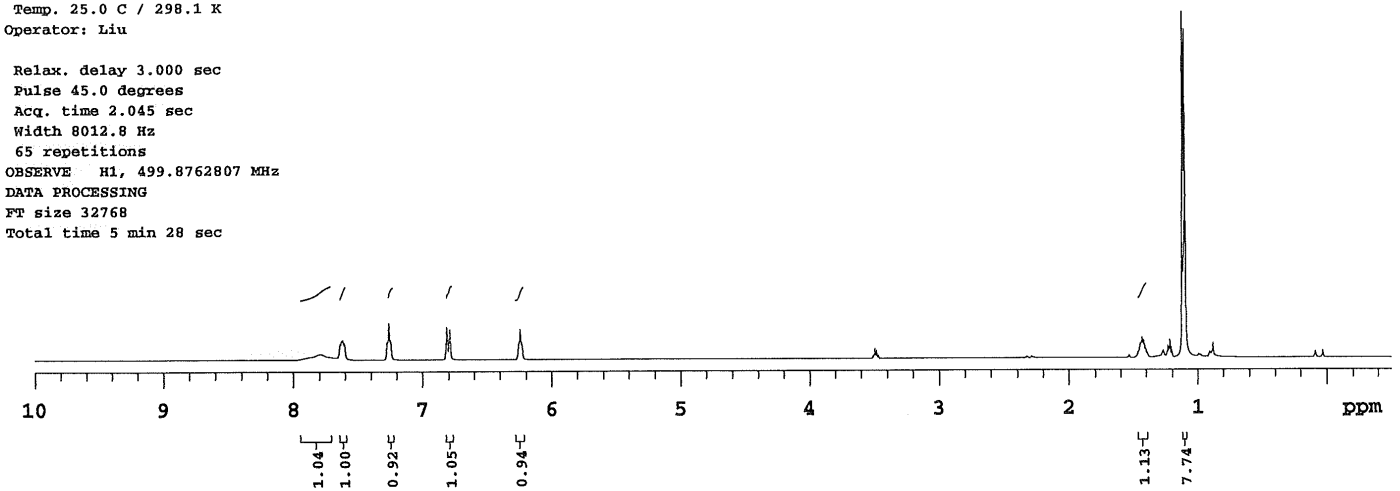

NH-BiPr-Characterization-11B-NMR

Sample Name:

Data Collected on:
nmr11-inova500
Archive directory:

Sample directory:

FidFile: B11

Pulse Sequence: s2pul
Solvent: cdcl3
Data collected on: May 27 2019

Temp. 25.0 C / 298.1 K
Operator: Liu

Relax. delay 0.100 sec
Pulse 22.2 degrees
Acq. time 0.064 sec
Width 32064.1 Hz
600 repetitions
OBSERVE B11, 160.3467538 MHz
DATA PROCESSING
Line broadening 0.5 Hz
FT size 4096
Total time 2 min 44 sec

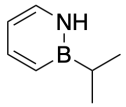

Agilent Technologies

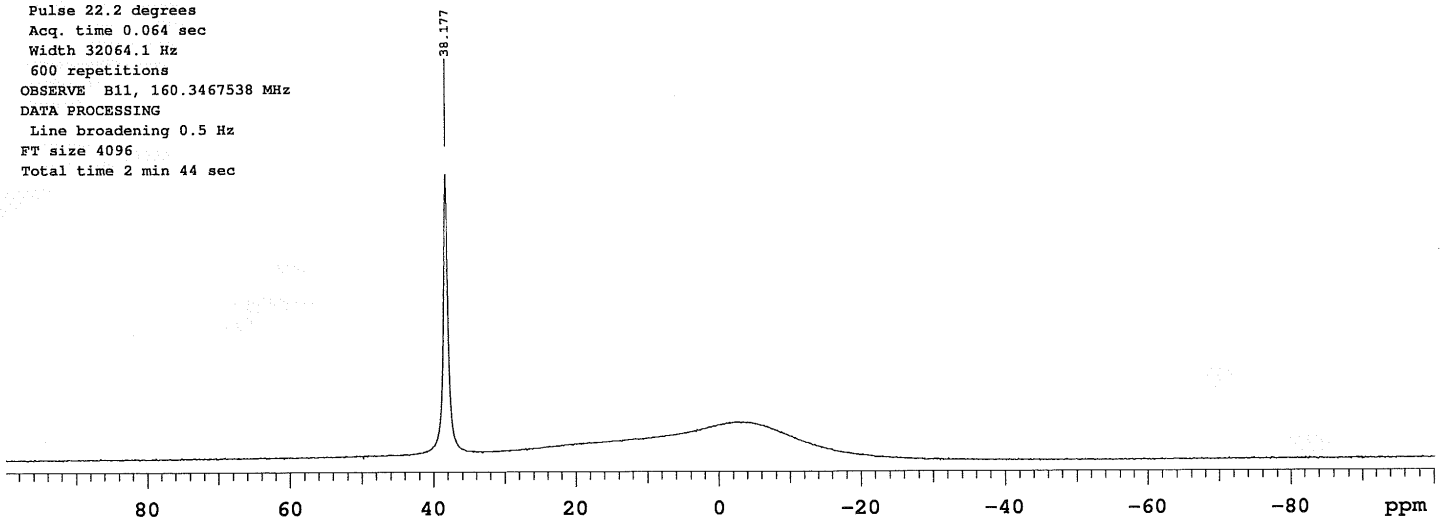

NH-BiPr-Characterization-13C-NMR

Sample Name:

Data Collected on:
nmr19-vnmrs600
Archive directory:

Sample directory:

FidFile: CARBON

Pulse Sequence: CARBON (s2pul)
Solvent: cdcl3
Data collected on: May 27 2019

Temp. 25.0 C / 298.1 K
Operator: Liu

Relax. delay 1.000 sec
Pulse 45.0 degrees
Acq. time 0.865 sec
Width 37878.8 Hz
550 repetitions
OBSERVE C13, 150.7898464 MHz
DECOUPLE H1, 599.6839027 MHz
Power 42 dB
continuously on
WALTZ-16 modulated
DATA PROCESSING
Line broadening 0.5 Hz
FT size 65536
Total time 17 min